ONCOLYTIC VIRUS VACCINATION TO EXPAND ENGINEERED T CELLS

DEVELOPING AN ENGINEERED T CELL PRODUCT FOR UNIVERSAL ONCOLYTIC VIRUS VACCINATION-BASED BOOSTING IN ADOPTIVE CELL THERAPIES

By Claire Morris, B.Sc (Hons)

A Thesis Submitted to the School of Graduate Studies in Partial Fulfilment of the Requirements for the Degree Master of Science

McMaster University

McMaster University MASTER OF SCIENCE (2024) Hamilton, Ontario (Biochemistry and Biomedical Sciences)

TITLE: Developing an Engineered T cell Product for Universal Oncolytic Virus Vaccination-Based Boosting in Adoptive Cell Therapies

AUTHOR: Claire Morris, B.Sc. (Hons) (Memorial University of Newfoundland)

SUPERVISOR: Dr. Jonathan L. Bramson

NUMBER OF PAGES: xiv, 86.

Lay Abstract:

Adoptive T cell therapy (ACT) uses a patient's immune cells to fight cancer but is often a last resort due to high costs and labor. Our research aims to make ACT more accessible by combining it with therapeutic cancer vaccines that can contain any protein, including cancer proteins, and boost ACT's effectiveness. We engineered T cells with synthetic receptors to recognize the vaccine's protein and developed a universal system pairing these T cells with a specially designed oncolytic virus vaccine (OVV).
This combination promotes T cell expansion and improves immune response against tumours. We tested this system in multiple models, demonstrating enhanced T cell function and tumour targeting in one model, but challenges in another. Investigating the mechanisms, we sought to identify ways to improve the therapy's efficacy. Our "off-the-shelf" solution reduces costs and resources, making this powerful cancer treatment more accessible to a wider range of patients.

Scientific Abstract:

Creating a universal-prime boost strategy using multi-specific T cells from the tumour infiltrating lymphocytes (TIL) population can enhance the success of adoptive T cell therapies (ACT). ACT, as a personalized living-drug, is often a last resort due to its extensive time, cost, and labor requirements, making it largely inaccessible. Vaccines encoding personalized tumour-associated antigens (TAA) have proven to be potent boosters for ACT. This combination has shown success in (1) promoting T cell proliferation in vivo and (2) inducing immune infiltration into the solid tumour microenvironment. TIL offer a plethora of TAA-specific T-cell receptors (TCRs) when successfully isolated and expanded. Synthetic receptors can be engineered into TIL to recognize any specified antigen, including those matched in vaccines. Previously, we validated combining ACT with an oncolytic virus vaccine (OVV) "boost" through a synthetic receptor to promote *in vivo* expansion of naïve splenocytes in a proof-of-concept TCR-transgenic synergetic murine model. Here, we report on the feasibility of isolating and engineering polyclonal, tumour-specific T cells from TIL and tumour-draining lymph nodes, evaluating them functionally. We further investigate the matched CAR/OVV system in another distinct TCR transgenic model and return to the first proof-of-concept model to uncover the biological mechanisms of our combination therapy to improve anti-tumour efficacy. Uniting a universal OV vaccine with a matched universal CAR creates an "off-the-shelf" combination, allowing any T cell product to be engineered. This approach reduces the resource burden of traditional ACT, making it more accessible to all cancer types.

Acknowledgements:

I'd like to begin this acknowledgment by speaking about the reason I began my journey into research and discovered my passion, Dr. Sheila Drover. Sheila, your belief in an undergraduate chemistry student with an interest in cancer immunotherapies has sustained me through my toughest days. Thank you for giving me that opportunity and I hope with each next step I take I make you proud.

Next, I'd like to extend my sincere thanks to my supervisor, Dr. Jonathan Bramson. None of this work would be possible without you, thank you for giving me the opportunity to complete it. I would also like to thank my supervisory committee, Dr. Matthew Miller and Dr. Amy Gillgrass. Your insights on this work were incredibly valuable, and I deeply appreciate the time you dedicated to my scientific training.

I'd also like to highlight the amazing staff I've encountered at McMaster. To Hong Liang and Zoya Tabunshchyk, thank you for your expertise in flow cytometry and dedication to keeping the machines in perfect condition and accommodating us students when things inevitably go wrong. Marion Corrick, Robin Howe, Maegan Gill, and the rest of the Central Animal Facility staff, thank you for your diligent care of our mice and the facility we worked in. Science would be incredibly more difficult without all your support.

I would also like to thank our collaborators through the Canadian Oncolytic Virus Consortium (COVCo) for providing their knowledge and materials for this project. Thank you to the funding sources who supported me and my research during my time as a graduate student: the Terry Fox Foundation, the Canadian Institutes of Health Research and Canadian Graduate Scholarships program.

I've been lucky to encounter some of the best people southern Ontario has to offer in my time here. Bonnie, there is no one else I'd like to debate with side-by-side in our BEAM TC suite. I'll miss chatting dogs and the outdoors with you. Derek, I'll miss you and our many inside jokes. Don't forget about me. Nick, you're the best big brother I never had. Your enthusiasm to listen to my every thought and idea was appreciated on my most challenging days. Chris, thank you for abandoning your introverted ways to socialize with me. Your friendship has meant more to me than you'll ever know, and I'll remember your sacrifice forever. Dr. Sam Afkhami, your support during this thesis writing process has been invaluable. Thank you for your insights, answering all my stupid questions with kindness and always being a second set of eyes for me. Dr. Rebecca Burchett, thank you for choosing me to join you as a mouse girl. We've had so much fun and shared so many ideas, figures and most importantly laughs together throughout this journey and I will never forget it.

Arwa, Ariya and Mira, you have moved past being my best friends and into being my sisters. I can't believe I spent the first 22 years of my life without you when it feels like I've known you forever. There is nothing more comforting and beautiful than having your best friends share your passions in life and in research. You girls are the reason I made it through the past 2 years, I adore you. We were written in the stars.

Throughout my degree, I've had momentous support coming from across the country. Dad, I appreciate all the phone calls, emails and how you somehow manage to move mountains here for me from home. You somehow know the solution to every

problem I encounter, and I would be so lost without you. To my mom, what is there to say? Appreciation seems like an understatement. You are the wind behind my sails and have always kept the fire burning when I wanted to put everything out. You kept me moving forward at my worst. While you will say I got all the brains, I will spend forever learning how to be half the woman you are. I love you both and only miss you more. My sister, Hannah, I know no matter what, you're in my corner. Thank you for your unwavering support and being proud of me when I am not proud of myself. Madi, my other "sister", sometimes I feel there aren't words to describe how someone has made you feel. I appreciate every trip you made to Hamilton to see me, every phone call you let me rant, and how you never let me lose myself. You're the best friend I've ever had, and I know you're waiting for me on the other side of this. Dawson, Sam, Grace and all the other amazing friends I've had visit me from home during my time here, thank you for choosing me as your vacation destination. I wouldn't be here without you all.

Finally, to my Gramps who I lost during my degree; I know you're looking out for me from somewhere in the fields, in the woods or on the water.

Long story short, I survived.

Table of Contents

Lay Abstract: ..... *iii*
Scientific Abstract: ..... *iv*
Acknowledgements: ..... *v*
Table of Contents ..... *vii*
List of Tables ..... *ix*
List of Figures ..... *ix*
List of Abbreviations and Symbols ..... *xi*
Abbreviations ..... **xi**
Symbols ..... **xiii**
Declaration of Academic Achievement ..... *xiv*
1 Introduction *1*
1.1 Cancer immunotherapies throughout history **1**
1.2 Adoptive T cell therapies; using transferred cytotoxic cells in an anti-cancer response **4**
1.3 Adoptive cell transfer of tumour infiltrating lymphocytes (TIL) **5**
1.4 Adoptive cell transfer of chimeric antigen receptor (CAR) T cells **6**
1.5 Viral immunotherapy using oncolytic viruses **8**
1.6 Rhabdovirus vaccines as a boosting agent **9**
1.7 Using a synthetic receptor as a boosting agent **10**
1.8 Further investigating CARs for a universal oncolytic virus boost **14**
1.9 Thesis scope and content **15**
1.9.1 Research objectives *15*
2 Materials and Methods *16*
3 Results *25*
3.1 Investigating the engineering and functionality of naturally occurring tumour-specific T cells as a T cell product for a CAR/OVV boost **25**
3.1.1 Optimizing the isolation of TIL from murine tumours in preliminary experiments *25*
3.1.2 TIL culturing and engineering from bulk tumour tissue *27*
3.1.3 Engineering and functionally testing T cells isolated from tumour-draining lymph nodes (TDLN) *29*
3.1.4 Invigorating the cytotoxic capacity of BCMACAR-T cells derived from TDLN 31

3.2 Evaluating a CAR-mediated OV vaccine boost in the DUC18/CMS-5 model 34

3.2.1 Depleting CD4+ T cells from splenocytes and mERK-activation of splenocytes to evaluate effects on memory phenotype and function.....34

3.2.2 Boosting CD4-negative DUC18 BCMACAR T cells and CD4+CD8+ DUC18 BCMACAR T cells with VSV-hBCMA 38

3.2.3 Monitoring DUC18 T cell expansion using non-invasive luminescent imaging 41

3.2.4 Comparing the boosting capacity and anti-tumour effects of CD4-negative and CD4+CD8+ DUC18 BCMACAR T cells boosted with VSV-mERK or VSV-hBCMA 47

3.3 Investigating the mechanisms involved in an effective CAR-mediated OV vaccine boost and achieving durable anti-tumour function in the P14/B16.F10-gp33 49

3.3.1 Assessing the contributions of CD4+ T cells to CD8+ T cell expansion in vivo 49

3.3.2 Assessing the inclusion of a mIL-15 transgene into the BCMACAR construct to improve T cell persistence and tumour clearance in vivo.....56

3.3.3 Tracking bioluminescent-VSV-HBCMA in vivo to investigate viral kinetics and distribution with transient type I IFN blockade.....58

4 Discussion.....62

5 References:.....68

List of Tables

Table 1.1: Examples of modern immunotherapies that are approved in Canada, the cancers they are used to treat and their mechanisms of action 3
Table 2.1: Constructs and transgenes used in this thesis.....17
Table 2.2: Recombinant hBCMA antigen transgene designs for VSV-vaccination used in this thesis.....24

List of Figures

Figure 1.1: P14 CAR-T cells can be boosted by VSV-hBCMA upon vaccination, expand in the periphery and clear B16-F10-gp33 tumour burdens but fail to persist and tumours relapse. 11
Figure 1.2: Transiently blocking type I IFN signaling during vaccination enhances transferred CAR-T cell expansion and efficacy in the P14/B16.F10-gp33 model. 13
Figure 1.3: DUC18 BCMACAR-T cells are not boosted by VSV-hBCMA upon vaccination and do not control tumour growth. 15
Figure 3.1: Endogenous TIL were successfully isolated from multiple murine tumours and isolation methods were optimized.....26
Figure 3.2: CD8+ T cells can be expanded from bulk tumour-isolated cells and can show cytotoxic effects on tumour targets. 28
Figure 3.3: TDLN-derived T cells from tumour-bearing mice were engineered to express the 28ζBCMA-CAR. 30
Figure 3.4: T cells isolated from TDLN of CMS-5 tumour-bearing mice proliferated only when stimulated through the CAR and were unable to kill tumour targets. 31
Figure 3.5: T cells isolated from TDLN of MC-38 tumour-bearing mice show cytotoxic effects after co-culture stimulation. 33
Figure 3.6: T cells isolated from TDLN of MC-38 tumour-bearing mice do not produce inflammatory cytokines in response to stimulation with tumour target.....34
Figure 3.7: Depleting CD4+ T cell populations from murine splenocytes lead to modest differences in memory phenotype bias and proliferative capacity. 36
Figure 3.8: Activating murine DUC18 splenocytes with mERK peptide led to some differences in growth and cell phenotype but does not lead to superior killing capacity. .38
Figure 3.9: ACT and recombinant VSV-hBCMA boosting of CD4-negative and CD4+CD8+ DUC18 CAR-T cells in CMS-5 tumour-bearing mice. 40
Figure 3.10: Adoptively transferred CD4+CD8+ DUC18 CAR-T cells in CMS-5 tumour-bearing mice peak at 4-days following vaccination with VSV-hBCMA. 42
Figure 3.11: CD4-negative and CD4+CD8+ DUC18 T cells were co-engineered with rsLuc and a BCMACAR and proliferative in functional assessments. 44
Figure 3.12: Adoptive transfer, recombinant VSV-hBCMA boosting and in vivo tracking of CD4-negative and CD4+CD8+ DUC18 CAR-T cells in CMS-5 tumour-bearing mice. 46

Figure 3.13: Adoptively transferred CD4-negative and CD4+CD8+ DUC18 CAR-T cells in CMS-5 tumour-bearing mice behave similarly in CAR- and TCR-activated boosting following VSV-hBCMA vaccination. 48
Figure 3.14: Non-differentiated (ND) C57BL/6 CD4+ T cells significantly reduced in vivo expansion of P14 T cells when included in the T cell product. 50
Figure 3.15: T helper 1 (Th1) CD4+ T cells can be engineered with a boosting CAR and produce cytokine in response to CAR stimulation....52
Figure 3.16: Th1 CD4+ T cells can proliferate in response to CAR stimulation and modestly increase proliferative capacity of P14-Thy1.1 T cells in vitro. 53
Figure 3.17: Including Th1 CD4+ T cells in ACT and recombinant VSV-hBCMA boosting of P14 T cells does not benefit P14 T cell persistence or prevent tumour relapse in B16-F10-gp33 tumour-bearing mice. 55
Figure 3.18: Adoptive transfer and recombinant VSV boosting of BCMACAR(28ζ)_mIL-15 P14 T cells does not augment T cell persistence in B16-F10-gp33 tumour-bearing mice. 57
Figure 3.19: Generating and validating VSV-rsLuc-hBCMA. 59
Figure 3.20: Tracking VSV-rsLuc-hBCMA with and without αIFNAR1 blockade shows differences in viral kinetics and infection levels. 61

List of Abbreviations and Symbols

Abbreviations

Ab – antibody
ACK - ammonium chlorine potassium
ALL - Adult acute lymphoblastic leukemia
ACT - adoptive (T) cell therapy
AICD – activation-induced cell death
APC - antigen-presenting cell
BCMA - B cell maturation antigen
CAR - Chimeric Antigen Receptor
CD – cluster of differentiation
CLL - Chronic lymphocytic leukemia
CRS – cytokine release syndrome
CTLA-4 - cytotoxic T-lymphocyte associated protein 4
CTV – CellTrace Violet dye
DC - dendritic cell
DLA- dog leukocyte antigen
DMSO – dimethyl sulfoxide
effLuc - enhanced firefly luciferase
EGFR - epidermal growth factor receptor
eTCR - engineered T cell receptor
FDA - American Food and Drug Administration
FLAG tag - DYKDDDDK peptide sequence
GALT - gut-associated lymphoid tissue
GM-CSF – granulocyte-macrophage colony stimulating factor
gRV - gammaretrovirus
GvHD - graft-versus-host disease
hBCMA - human B cell maturation antigen
HER2 - human epidermal growth factor receptor-2
HEVs - High endothelial venules
HLA - human leukocyte antigen
HSC - hematopoietic stem cells
HSV – herpes simplex virus
IC - intracellular
ICS – intracellular cytokine staining
IFN - interferon
IFN-I - type I interferon
IFNAR1 - interferon alpha and beta receptor subunit 1
IL – interleukin
IVIS - In vivo imaging system
KO - knockout
LCMV - lymphocytic choriomeningitis virus
mAb – monoclonal antibody

MAGE-A3 – melanoma-associated antigen A3
mERK - mutated extracellular signal-regulated kinases
MDSCs - myeloid-derived suppressor cells
MFI - mean/median fluorescence intensity
MHC - major histocompatibility complex
MOI - multiplicity of infection
MSCV – murine stem cell virus
ND - non-differentiated
NGFR – nerve growth factor receptor
NIH – U.S. National Institutes of Health
NIS - sodium iodine symporter
OV- oncolytic virus
OVV - Oncolytic virus vaccine
pAPC - professional antigen presenting cell
PBS - phosphate-buffered saline
PD-1 - programmed cell death protein-1
PD-L1 – programmed cell death ligand-1
PFU - plaque-forming unit
PLAT-E – platinum-E
PMA - PHORBOL 12-MYRISTATE 13-ACETATE
PSMA - prostate-specific membrane antigen
RAG2 - Recombination activating gene 2 protein
REP - rapid expansion protocol
RNA - ribonucleic acid
rsLuc - red-shifted firefly luciferase
ScFv - single chain variable fragment
TAA - Tumour-associated antigen
TAMs - tumour associated macrophage
TANs - tumour associated neutrophils
Tcm - T central memory
TCR - T cell receptor
TDLN - tumour-draining lymph nodes
Teff - T effector
Tem - T effector memory
Th1 - T helper 1
Th2 - T helper 2
Th9 - T helper 9
TME - tumour microenvironment
TNF – tumour necrosis factor
Treg - Regulatory T cell
Tscm - T stem cell memory
TIL - tumour-infiltrating lymphocytes
TIL-ACT - adoptive T cell therapy using tumour-infiltrating lymphocyte
TME - tumour microenvironment

TTDR - tumour tissue dissociation reagent
T-VEC - talimogene laherparepvec
UT – untransduced (non-engineered)
VSV - Vesicular stomatitis virus
WT - wild-type

Symbols

α – alpha
β – beta
˚C – degrees Celsius
d – day(s)
δ – delta
Δ - delta
γ – gamma
μ - micro
ζ – zeta
% - percent

Declaration of Academic Achievement

This document was independently authored by Claire Morris, with editorial support from Dr. Jonathan Bramson. The studies described were designed, conducted, and analyzed by Claire Morris with guidance from Dr. Jonathan Bramson. Claire Morris was the primary researcher for all described experiments, with assistance from colleagues and collaborators as outlined below:

- Ricardo Marius, Dr. John Bell, Natasha Kazhdan, and Dr. Brian Lichty helped with preparation of the recombinant VSVΔM51 vaccines used throughout this thesis.
- Cloning of the dual-expression VSV-hBCMAtNGFR/rsLuc constructs in Figure 3.19 was completed by Mira Ishak and me. Preparation of the dual-expression VSV-hBCMAtNGFR/rsLuc viruses was done with technical assistance from Natasha Kazhdan. IVIS imaging and image analysis were performed by Craig Aarts.
- IVIS imaging and image analysis in Figure 3.10 and 3.12 were performed by Chris Baker.
- Mira Ishak assisted with the experiments outlined in Figure 3.10.
- Dr. Rebecca Burchett generated the CMS-5-TR-BCMA and CMS-effLuc cell lines used in this thesis
- Dr. Rebecca Burchett generated the data outlined in Figures 1.1, 1.2, 1.3, 3.14, 3.18A/B, 3.19
- Dr. Rebecca Burchett generated all gRV constructs used in this thesis.
- Dr. Scott Walsh cloned the VSV-mERK and preparation was done by Natasha Kazhdan.
- Dr. Scott Walsh, Lan Chen, Dr. Joanne Hammill, and Christopher Baker assisted with maintenance of the P14-Thy1.1 and DUC18 mouse colonies.
- Experimental schematics and diagrams throughout this thesis were generated using assets from BioRender by Dr. Rebecca Burchett or me.

1 Introduction

1.1 Cancer immunotherapies throughout history

While in 2013, the journal Science declared immunotherapy for the treatment of cancer the "Breakthrough of the Year", the reality is that the idea of the immune system recognizing and destroying malignant cells has existed for hundreds of years[1]. Some of the earliest documentation of an activated immune system resulting in regression of cancer burden comes from ancient Egypt, where there are documented observations of tumourous growths regressing or disappearing after a high febrile episode or infection[2]. Indeed, the synergy between immune activation and cancer regression has been documented for most of history, but it is only in the last century that we have truly began to uncover the power of cancer immunotherapy.

Now known as the "Father of Immunotherapy", William B. Coley observed tumour regression in his sarcoma patients who also contracted erysipelas, a skin infection[3,4]. He began to treat patients with "Coley's mixed toxin", which contained a mixture of live and inactivated *Streptococcus pyogenes* and *Serratia marcescens* and he achieved disease-free survival in many cancers[3]. In the late 1800s, Busch and Fehleisen, independently made similar observations when they also saw co-current infection causing reduced tumour burdens in their patients[2]. While at that point the relationship between the immune system and cancer was not well understood, we can now hypothesize that the inflammatory response due to infection in cancer patients mediated some anti-cancer responses, resulting in the observed regression. Despite these independent findings, Coley's work was widely rejected by the medical community due to the lack of understanding of the treatment's mechanism of action and the risks of infecting patients with pathogenic bacteria[4]. The proposed prospect of using one's immune system to fight malignancies was then neglected until the 20th century.

Cancer immunotherapies did not emerge again until the late 1950s, when E. Donnall Thomas performed bone marrow transplant from healthy donors to leukemia patients[4]. His treatment, now known as hematopoietic stem cell (HSC) transplantation, yielded some success despite patients experiencing severe side effects. Patients first suffered from toxicities due to the preparative high-dose chemotherapy and radiation prior to treatment[5]. If cells had engrafted, patients displayed what is now thought to be graft-versus-host disease (GvHD) due to engrafted allogenic bone marrow cells mounting an immune attack against the host[6]. Later studies in canines in the 1960s revealed the importance of histocompatibility in HSC transplant when marrow grafts from littermates matched for dog leukocyte antigen (DLA) in combination with immunosuppressive agents gave long-term, healthy survival without GvHD. It is now known that these antigens, DLA or human leukocyte antigen (HLA), provoke immune responses when tissues are grafted from a donor to a patient and that genetic control of these antigens resides on the major histocompatibility complex (MHC)[6]. This discovery was also relevant to humans as when sibling donor-recipient pairs were assessed and matched for HLA haplotypes, this led to successful HSC transplantation. Today, bone marrow

transplantation occurs between non-related, HLA matched individuals routinely due to this discovery.

Modern immunotherapies focus on enhancing the immune system to better recognize and target malignancies. A theory of cancer immunosurveillance proposes the idea that the immune system can recognize and destroy the majority of precursor transformed cells, but that the survival of the non-immunogenic, "escaped" cancer cells and homeostatic suppression of the immune system allows for disease development[7,8]. This led researchers to investigate how to overcome this suppression or effectively target these escaping cells. Today, many immunotherapies are utilized alone or in combination with other therapies. These treatments can be based on cellular therapy, eliminating immunosuppression or broad immune activation. A selection of some example cancer immunotherapies that will not be thoroughly discussed throughout this thesis and their proposed mechanisms are represented in Table 1.1

Table 1.1: Examples of modern immunotherapies that are approved in Canada, the cancers they are used to treat and their mechanisms of action

Types of immunotherapies	Examples of therapies (Commercial Names)	Some treated cancers	Proposed mechanisms of action	Reference
Hematopoietic stem cell (HSC) transplant	Bone marrow transplant	Leukemia, lymphoma, multiple myeloma	Re-establishment of immune cells using transfer of healthy allogenic or autologous stem cells	9
Cytokines	IL-2 (Aldesleukin)	Melanoma, renal cell carcinoma	Bulk activation of the immune system	10,11
	Type I Interferons (Intron A, Wellferon)	Melanoma, lymphoma, leukemia		12,13
Checkpoint inhibitors	Anti-PD-1 (Keytruda, Opdivo)	Melanoma, non-small cell lung cancer	Blocks inhibition of lymphocyte activation	12,14
	Anti-PD-L1 (Tecentriq, Imfinzi)	Melanoma, small cell lung cancer		12,15
	Anti-CTLA-4 (Yervoy, Imjudo)	Melanoma, Urothelial carcinoma		12,16
Tumour-antigen targeting monoclonal antibodies	Anti-HER2 (Trastuzumab)	Breast cancer	ADCC, inhibition of growth	5,17
	Anti-CD20 (Rituximab)	Lymphoma, leukemia	ADCC, complement-mediated cytotoxicity (CMC)	12,18
	Anti-EGFR (Cetuximab)	Metastatic colorectal cancer	ADCC, inhibition of growth	19

1.2 Adoptive T cell therapies; using transferred cytotoxic cells in an anti-cancer response

Adoptive cell therapy (ACT) is a personalized "living" cancer treatment which involves the isolation of host lymphocytes and subsequent administration of immune cells that can proliferate *in vivo* and mediate an anti-cancer response[20]. The first demonstration of ACT was the transfer of syngeneic lymphocytes from rodents heavily immunized against a tumour to tumour-bearing recipient rats, which led to tumour growth inhibition[20,21]. T lymphocytes, or T cells were assumed to be predominately responsible for these observations and were later further characterized by Dr. Jacques Miller and Dr. Graham Mitchell as thymic-derived immune cells that react specifically with antigen and are necessary in a normal immune response[22,23].

T cells recognize peptide epitopes, which are derived from degraded proteins and presented on cell surface molecules called major histocompatibility complexes (MHC), using the T cell receptor (TCR). T cells can be categorized into two broad groups depending on whether they express a CD4 or CD8 co-receptor[22]. CD4+ T cells recognize antigen epitopes in the context of MHC class II molecules and can direct the adaptive arm of the immune system by producing chemotactic, pro-inflammatory or immunoprotective cytokines[24]. CD8+ T cells, which have been the focus of ACT for many years due to their direct cytotoxic capacity, recognize antigen epitopes in the context of MHC class I molecules[22]. The TCR is a cell surface protein complex on T cells that recognizes antigens through MHC:TCR interactions[25]. The TCR complex itself is comprised of diverse single α- and β-glycoprotein chains and rare T cell populations harbour γ- and δ-chains[26]. Naïve T cell priming requires antigen stimulation through the TCR via MHC and a co-stimulatory signal, exemplified by the protein, CD28[27]. Following T cell activation, differentiation and elimination of a pathogen, the majority of effector T cells (T_{eff}) die and leave behind a heterogeneous pool of memory T cells. Formation of memory T cells allows for experienced T cells to be recalled upon re-exposure to the same antigen and improve immune efficacy, leading to no or subclinical symptoms of maladies[28]. Conversely, exposure to high level, persistent antigen can lead to T cell exhaustion, which leads to dysfunction[29].

Clinical trials using ACT have shown some positive results in the treatment of solid tumours that are resistant to other therapies[30]. In one clinical trial, 20% of metastatic melanoma patients that had prior systemic treatment with no observable benefit, were treated with ACT of autologous tumour-infiltrating lymphocytes (TIL) and experienced complete regression without reoccurrence for up to 5 years[31]. In another Phase I clinical trial, 80% of hepatocellular carcinoma patients treated with ACT of TIL had no evidence of disease after 14 months[32]. The efficacy of ACT in solid and liquid cancers often can depend on the persistence of adoptively transferred T cells as the long-lasting tumour-specific memory CD8+ T cells are thought to prevent recurrent malignancies[33].

1.3 Adoptive cell transfer of tumour infiltrating lymphocytes (TIL)

One of the first methods of ACT utilized immune cells that were isolated from tumours, later named TIL. Following isolation, these immune cells are cultured with high levels of IL-2, tested for tumour recognition and tumour reactive cultures are then expanded *in vitro* before being infused back into the patient[20]. The first study utilizing TIL as a cell product for ACT (TIL-ACT) in cancer immunotherapy against metastatic melanoma occurred in 1988 and combined TIL-ACT, cyclophosphamide and IL-2[34]. Rosenberg et al. demonstrated that the combination therapy could achieve cancer regression in 60% of patients who had not had prior IL-2 treatments and in 40% of patients who had failed IL-2 treatments[34].

Since then, many clinical trials of TIL-ACT have emerged with mixed success in treating melanoma and TIL-expansion methods have expanded to other cancers, including non-small cell lung cancer, pancreatic cancer and glioma[35,36,37]. In February of this year, the FDA approved the first TIL therapy for patients with unresectable or metastatic melanoma[38]. At present, effective TIL therapy requires intensive lymphodepletion and high doses of systemic IL-2 to achieve anti-tumour effects. Lymphodepletion creates a niche for transferred T cells to reside in and can give these cells an advantage by eliminating regulatory cells and competing cell populations as well as enhancing the availability of vital cytokines[39]. IL-2 is administered systemically to support the transferred cells[40]. Unfortunately, intensive lymphodepletion can result in neurotoxicity, neutropenia, anemia, and a greater risk of infection[39]. In addition, high dose IL-2 has shown severe toxicities to patients[40].

One of the most attractive features of TIL-ACT is the potential to overcome heterogeneity in tumour antigen expression. TIL have the capacity to recognize multiple tumour antigens[41]. Immune profiling has revealed that most tumours that have identifiable TIL populations have a T cell population capable of recognizing neoantigens[42]. It is thought that the anti-tumour activity of TIL is due to this ability to recognize tumour associated antigens (TAAs) that emerge from genetic mutations that are characteristic of cancer. It has been demonstrated in clinical studies of TIL-ACT, that T cell recognition of cancer-driven mutations can mediate clinical responses in patients. In a study investigating a cohort of 75 patients with gastrointestinal cancers, 83% of patients had neoantigen-reactive TIL[42]. Of the 124 total TIL populations found, only one neoantigen was recognized by more than one population, indicating a broad immune response to each unique antigen that is utilized in TIL therapy[42].

In the initial expansion of TIL, tumour fragments are placed in IL-2 supplemented media until lymphocytes grow out and eliminate tumour tissue[43]. Following this, the cells advance to the rapid expansion protocol (REP) where these young TIL are largely expanded using IL-2, anti-CD3 antibodies and allogenic feeder cells[44,45]. In TIL therapy, it is thought that less differentiated T cells are more effective in generating a robust and prolonged response[46]. In fact, melanoma patients treated with TIL were more responsive to TIL-ACT when the infusion product contained T cells with elongated telomeres and high levels of CD27 expression, a marker for less differentiated cells[31]. TIL with shorter telomere, which has shown to be proportional with time in culture, have been associated with reduced clinical responses and *in vivo* persistence[47]. Infusing patients with TIL

containing CD8+CD27+ cells and longer average telomeres can both be associated with reduced differentiation, enhanced proliferative capacity and *in vivo* persistence[31]. Through the intensive expansion process used to generate the number of cells necessary for successful TIL-ACT, CD8+ T cells often terminally differentiate into T_{EFF} cells. These T_{EFF} cells can demonstrate less CD28 and CD27 expression and shorter telomere length when compared to T_{CM} cells, which are less differentiated and considered more functional cells for long-lasting treatment[31,48]. Unfortunately, these standard TIL *in vitro* expansion methods tend to promote T cell differentiation and functional exhaustion. This is attributed to extended culture in high concentrations of IL-2, which is known to promote CD8+ T cell terminal effector differentiation[49]. Minimal culture of any T cell product, TIL included, can evade this terminal differentiation, and maintain a proliferative, Tcm phenotype.

1.4 Adoptive cell transfer of chimeric antigen receptor (CAR) T cells

Introducing a synthetic receptor into T cells proved revolutionary for cancer cell therapies. Canonical T cell stimulation relies on TCR recognition of MHC-presented antigens. Alternatively, chimeric antigen receptors (CARs) can be engineered to recognize any surface antigen with high affinity, independent of MHC. Second generation CAR constructs, which are considered the most mature generation clinically, are composed of three domains; an extracellular single-chain variable fragment (scFv), a transmembrane spacer, and an intracellular co-stimulatory signaling domain followed by the intracellular region of CD3 ζ[50,51]. The additional co-stimulatory signalling domain of the second-generation CAR can consist of 4-1BB or CD28, to induce T cell expansion and longer persistence[51]. The scFv is composed of variable light (V_L) and variable heavy (V_H) regions of a monoclonal antibody against target tumour antigens[52]. The spacer/hinge domain connects the scFv to the transmembrane region, allowing the scFv domain to bind its specific antigen due to the hinge's flexibility[50,53]. When the scFv portion recognizes and binds to a tumour antigen, the intracellular 4-1BB or CD28 co-stimulatory domain, along with CD3ζ, signals to the downstream intracellular pathway[54]. Subsequently, activated T cells release perforin, which creates pores in the tumour cell membranes, allowing cytotoxins and granzyme B to enter and activate the apoptosis-related caspase cascades, initiating cell death[50].

The first B cell leukemia patients received CD19-targeted CAR T cells in 2006 and exhibited robust and long-lasting responses[55]. Several clinical trials directing CAR T cells toward hematological cancers followed this until the eventual approval of CD19-CAR T cell treatment for adult acute lymphoblastic leukemia (ALL) in 2017[50,56]. Following this success in treating hematological malignancies, CAR T cell therapies began expanding to solid tumours, but treatment efficacy has been difficult to achieve.

Using personalized tumour-antigen identification is an attractive approach to ACT as it has been very successful in treating leukemias in which all malignant cells express CD19, however solid tumours rarely express a singular antigen. In addition, the loss, or downregulation of a targeted antigen on tumour cells is common[57]. Some solid tumours do have identified TAAs, where TAAs can be highly expressed on tumour tissue, but these antigens are also expressed at low levels on normal tissue[57]. This can result in on-

target off-tumour toxicity. An example of this occurred in a colon cancer patient, in which this on-target off-tumour toxicity resulted in death 5-days following HER2CAR T cell therapy as low levels of HER2 on the lungs were targeted by CAR T cells[58].
Many challenges for CAR T cells in the treatment of cancers can also arise from the tumour microenvironment (TME). The TME can implement physical and chemotactic barriers to promote T cell exclusion. Cancer-associated fibroblasts and abnormal vasculature limit the ability of transferred cells to traffic to the tumour through formation of dense extracellular matrices[59]. High endothelial venules (HEVs) are hypothesized to be critical for T cell infiltration and have been associated with tumour regressions in some cancers, but these blood vessels can be distorted and immature in many solid tumours[60]. Chemokines are also important in promoting T cell homing and the dysfunctional HEVs can also inhibit the chemotactic-dependent migration of T cells to the tumour[57]. Even once trafficked to the tumour, the TME relies on immunosuppressive cells such as myeloid-derived suppressor cells (MDSCs), tumour associated macrophages (TAMs), tumour associated neutrophils (TANs) and regulatory T cells (Tregs) to manufacture a hostile environment for T cells[61]. These immunosuppressive cells can secrete soluble factors which can contribute to abnormal tumour vasculature formation and promote anti-inflammatory polarization of TAMs, which can produce reactive oxygen species that both indirectly and directly suppress T cells[62]. Immunosuppressive cells in the TME can also contribute to T cell exhaustion and dysfunction, which can limit the efficacy of transferred CAR T cells in solid tumours.

Another important factor of CAR T cell efficacy is the proportion of CD4+ and CD8+ T cells in the product. CD4+ T cells can provide indirect and direct “help” to developing CD8+ T cells by licensing dendritic cells to improve antigen presentation, stimulating naive CD8+ T cells, and producing pro-survival cytokines to maintain the CD8+ effector pool[63]. Furthermore, differentiated CD4+ T cells can produce inflammatory cytokines that polarize macrophages and indirectly contribute immunostimulation to CD8+ T cells[63]. Some reports indicate that while CD4+ CAR T cells may be beneficial, as they increase CD8+ CAR T cell expansion and are crucial for long-term responses, they also heavily contribute to severe toxicities, through eliciting and exacerbating cytokine release syndrome (CRS)[64,65]. Conversely, engineering CAR T cells from defined CD4+ and CD8+ subsets and transferring equivalent numbers of CD4+ and CD8+ T cells can confer synergistic anti-tumour activity in both human and murine studies[66,67]. In addition, the persistence of CD4+ CAR T cells in two patients who received CD19-CAR T cells for chronic lymphocytic leukemia (CLL) for greater than 10 years has also recently been reported, indicating that CD4+ T cells have increased tolerance of repeated stimulation without functional exhaustion[68]. In unedited T cells, without CD4+ T cell help, CD8+ T cells can demonstrate a “helpless” phenotype, resulting in reduced expansion, exhaustion, tumour necrosis factor-related apoptosis-inducing ligand (TRAIL)-mediated apoptosis and poor long-term memory formation[69,70,71,72]. This observation has been observed in unengineered T cells, where CD4+ T cells indirectly prime CD8+ T cells through APCs’ MHC-TCR interactions[72]. Engagement of APCs by CD4+ T cells during CD8+ T cell activation leads to licensing and subsequent production of IL-12 and IL-15. These cytokines can promote CD8+ T cell

polyfunctionality, memory formation, and persistence[73]. In the context of CAR T cells, CAR-antigen engagement may occur in an immunological environment that is spatially or temporally separated from MHC-dependent CD4+ T cell assistance. This may cause the "helpless" CD8+ T cell phenotype and subsequent dysfunction if CD4+ T cells are not also engaged. Indeed, CD4+ CAR T cells do seem to be required for optimal anti-cancer effects, despite their association with serious toxicities such as CRS, in some instances.

1.5 Viral immunotherapy using oncolytic viruses

Oncolytic viruses (OVs) have the unique capacity to selectively infect and replicate in transformed cells while leaving healthy cells unaffected. In 2015, the first OV was approved for the treatment of advanced melanoma. The OV, named T-VEC is a herpes simplex virus 1 (HSV-1) expressing granulocyte-macrophage colony-stimulating factor (GM-CSF). The virus was designed to selectively replicate within tumours and produce GM-CSF to augment systemic anti-tumour responses[74]. Beyond direct lysis, OVs can also arouse a broad immune event, through the release of TAAs during lysis, promoting immune infiltration, improving recognition and cytotoxic capacity of immune cells and dampening the immunosuppressive TME[75]. This allows OVs to be regarded as a multi-pronged therapy, as they can eliminate tumours through multiple direct and in-direct methods.

Vesicular stomatitis virus (VSV) is an enveloped negative sense RNA virus from the Rhabdovirus family, that has a low seroprevalence in humans[76]. Wildtype VSV (WT-VSV) is sensitive to type I IFN signalling as it inhibits WT-VSV replication. As transformed cells often have dysfunctional type I IFN signalling, VSV preferentially replicates in cancer cells, giving it oncoselectivity[77]. However, this inherent oncoselectivity of WT-VSV is not sufficient, as one function of its VSV matrix (M) protein is to inhibit type I IFN signalling[78]. When intact, this function of the M protein causes WT-VSV to exhibit neurotoxicity in rodents and severe neurological disease in nonhuman primates[79,80]. VSV-ΔM51, a VSV-mutant that contains a deletion of the methionine at amino acid position 51 of the VSV M protein, is a safer alternative as it induces a strong interferon response upon infection but cannot replicate in healthy cells[81]. VSV-ΔM51 is unable to inhibit antiviral responses, which causes the lack of replication in healthy cells. This is because the intact anti-viral interferon response in healthy cells ensure they are protected from VSV-ΔM51 replication. The defects in interferon signalling in transformed cells allows for the selective infection, replication and lysis of transformed cells[77]. This mutation increases the therapeutic index of VSV-ΔM51. VSV-ΔM51 has also been shown to abortively infect healthy cells, allowing the virus to enter and present viral antigens on cell surfaces upon infection without pathogenesis[82].

VSV-IFNβ is another variant of WT-VSV that has been edited to increase safety. VSV-IFNβ has been engineered to express IFNβ to stimulate an innate immune response in normal cells but not in type I IFN defective cells and has been shown to stimulate anti-tumour immunity[83]. VSV-IFNβ has also shown no signs of neurotoxicity in rhesus macaques[84]. This promoted multiple VSV-IFNβ based therapies, with the inclusion of a thyroidal sodium iodide symporter (NIS) that permits *in vivo* trackability (VSV-IFNβ-NIS), be evaluated clinically[85,86,87]. A 2022 report on a trial treating patients with T cell

lymphoma showed that VSV-IFNβ-NIS had single-agent activity and treatment gave durable disease remissions[88]. Since then, additional arms have been added to the clinical trial to investigate using VSV-IFNβ-NIS in combination with other immunomodulatory drugs, which may yield interesting results.

1.6 Rhabdovirus vaccines as a boosting agent

The ability of VSV-ΔM51 to abortively infect healthy cells and its small genome make it an attractive OV for wider uses beyond lysis of tumour cells[82,89]. Indeed, our group has previously found ΔM51-VSV to be an efficient gene-delivery vector with the ability to aid in DC maturation[90]. These matured DCs previously infected with VSV-ΔM51 encoding a tumour-associated antigen mediated significant control of tumour growth by engaging both NK and CD8+ T cells in tumour-bearing mice[90].

Our group has further investigated using VSV-ΔM51 as a vaccine in a heterologous prime-boost vaccination. In this prime-boost vaccination, two different viral vectors, adenovirus and VSV-ΔM51, encoding a common TAA are delivered sequentially to minimize an anti-vector response and maximize the T cell response[91,92,93,94]. In these prime-boost vaccination studies, we have used an adenovirus vector to "prime" the endogenous T cell population against the encoded TAA and generate antigen specific memory T cells. The "boost" can then be provided by VSV, to expand this memory T cell population and further initiate an anti-tumour response. Notably, this prime-boost mechanism, improved tumour control and survival when compared to each vaccine independently.

Our group also investigated the use of VSV-ΔM51 as a potential vector to boost adoptively transferred tumour-specific T cells upon vaccination[94,95,96]. In combination with VSV-ΔM51, using central memory T cells (T_{cm}) ($CD62L^{hi}$ $CD44^{hi}$) is advantageous due to the increased proliferative capacity and anti-tumour effects they demonstrate when compared to effector T cells[96,97]. The transfer of minimal T_{cm} cells allows for *in vivo* expansion of transferred cells upon interaction with the VSV-ΔM51-encoded antigen. In addition, VSV-ΔM51 has previously shown a tropism for infecting professional antigen presenting cells (pAPCs)[97]. To allow for the interaction of transferred T cells with the VSV-ΔM51-encoded antigen, T_{cm} cells must traffic to lymphoid follicles, which effector T cells cannot do[97]. In syngeneic mouse models, tumour-specific T_{cm} cells from TCR transgenic mice were infused into tumour bearing recipient mice and boosted with engineered-VSV-ΔM51 expressing a tumour antigen. Combining ACT of tumour-specific T_{cm} cells with known TCR specificity and VSV-ΔM51 vaccination showed complete and durable tumour regression. Neither the T cells nor VSV-ΔM51 alone could achieve tumour clearance, showing the benefit of combining the two agents. Importantly, unlike methods of ACT previously discussed in this thesis, neither lymphodepletion nor exogenous IL-2 was necessary for successful engraftment, expansion, and anti-tumour function of the transferred cells in immunocompetent animals. If these characteristics of the OV vaccine (OVV) are confirmed in human trials, they could be transformative.

However, there are still challenges to translating this therapy to clinical use. Primarily, in this tumour model, the TAA was known and singularly targeted, which is not practical in a clinical setting where solid tumours vary between patients, necessitating the

engineering of a personalized recombinant vaccine for each patient. Additionally, antigen expression within a solid tumour is heterogeneous, and in experiments where tumours relapsed, antigen loss was identified as the cause[94,95].

1.7 Using a synthetic receptor as a boosting agent

Our lab is investigating a combination approach that pairs a chimeric antigen receptor (CAR) with a cancer vaccine, aiming for a universal vaccination-mediated T cell boost. In this system, a universal boosting vaccine can be engineered to express any antigen, which eliminates the need for a personalized recombinant vaccine for each patient. This engineered vaccine can be matched with a CAR that recognizes this antigen and can expand upon interaction. Within the CAR/OVV boosting strategy, the CAR can be engineered into any T cell product, including multi-specific tumour-targeted T cell populations, such as TIL. This approach could eliminate the need to manufacture large numbers of cells for effective treatment and minimize *in vitro* differentiation. By transferring fewer CAR T cells into a recipient, expansion and T cell differentiation can occur *in vivo* following vaccination and interaction with the engineered viral transgene[98]. Importantly, others have shown that the combination of CAR T cells with CAR-targeted lipid- or RNA-based vaccines enhanced *in vivo* expansion and persistence of CAR-T cells, demonstrating that CARs can effectively function as boosting receptors[99,100,101] . Previous literature has also demonstrated that CAR expression does not affect TCR function and that engineered CAR T cells can expand following exposure and re-exposure to viral antigens[102,103]. We aim to leverage this dual CAR and TCR functionality in a novel way: the adoptively transferred CAR T cells possess boosting antigen specificity through the CAR and tumour specificity via the TCR.

To date, only one model has been assessed in this boosting CAR system. P14 transgenic mice were designed to have a TCR reservoir of CD8+ T cells that exclusively recognize the lymphocytic choriomeningitis virus (LCMV) glycoprotein gp33 as they are on a RAG2 KO and C57BL/6 background[104]. These CD8+ T cells from P14 mice target the gp33 peptide engineered into the murine melanoma cell line, B16-F10-gp33, allowing for the assessment of the TCR driven anti-tumour response. For our boosting CAR, we chose to use the second-generation CAR starting scaffold that has been validated and previously published by our group[105,106] targeting human BCMA (hBCMA-CAR) as the boosting antigen. The matched vaccine in our boosting system is recombinant VSV-ΔM51 which has been engineered to express truncated human BCMA (VSV-hBCMA), as it allows for evaluation of this treatment in a syngeneic murine model, where the CAR does not react with murine BCMA. VSV is also advantageous as its tropism for APCs in secondary lymphoid organs allows for the CAR T cells to engage with their antigen in a supportive setting[97]. Using a completely syngeneic model allows for the assessment of the endogenous immune system response following T cell transfer and vaccination.

Preliminary data in a proof-of-concept study in our lab has indicated that a vaccine-mediated CAR-T cell boost is possible. To achieve this, we adoptively transferred P14 TCR-transgenic BCMACAR T cells in B16.F10-gp33 tumour bearing C57BL/6 hosts. 24 hours following this adoptive T cell transfer, we vaccinate hosts with our VSV-hBCMA. We assess for presence of the T cells in the peripheral blood 5 days following

vaccination to monitor expansion and again 12 days following vaccination to monitor T cell persistence. Within the P14/B16.F10-gp33 model, we have seen that CAR-mediated boosting is possible and markedly expands transferred T cell populations *in vivo*. In response to this combination treatment, we have also seen complete tumour regression. Despite the initial T cell expansion and anti-tumour effects, we fail to observe persistence of our transferred T cells to 12 days following vaccination and tumours consistently relapse (Figure 1.1)

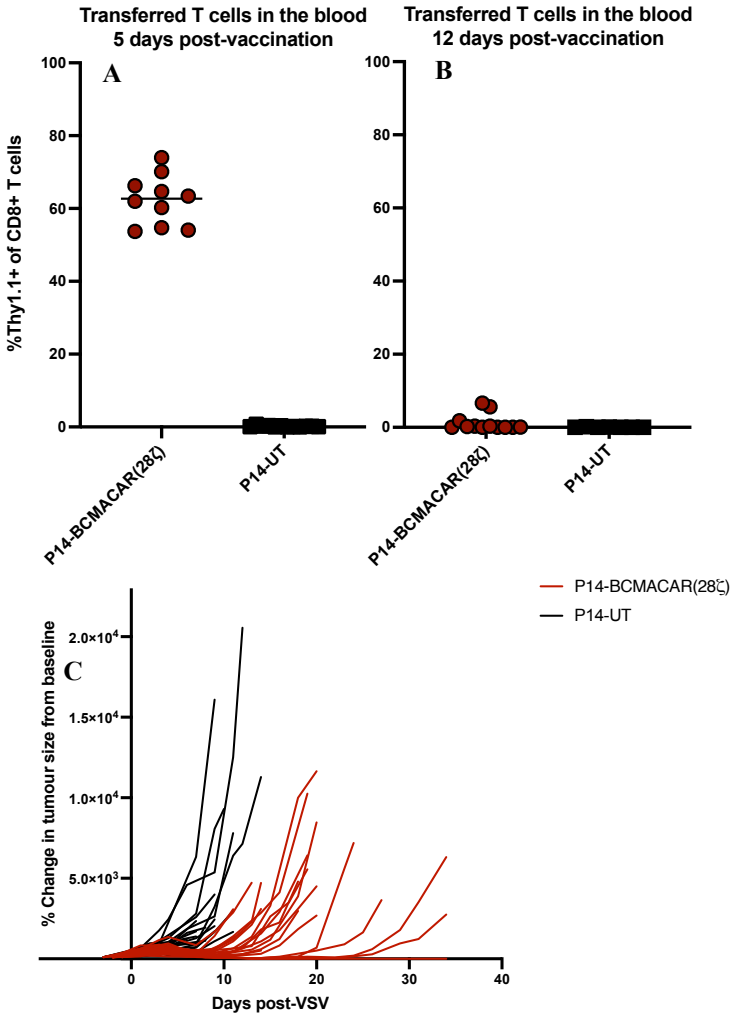

Figure 1.1: P14 CAR-T cells can be boosted by VSV-hBCMA upon vaccination, expand in the periphery and clear B16-F10-gp33 tumour burdens but fail to persist and tumours relapse. 1x106 cryopreserved P14 BCMACAR-T cells or P14 UT T cells were administered intravenously 7 days after 1e5 B16-F10-gp33 tumours were implanted in 6-8 w.o. C57BL/6 recipients. 24 hours after ACT, 2x108 PFU of rVSV-hBCMA was administered intravenously. (A) 5 and (B) 12 days after vaccination, non-terminal bleeds were collected from the facial vein of each mouse. Following ACK lysis to remove erythrocytes, cells were stained with a fixable viability dye and αCD8, αCD4, αThy1.1, and αCAR antibodies for quantification of cell populations by flow cytometry. Plots represent the percentage of total CD8+ T cells in peripheral blood that express the congenic marker, Thy1.1, in each C57BL/6 recipient post-boost. (C) Tumour volume was monitored by manual caliper measurement every 2-3 days for the duration of the experiment. Figure adapted from Rebecca Burchett.

Our group has also observed (Figure), as well as others, that intact type I interferon (IFN) signalling can be detrimental to transferred CAR T cell function and can confer autoimmune toxicities[107,108,109]. We concluded that transiently blocking the type I IFN response prior to vaccination was necessary to maximize the magnitude of the boost and anti-tumour function of transferred T cells. Robust boosting through the CAR is observed when type I IFN signalling is transiently blocked in this model, leading to temporary tumour regression, but since the transferred T cells still fail to persist, eventual tumour relapse is consistently observed (Figure 1.2).

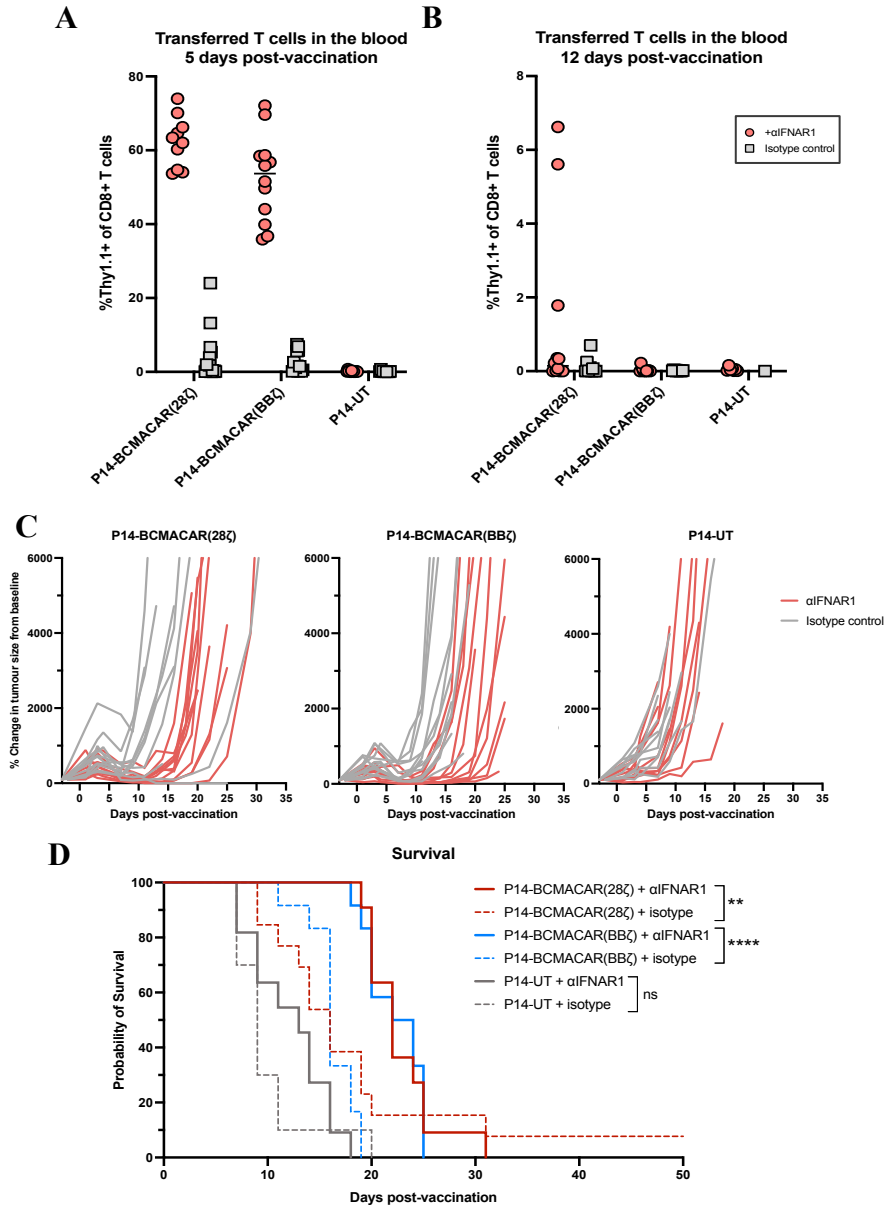

Figure 1.2: Transiently blocking type I IFN signaling during vaccination enhances transferred CAR-T cell expansion and efficacy in the P14/B16.F10-gp33 model. $1x10^6$ cryopreserved P14 BCMACAR-T cells or UT P14 T cells were administered intravenously 7 days after 1e5 B16-F10-gp33 tumours were implanted in 6-8 w.o. C57BL/6 recipients. 16-22 hours prior to OVV, mice were given αIFNAR1 blocking antibody or isotype control antibody intraperitoneally. 24 hours after ACT, $2x10^8$ PFU of rVSV-hBCMA was administered intravenously. (A) 5 and (B) 12 days after vaccination, non-terminal bleeds were collected from the facial vein of each mouse. Following ACK lysis to remove erythrocytes, cells were stained with a fixable viability dye and αCD8, αCD4, αThy1.1, and αCAR antibodies for quantification of cell populations by flow cytometry. Plots represent the percentage of total CD8+ T cells in peripheral blood that express the congenic marker, Thy1.1, in each C57BL/6 recipient post-boost. (C) Tumour volume was monitored by manual caliper measurement every 2-3 days for the duration of the experiment. Figure adapted from Rebecca Burchett.

1.8 Further investigating CARs for a universal oncolytic virus boost

In this thesis, we first assess the feasibility of isolating and engineering TIL and other naturally occurring tumour specific T cells with a CAR. This would allow a polyclonal T cell population to be expanded *in vivo* following vaccination when the CAR interacts with the engineered transgene. This expanded TIL population can then target multiple TAAs with native TCRs. We test the cytotoxic capacity of the TIL and evaluate their ability to be expanded when stimulated through their CAR. Using TIL can exploit the existing multi-specific T cell population to target multiple tumour antigens without prior knowledge of TCR specificity. Others have engineered isolated TIL with CARs[110,111,112], indicating the feasibility of engineering TIL.

Next, we will further investigate vaccination-driven expansion of an adoptively transferred T cell population through the CAR in the context of DUC18 transgenic T cells. DUC18 mice are transgenic mice from a BALB/C background with rearranged Vα10.1 and Vβ8.3 genes to produce a T cell receptor restricted by H-2K^d and specific for the tumour-expressing mutated ERK2 (mERK2) peptide, present on the methylcholanthrene-induced immunogenic fibrosarcoma, CMS-5[113]. A single-base pair mutation that translates to an amino acid substitution distinguishes the mERK2 from the wild-type ERK2 gene, but this difference is sufficient to form a unique tumour-rejection antigen. Unlike P14 transgenic mice that have only CD8+ T cells which all express the transgenic TCR, DUC18 transgenic mice possess both CD4+ and CD8+ T cells and only 35%–50% of the CD8+ T cells are specific for the mERK peptide[113]. Preliminary experiments in the DUC18/CMS-5 model showed no expansion of transferred CAR DUC18 T cells upon VSV-HBCMA vaccination and no anti-tumour effects (Figure 1.3). For this reason, in this thesis we aimed to investigate the reasons behind the striking differences observed in this TCR transgenic model and to further expand our understanding of the biology of VSV vaccination-mediated expansion of CAR T cells in both models.

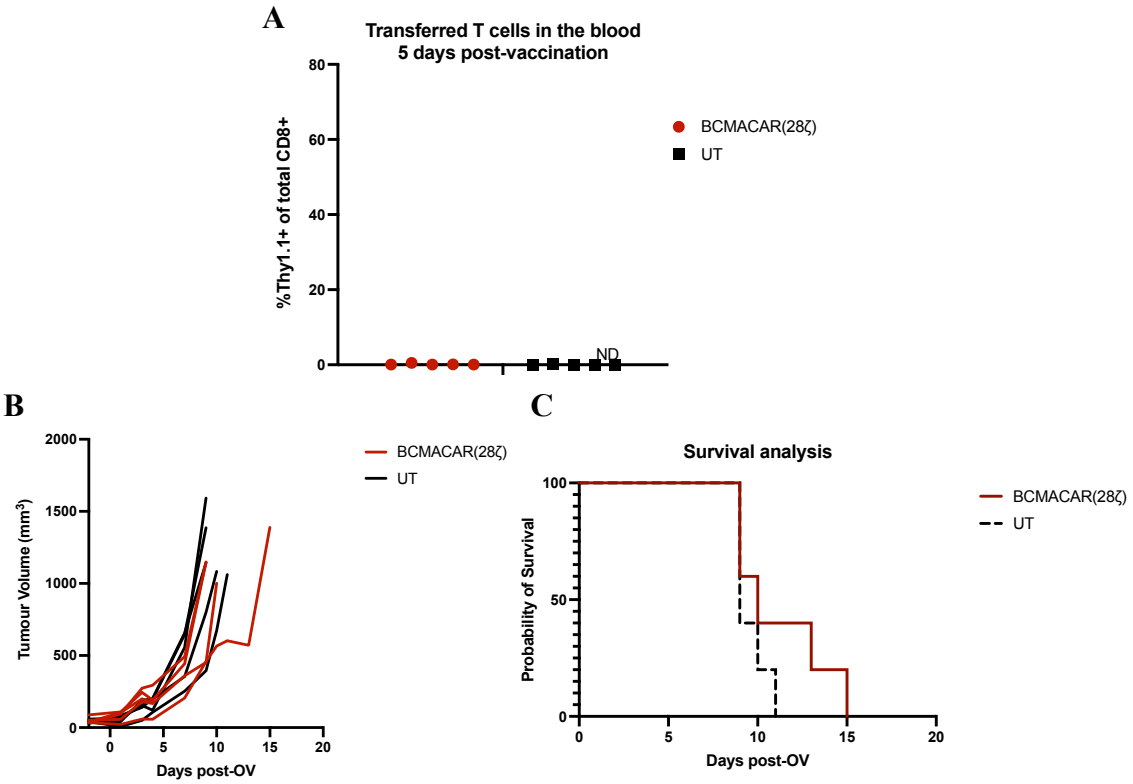

Figure 1.3: DUC18 BCMACAR-T cells are not boosted by VSV-hBCMA upon vaccination and do not control tumour growth. 1x106 cryopreserved DUC BCMACAR-T cells or DUC18 UT T cells were administered intravenously 0.5 mg of αIFNAR1 blocking antibody was delivered intraperitoneally 7 days after 1e6 CMS-5 tumours were implanted in 6-8 w.o. BALB/C recipients. 24 hours after ACT, 2x108 PFU of rVSV-HBCMA was administered intravenously. (A) 5 and (B) 12 days after vaccination, non-terminal bleeds were collected from the facial vein of each mouse. Following ACK lysis to remove erythrocytes, cells were stained with a fixable viability dye and αCD8, αCD4, αThy1.1, and αCAR antibodies for quantification of cell populations by flow cytometry. Plots represent the percentage of total CD8+ T cells in peripheral blood that express the congenic marker, Thy1.1, in each BALB/C recipient post-boost. (C) Tumour volume was monitored by manual caliper measurement every 2-3 days for the duration of the experiment. Figure adapted from Rebecca Burchett.

1.9 Thesis scope and content

The objective of this MSc thesis research was to further evaluate a novel strategy for vaccine-boosting adoptively transferred tumour-specific T cells using an engineered synthetic receptor and a paired oncolytic vaccine vector. This research builds on previous findings from the Bramson and Wan labs, which described and characterized the unique interaction between endogenous or adoptively transferred memory T cells and oncolytic vaccines expressing a cognate tumour-associated antigen.

1.9.1 Research objectives

By building on the success of OV vaccines in enhancing tumour-specific T cell responses, this thesis broadly aims to further evaluate a universal method for expanding

adoptive T cell therapies for cancer. This research can be divided into three research objectives, which are detailed in Chapter 3.

- **Objective 1:** Investigate the use of naturally occurring tumour-specific T cells as a T cell product in our universal T cell boosting method. Optimize the isolation and culture of tumour-specific T cells from TIL and tumour draining lymph nodes and assess their functionality.
- **Objective 2:** To extend the horizons of the vaccination-based CAR T cell boosting, we aim to replicate the proof-of-concept data we have observed in the P14/B16-F10gp33 model in the DUC18/CMS-5 model, another syngeneic model.
- **Objective 3:** Elucidate the immunological mechanisms involved in effective OV vaccine boosting and durable anti-tumour T cell function within the P14/B16.F10-gp33 model.

2 Materials and Methods

Mice and Mouse Models. C57BL/6, BALB/c and B6 albino mice (B6N-Tyr$^{c\text{-}Brd}$/BrdCrCrl) mice were purchased from Charles River Laboratories. DUC18 mice were kindly provided by Dr. Lyse Norian (University of Iowa). The P14-Thy1.1 strain was generated in-house by Dr. Scott Walsh by crossbreeding P14 mice (B6.Cg-Tcratm1Mom Tg(TcrLCMV)327Sdz; purchased from Taconic Laboratories, MMRRC stock #37394) onto a homozygous Thy1.1+/+ background (B6.PL-Thy1a/CyJ; purchased from Charles River Laboratories). Mice were housed under controlled lighting (12:12 L:D) and temperature (22°C) with ad libitum access to a low-fat irradiated chow diet containing 18.6% protein, 6.2% fat, and 3.5% fibre (2918, Tekland Global Diets) and water in specific pathogen-free conditions in the Central Animal Facility at McMaster University. All animal studies were conducted in compliance with the Canadian Council on Animal Care guidelines and were approved by McMaster University's Animal Research Ethics Board.

CAR retroviral vectors. The starting scaffold for all murine CAR vectors used in this thesis was generated in the Bramson lab and has been previously described[105,106]. The CAR sequence was cloned into an MSCV-based gammaretrovirus vector, pRV2011-oFL, originally provided to us by Dr. Brian Rabinovich (MD Anderson Cancer Center; Houston, Texas). Either traditional restriction and insertion cloning and NEBuilder® HiFi DNA Assembly cloning techniques were used to generate all pRV2011 constructs outlined in Table 2.1. Sanger sequencing was performed to validate the correct sequence and integration of each transgene.

Table 2.1: Constructs and transgenes used in this thesis.

Construct name	First transgene	Signalling Domain	Tag	Second transgene	Notes
BCMACAR(FLAG)-28ζ	BCMACAR	CD28/ CD3ζ	FLAG	N/A	Construct previously generated in Bramson Lab (105,106)
BCMACAR(FLAG)-BBζ-TRAF1/3mut	BCMACAR	murine CD137 domain TRAF1/3 mutant/murine CD3ζ	FLAG	N/A	
BCMACAR(FLAG)-28ζ_ mIL-15	BCMACAR	CD28/ CD3ζ	FLAG	native murine IL-15	
Red-shifted firefly luciferase (rsLuc) (Ppy- RE9)	BCMACAR	N/A	N/A	N/A	

Ecotropic gammaretrovirus production. Platinum-E (Plat-E) cells were thawed into DMEM media containing 8.90% heat inactivated fetal bovine serum (Gibco), 8.90 mM HEPES, 1.78 mM L-Glutamine, 89 ug/mL Normocin, 8.9 ug/mL Blasticidin, 0.89 ug/mL Puromycin (Invivogen; Cat#ant-pr-1), cultured at 37℃ and 5% CO_2 until confluent and split as needed. The day before transfection, the cell monolayer was washed with phosphate buffered saline (PBS), lifted from flask with 1x Trypsin. Cells were counted using trypan blue on the Thermo Scientific Invitrogen Countess II, plated at $6x10^6$ cells in a final volume of 10 mL transfection media (DMEM media containing 8.90% heat inactivated fetal bovine serum, 8.90 mM HEPES, 1.78 mM L-Glutamine and 89 ug/mL Normocin) in each T-75 flask and cultured at 37℃ and 5% CO_2 overnight. For each transfection, 10 μg of both the construct and packaging plasmid were diluted into Gibco Opti-MEM™ (Gibco; Cat#31985-070). 45 μL of Lipofectamine™ 2000 (Thermo Fisher Scientific; Cat#11668-019) was also diluted in 2.25 mL of Gibco Opti-MEM™ and incubated for 5 minutes at room temperature. The two Gibco Opti-MEM™ mixtures were then combined and incubated for 20 minutes at room temperature. The Gibco Opti-MEM™ mixtures were then added to the side of each flask containing PLAT-E cells and rocked to mix before being incubated overnight at 37℃ and 5% CO_2. 16-20 hours post-transfection media was aspirated off the transfected PLAT-E cells and replaced with 10 mL fresh transfection media before being incubated for 24 hours at 37℃ and 5% CO_2. 24

hours after the media change Amicon® Ultra 100K centrifugal filters (Cat#UFC910024) were washed with cold, sterile PBS and centrifuged at 2100xg at 4℃ for 5-8 minutes until all PBS has passed through the filter. The viral supernatant was collected from the flasks and filtered through a 0.45 μm syringe filters and then kept on ice after filtration. Filtered supernatants are then loaded into the Amicon® Ultra 100K centrifugal filters and centrifuged at 2100xg at 4℃ for 15 minutes. To concentrate the virus 20x, for each 10 mL of viral supernatant 500 μL of concentrated virus was collected. The concentrated viral supernatant was then transferred to a sterile Eppendorf tube, mixed well, aliquoted and stored at -80℃ until required.

Retroviral transduction and culture of murine T cells. The day before T cells were activated, the number of wells required for culture in a 24-well plate were coated with an αCD3e antibody (Clone 145-2C1, BioXCell; Cat# BE0001-1) diluted in PBS. The day of activation, a spleen (or TDLN) was acquired from the desired mouse source after euthanasia according to AUP 22-11-35 and kept in 10 mL T cell media (RPMI media containing 8.76 % heat inactivated fetal bovine serum, 8.69 mM HEPES, 0.87x non-essential amino acids [Gibco], 87 U/mL penicillin+87 U/mL streptomycin [Gibco], 0.87 mM sodium pyruvate and 1.78 mM L-GlutaMax [ThermoFisher; Cat# 35050061]) on ice during transport to a biological safety cabinet. Cells were isolated by grinding pieces of the spleen between two sterile glass microscope slides and filtering through a 40 μm cell strainer (Fisher Scientific; Cat#08-771-1). Cells were centrifuged at 500xg for 5 minutes at room temperature and resuspended in 5 mL of Gibco™ ACK Lysing Buffer (Cat#A1049201) for 5 minutes, in the dark at room temperature to lyse red blood cells. The reaction was quenched with 45 mL PBS and centrifuged at 500xg for 5 minutes at room temperature. The cells were resuspended in T cell media and filtered through a 40 μm cell strainer before being counted using AOPI dye and Cellometer Auto 2000 Cell Viability Counter. The required number of cells were plated in the pre-coated wells at $3x10^6$ cells per well in T cell media supplemented with 10 ng/mL IL-7 (Peprotech; Cat#200-07) or other required cytokines and an αCD28 antibody (Clone 37.51, BioXCell; Cat# BE0015-1) and incubated for 24 hours at 37℃ and 5% CO_2. If DUC18 splenocytes cells were activated via mERK peptide (QYIHSANVL), 0.1 μg/mL of mERK peptide (Biomer Technologies), was added to T cell media. In CD4+ T cell optimization experiments, Th1 cells were maintained in T cell media containing 15 ng/mL IL-12 (BioLegend; Cat # 577002), 30 IU/mL IL-2 (Peprotech; Cat# 200-02) and 5 ug/mL αIL-4 antibody (Clone 11B11, BioXCell; Cat # BE0045).
In the CD4 depletion experiments, the EasySep™ Mouse CD4 Positive Selection Kit II (StemCell;Cat #18952RF) was used. In CD4+ T cell optimization experiments, the EasySep™ Mouse CD4+ T cell Isolation Kit (StemCell;Cat #19852RF) was used with the same following processes. After cells were isolated and counted, the desired number of cells were centrifuged and resuspended in the separation buffer (PBS containing 2% FBS and 1 mM EDTA). The separation cocktail was prepared and incubated at room temperature for 5 minutes. Rat serum was added to the cells along with the separation cocktail and this mixture was incubated at room temperature for 5 minutes. Magnetic spheres were then added to the sample, incubated at RT for 3 minutes and the cells were

placed into a magnet. This was then incubated for 3 minutes at room temperature before the supernatant was dumped and the separation buffer was used to top up the cells in the magnet and repeat this isolation process 2 times. 10 mL of T cell media was added to the isolated cells, and they were counted before being plated as described.

To transduce cells with the gammaretrovirus, a master mix was prepared consisting of 0.8 µL of 1.0 mg/mL Polybrene and 1.0 µL of Lipfectamine 2000 per well. The volume required to add the retrovirus plus 500 µL of media was removed from the wells and the retrovirus and 1.8 µL of the master mix was added to each well. The plate was carefully balanced and centrifuged for at 930xg for 90 minutes at 32℃ with the brakes off. After the spin, cells were transferred to an incubator at 37℃ and 5% CO_2 for 3-4 hours. After this incubation period, each well was topped off with 500 µL of warm T cell media supplemented with 10 ng/mL IL-7 or other required cytokines and placed in the 37℃, 5% CO_2 incubator overnight.

14-16 hours after media replacement, each well was washed out with warm T cell media supplemented with 10 ng/mL IL-7 or other required cytokines and added to T-25 flasks. On day 4, cells were centrifuged and scaled as needed with T cell media supplemented with 10 ng/mL IL-7 and 10 ng/mL IL-15 (BioLegend; Cat# 570304) or other required cytokines. On day 6 of culture, cells were fed with T cell media supplemented with 10 ng/mL IL-7 and 10 ng/mL IL-15 and scaled as needed.

On days 5-7 of culture, cells were counted and 0.5-1x10^6 cells were stained on ice. Cells were stained for CD90.1 (Thy1.1), a transgenic T cell marker, or CD45.2, CD4, CD8, CD62L and CD44 and FLAG, used to recognize the tag on the BCMACAR construct and used to evaluate transduction. Cells were filtered through mesh filter paper and data was collected on a Beckman Coulter Cytoflex LX Flow Cytometer. Flow cytometry data was analyzed via FCSExpress 7 from Denovo Software.

Adoptive transfer and vaccination. 1e6 CMS-5 cells in PBS (cultured in DMEM media containing 8.93 % heat inactivated fetal bovine serum, 8.85 mM HEPES, 87 U/mL penicillin+87 U/mL streptomycin and 1.78 mM L-GlutaMax) or 5e5 B16-F10-gp33 (cultured in MEM EARLS media containing 8.93 % heat inactivated fetal bovine serum, 8.85 mM HEPES, 87 U/mL penicillin+87 U/mL streptomycin, , 0.87x non-essential amino acids, MEM vitamins (Gibco), 0.87 mM sodium pyruvate and 1.78 mM L-GlutaMax) cells were injected intradermally to 6–8-week-old BALB/c or C57BL/6 mice obtained from Charles River Laboratories, Wilmington, MA. To maintain stable expression of the gp33 peptide, B16.F10-gp33 cells were further supplemented with 0.2 mg/mL G418. 5 or 7-days post implantation, cryopreserved DUC18 or P14 T cells were thawed and transferred into CMS-5 bearing BALB/c or B16-F10-gp33 bearing C57BL/6 hosts through intravenous injection (IV). 16 hours prior to rVSV administration, 0.5-1 mg of anti-mouse IFNAR1 blocking antibody (Clone MAR1-5A3, BioXCell; Cat #BE0241) was administered via intraperitoneal injection. 24 hours after T cell transfer, 2e8 pfu rVSV was administered through IV. At 4 to 5 and 11 to 12 days post-VSV, blood samples were taken via facial vein bleed.

Intracellular cytokine staining. Required tumour cells were washed with PBS and lifted using TrypLe Express Enzyme™ (Gibco; Cat # 12604021). Cells were counted using trypan blue on the Thermo Scientific Invitrogen Countess II and left to adhere at 37℃ and 5% CO_2 and double in number overnight. TDLN-derived T cells were thawed 24 hours prior to assay assembly and left to rest in T cell media containing 10 ng/mL IL-7 and 20 ng/mL IL-15 or other required cytokines. These T cells were then counted using AOPI dye and Cellometer Auto 2000 Cell Viability Counter and plated on the wells containing the adherent tumour target, except for the cells used as a positive control with Ionomycin (Sigma-Aldrich; Cat # I13909) and PMA (Sigma-Aldrich; Cat P1585-10MG), which were added in the media to be at 1 mM and 50 ng/mL, respectively. This co-culture was incubated for 2 hours at 37℃ and 5% CO_2 until Golgiplug (BD Biosciences; Cat # 555029), containing Brefeldin A, was added and incubated for 4 hours at 37℃ and 5% CO_2. At the end of this incubation period, 0.02 M EDTA was added to each well and incubated at RT for 15 minutes to stop the stimulation. Following this, cells were stained with a fixable viability dye and αCD8, αCD4, αCD45.2, and αCAR antibodies for identifications of cell populations by flow cytometry. Cells were then fixed and permeabilized using Cytofix/Cytoperm™ (BD Biosciences; Cat# 554722) and stained with αIFN-γ and αTNF-α antibodies for cytokine production identification.

Dye-based Proliferation Assay. Target tumour cells, CMS-5 and CMS-5-TR-BCMA (cultured in DMEM media containing 8.85 % heat inactivated fetal bovine serum, 8.85 mM HEPE, 87 U/mL penicillin+87 U/mL streptomycin, and 1.78 mM L-GlutaMax) were counted using trypan blue on the Thermo Scientific Invitrogen Countess II, plated, and left to adhere for 3-4 hours. CMS-5-TR-BCMA cells were derived from relapsed CMS-5 tumour cells that had lost expression of the tERK peptide and were engineered via lentiviral transduction by Rebecca Burchett to express hBCMA, the antigen the CAR is specific for. T cells were counted, washed with PBS, and centrifuged at 500xg for 5 minutes at room temperature. The reconstituted CellTrace Violet (CTV) (Invitrogen; Cat# C34557) was diluted and added to T cells and incubated at 37˚C for 20 minutes in the dark. After the incubation period, 5x warm T cell media was added to quench the dye and the cells were incubated at 37˚C for another 5 minutes with minimal light exposure. Stained T cells were centrifuged at 500xg for 5 minutes at room temperature and resuspended in T cell media containing 10 ng/mL rhIL-7. The media was aspirated from the tumour cells in each well and the stained T cells were added to the plate. The cells were incubated at 37˚C, 5% CO2 for 3-5 days. On the final day, cells in each cell were resuspended and transferred to the staining vessel. The cells were stained on ice and stained for live cells, Thy1.1 or CD45.2, CD4 and CD8. Cells were filtered through mesh filter paper and data was collected on a Beckman Coulter Cytoflex LX Flow Cytometer. Flow data was analyzed via FCSExpress 7 from Denovo Software.

Cell Irradiation. Irradiation was performed using the X-ray machine irradiator (Faxitron X-ray Corporation Cabinet X-ray System; ID # 23221) and was optimized using protocols graciously shared by William Maich in the Singh Lab. Using the Singh lab SOP for using the X-ray machine for irradiation, which considered an irradiation period of 40 seconds at

120V on shelf #6 as 1 Gy, a dosage titration of irradiation was performed to optimize the dose capable of hindering growth without cytolytic effects on the tumour cells and 25 Gy was considered the optimal dose for inhibiting tumour cell growth with minimal tumour cell death.

Co-culture Experiments. Tumour cells were washed with PBS and lifted using TrypLe Express Enzyme™. Cells were counted using trypan blue on the Thermo Scientific Invitrogen Countess II, plated, and left to adhere at 37℃ and 5% CO_2 for 3-4 hours. After cells had adhered, they were either irradiated (or not) using X-ray irradiation at 25 Gy. Various T cell products (TDLN-derived T cells or isolated TIL) were counted using AOPI dye and Cellometer Auto 2000 Cell Viability Counter and plated in the co-culture at defined E:T cell ratios with supporting cytokines including IL-2 and IL-7. These co-cultures were monitored daily, fed with fresh media containing cytokine as required, and cultured for 4-5 days until cells were harvested to be placed in killing assay.

Luciferase-Based Killing Assay. The target tumour cells (CMS-5-effLuc or MC-38-effLuc) were engineered via lentiviral transduction to express enhanced firefly luciferase (effLuc) for killing assay analysis. These cells were counted using trypan blue on the Thermo Scientific Invitrogen Countess II, plated, and left to adhere for 3-4 hours. T cells were counted and plated in serial dilutions of E:T ratios in triplicates. After 19-48 hours of incubation at 37°C, 5% CO_2, 22 uL of 1x D-Luciferin (PerkinElmer; Cat# 122799) was added to each well and spectrophotometry results were read on the i3 SpectraMax®.

TIL Isolation from tumour-bearing mice. 7-9 days prior to isolation, $2x10^5$ MC-38 cells in PBS (cultured in DMEM media containing 8.93 % heat inactivated fetal bovine serum, 8.85 mM HEPES, 87 U/mL penicillin+87 U/mL streptomycin and 1.78 mM L-GlutaMax) were injected intradermally to 6–8-week-old C57BL/6 mice obtained from Charles River Laboratories, Wilmington, MA. On the day of isolation, the tumour was acquired from the desired mouse source after euthanasia according to AUP 22-11-35 and kept in pre-weighed tubes containing 10 mL T cell media on ice. The tubes were weighed to obtain tumour weight and determine the amount of enzymatic tissue dissociation solution required. The digest solution, containing HANKS HBSS (Fisher Scientific; Cat# SH30015.03), 0.5 mg/mL Collagenase (Type I) (Thermo Fisher Scientific; Cat # 17100017) and 0.2 mg/mL DNaseI (Millipore Sigma; Cat # 11284932001) was added to minced tumour tissue (10 mL of Digest Solution for every 0.25 g of tumour) and tubes were kept on ice until incubation at 37°C for 1 hour with shaking. After the incubation period, the dissociated tissue was passed through a 70 µm nylon cell strainer (Corning; Cat# 431751), a syringe plunger was used to lightly grind the pieces of tissue through the strainer then the filter was rinsed with HANKs. This was repeated through a 40 µm nylon cell strainer. The cell suspension was centrifuged at 500xg for 5 minutes at 4°C, resuspended in 5 mL T cell media and counted using AOPI dye and Cellometer Auto 2000 Cell Viability Counter.

Recombinant VSV. Vesicular stomatitis virus (VSV) is an enveloped, negative-strand RNA *Rhabdovirus*. The 11-kb VSV genome encodes five structural proteins, including the nucleocapsid protein (N), phosphoprotein (P), matrix protein (M), glycoprotein (G), and the large polymerase protein (L). VSV-G binds to the low-density lipoprotein receptor (LDL-R), lending to the broad tropism of VSV[114]. A recombinant B cell maturation antigen (BCMA/CD269) with or without red shifted luciferase (rsLuc) (codon-optimized for murine cell expression) was used as the recombinant antigen in this thesis Table. For VSV-hBCMA-tNGFR, the recombinant antigen was created by fusing the extracellular and transmembrane domains of native human BCMA to a short truncated intracellular domain of human nerve growth factor receptor (NGFR/CD271) to remove any signaling capacity from the protein. The hBCMA-tNGFR sequence was cloned into a pCCL lentiviral vector. For VSV-rsLuc-hBCMA, dual-expression constructs were purchased as GBlocks (Integrated DNA Technologies) and cloned directly into the multiple cloning site of a pVSV plasmid kindly provided to us by Dr. John Bell (The Ottawa Hospital Research Institute). VSV-VSVΔ51 viruses encoding hBCMA (VSV-hBCMA) and rsLuc_T2A_huBCMA (VSV-rsLuc-hBCMA) were rescued in HEK293T cells (cultured in Dulbecco's Modified Eagle's Media (DMEM) supplemented with 8.9% heat-inactivated fetal bovine serum, 0.89x GlutaMAX, 8.85 mM Hepes, and 88.5 U/mL penicillin + 88.5 µg/mL streptomycin) and propagated in Vero cells by Rebecca Burchett. High-titer, sucrose gradient-purified VSV-hBCMA and VSV-rsLuc-hBCMA viruses were generated in-house with technical assistance from Natasha Kazhdan in Dr. Brian Lichty's lab. VSVΔ51-Erk9m (VSV-mERK) was provided by Dr. Brian Lichty (McMaster University).

All samples taken for virus titrations were frozen at -80°C prior to titration and thawed to assemble the plaque assay. Virus titers for VSV were determined using confluent Vero cells (cultured in Dulbecco's Modified Eagle's Media (DMEM) supplemented with 8.9% heat-inactivated fetal bovine serum, 0.89x GlutaMAX, 8.85 mM HEPES, and 88.5 U/mL penicillin + 88.5 µg/mL streptomycin) in 6-well tissue-culture treated plates. Serial virus dilutions were prepared and incubated on Vero cells for 45 minutes. After allowing for viral adsorption, the viral inoculate was aspirated off the monolater and 2 mL of prepared agarose overlay was added to each well (1:1 of 1% agarose, 2x MEM-F11 medium with 20% FBS). 24 hours later, wells were fixed with a 3:1 methanol: glacial acetic acid solution, agarose overlays were removed, and monolayers were stained with 0.2% crystal violet to visualize and enumerate the plaques.

***In vivo* Imaging System (IVIS).** Experimental mice were weighed the day before or day of *in vivo* imaging. Preprepared aliquots of 15 mg/mL D-luciferin were thawed at room temperature and kept on ice until sterile filtering immediately prior to administration. Mice were given D-luciferin at a dose of 150 mg/kg according to body weights through intraperitoneal injection. Mice were placed under isoflurane anaesthesia, eye lubricant was applied, and imaging was completed between 13-16 minutes post administration of D-luciferin on the IVIS Spectrum imager (Revvity). Total flux signal was quantified with LivingImage v4.2 software (Perkin Elmer).

Flow Cytometry Antibodies. Thy1.1-FITC (eBioscience; Cat# 11-0900-85); CD45.2 (BD Biosciences; Cat# 553772); CD8α-PE-CF594 (eBioscience; Cat# 562283); CD4-

AF700 (Invitrogen; Cat# 56-0041-82); CD44-APC (BD Biosciences; Cat# 559250); CD62L-APC-Cy7 (BD Biosciences; Cat# 560514); IFN-γ (BD Pharmingen; Cat# 554413); IL-2-PE (BD Pharmingen; Cat# 554428); TNF-α (BD Pharmingen; Cat# 560659); BV605 (BD Biosciences; Cat# 564169); FLAG-BV421 (BioLegend; Cat# 637322); LIVE/DEAD™ Fixable Near-IR Dead Cell Stain Kit (Invitrogen; Cat# L10119).

Statistical analyses. A Student's t-test was used to compare the means of two groups, while a one-way analysis of variance (ANOVA) with the Dunnett multiple comparison test was employed to compare three or more groups within an experiment. The Log-rank (Mantel-Cox) test was used to compare survival curves unless otherwise noted. Statistical significance and p-values were calculated using GraphPad Prism 10.2.3 for macOS. The significance levels were as follows: * $p < 0.05$, ** $p < 0.01$, *** $p < 0.001$, **** $p < 0.0001$, and ns = not significant.

Table 2.2: Recombinant hBCMA antigen transgene designs for VSV-vaccination used in this thesis.

Antigen	Vector	Transgene elements	Amino acid sequence
hBCMA-tNGFR	pCCL	hBCMA extracellular & transmembrane hNGFR truncated intracellular domain	MLQMAGQCSQNEYFDSLLHACIPCQLR CSSNTPPLTCQRYCNASVTNSVKGTNA ILWTCLGLSLIISLAVFVLMFLL KRWNRGIF*
rsLuc_T2A_hBCMA-tNGFR	pVSV	rsLuc (codon-optimized) *T2A* hBCMA-tNGFR (codon-optimized)	MEDAKNIKKGPAPFYPLEDGTAGE QLHKAMKRYALVPGTIAFTDAHIE VNITYAEYFEMSVRLAEAMKRYG LNTNHRIVVCSENSLQFFMPVLGA LFIGVAVAPANDIYNERELLNSMNI SQPTVVFVSKKGLQKILNVQKKLP IIQKIIIMDSKTDYQGFQSMYTFVT SHLPPGFNEYDFVPESFDRDKTIAL IMNSSGSTGLPKGVALPHRALCVR FSHARDPIFGNQIAPDTAILSVVPFH HGFGMFTTLGYLICGFRVVLMYRF EEELFLRSLQDYKIQTALLVPTLFS FLAKSTLIDKYDLSNLHEIASGGAP LSKEVGEAVAKGFHLPGIRQGYGL TETTSAILVTPIGDDKPGAVGKVVP FFEAKVVDLDTGKTLGVNQRGELC VRGPMIMSGYVNNPEATNALIDKDG WLHSGDIAYWDEDEHFFIVDRLKSL IKYKGYQVAPAELESILLQHPNIRDA GVAGLPDDDAGELPAAVVVLEHGK TMTEKEIVDYVASQVTTAKKLRGGV VFVDEVPKGLTGKLDARKIREILIK AKKGGKI *GSGEGRGSLLTCGDVEENPGPGTS* MLQMAGQCSQNEYFDSLLHACIPC QLRCSSNTPPLTCQRYCNASVTNSV KGTNAILWTCLGLSLIISLAVFVLMFL LKRWNRGIF*

3 Results

3.1 Investigating the engineering and functionality of naturally occurring tumour-specific T cells as a T cell product for a CAR/OVV boost

3.1.1 Optimizing the isolation of TIL from murine tumours in preliminary experiments

As a first step towards engineering a multi-specific T cell population from tumour-bearing mice, we set out to optimize isolation of tumour infiltrating lymphocytes (TIL) using the BD Horizon™ Dri Tumour & Tissue Dissociation Reagent (TTDR)[115]. 10 days following tumour implantation, a murine colon carcinoma tumour cell line, MC-38, was processed through the provided TTDR protocol to isolate TIL (Figure 3.1). Using a spleen as a positive control for gating flow cytometry populations, the isolated cells were assessed for CD45 expression, a common antigen on hematopoietic cells, and CD4 and CD8 expression to characterize T cell subsets. These data revealed that live CD45+CD4+ and CD45+CD8+ cells were present (Figure 3.1

FigureA) and could be isolated from MC-38 tumour-bearing mice. We next evaluated a murine fibrosarcoma tumour cell line, CMS-5, as a source of TIL. Splenocytes were again used as a positive control to identify immune cell populations. There were similar percentages of cells present expressing CD45 and CD4 or CD8 (Figure 3.1B), confirming the utility of this method for isolation of TIL from murine tumours.

Given the high cost of TTDR, we also evaluated a lower cost method (Lab Method) used previously by our lab in a head-to-head experiment with the TTDR method (Commercial Method). For this experiment, large and small MC-38 tumours were dissociated through each protocol to evaluate whether differences in tumour sizes could affect outcome. Interestingly, the Lab Method yielded TIL with greater overall viability, regardless of tumour size (Figure 3.1C). The Lab Method yielded more CD45+/CD8+ and CD45+/CD4+ cells (Figure 3.1D). As such, the Lab Method was selected for future TIL isolation.

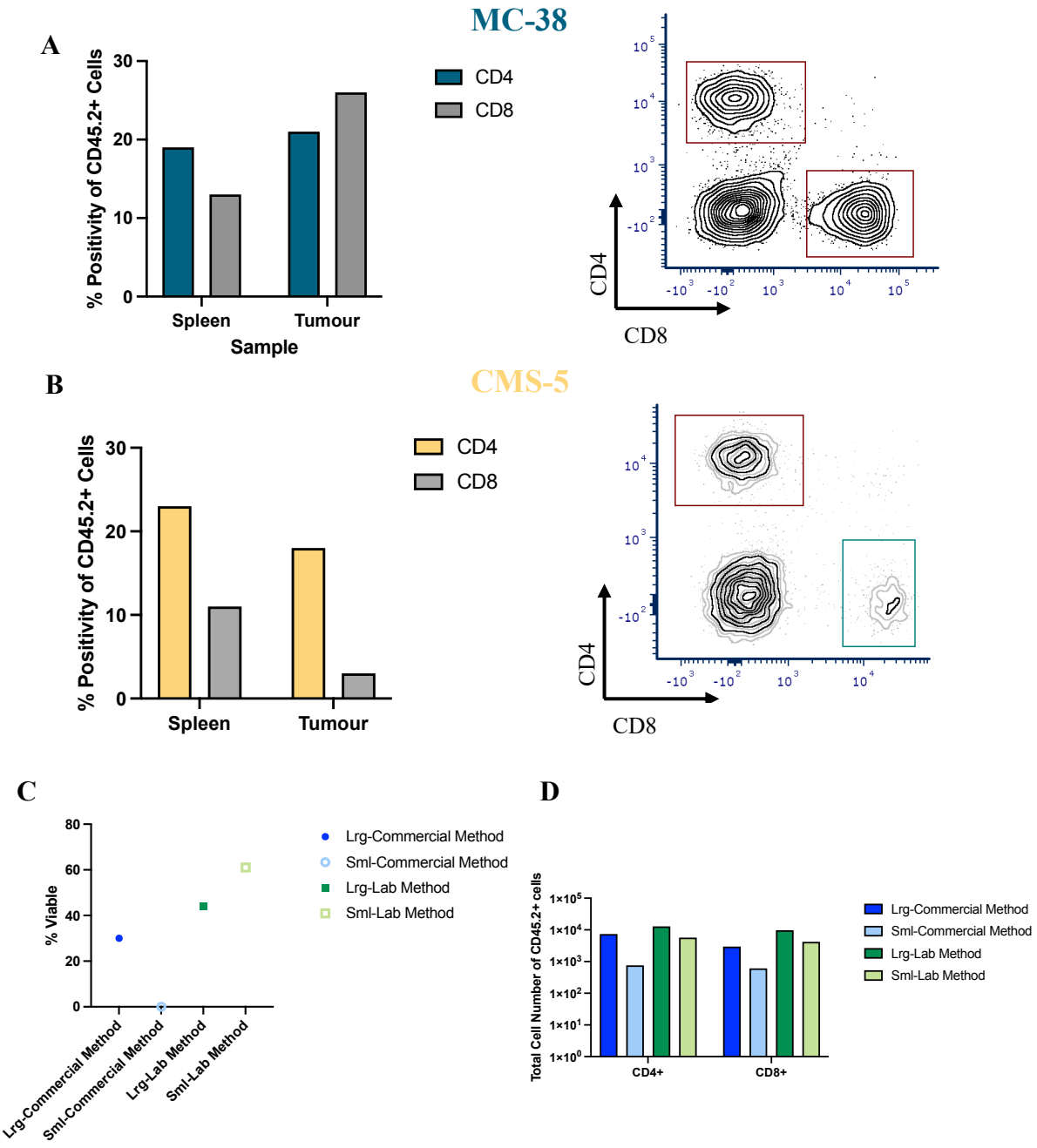

Figure 3.1: Endogenous TIL were successfully isolated from multiple murine tumours and isolation methods were optimized. The tumours were processed 10 days post-implantation and stained with fluorescently conjugated anti-mouse antibodies against CD45.2, CD4 and CD8 markers prior to FACS analysis. Representative flow cytometry plots and percentages of CD4+ and CD8+ CD45.2+ cells isolated from an (A) MC-38 (B) CMS-5 tumours and spleens, as a control tissue. (C) Indicates the viability of the cells post isolation determined using an automated cell counter and AOPI staining. (D) represents the number of cells positive for each marker. (A) (B) (D) Gating strategy: Live Cells> Lymphocytes> CD45.2+> CD4+ and CD8+. Lrg= Large tumour; Sml=Small tumour. (n=1 sample per tumour type)

3.1.2 TIL culturing and engineering from bulk tumour tissue

We next adapted a protocol for TIL expansion from MC-38 tumours[116]. The TIL were harvested from MC-38 tumours cells 9 days post-implantation and cultured in medium containing 1000 IU/mL of IL-2 in media and fed with fresh media containing 1000 IU/mL IL-2 every 4 days. On day 21, the cells were assessed via flow cytometry to phenotype the live cells present in culture to reveal a dominant population of live CD45.2+CD8+ T cells (Figure 3.2A/B). These data confirmed that TIL could be cultured using these methods and revealed that CD8+ T cells become the dominant cell population in the TIL.

In an effort to further expand tumour-specific T cells, the 21-day TIL culture was stimulated with irradiated MC-38 cells as outlined in FigureC. In this co-culture, the T cell media was supplemented with 500 IU/mL of IL-2 and 10 ng/mL of IL-7. The co-culture resulted in further TIL expansion (Figure 3.2D). Prior to these experiments, MC-38 cells were engineered via lentiviral transduction to express enhanced firefly luciferase as a marker of cell viability. Five days after the secondary stimulation with tumour cells, the cytotoxicity of the TIL culture was determined using a luciferase-based killing assay to assess their cytotoxic capacity against their tumour target (Figure 3.2E) and CMS-5 (Figure 3.2F) to observe any non-specific killing. The expanded TIL killed MC-38 cells expressing luciferase even at the lowest effector to target (E:T) ratio but did exhibit some non-specific killing at the highest E:T ratios.

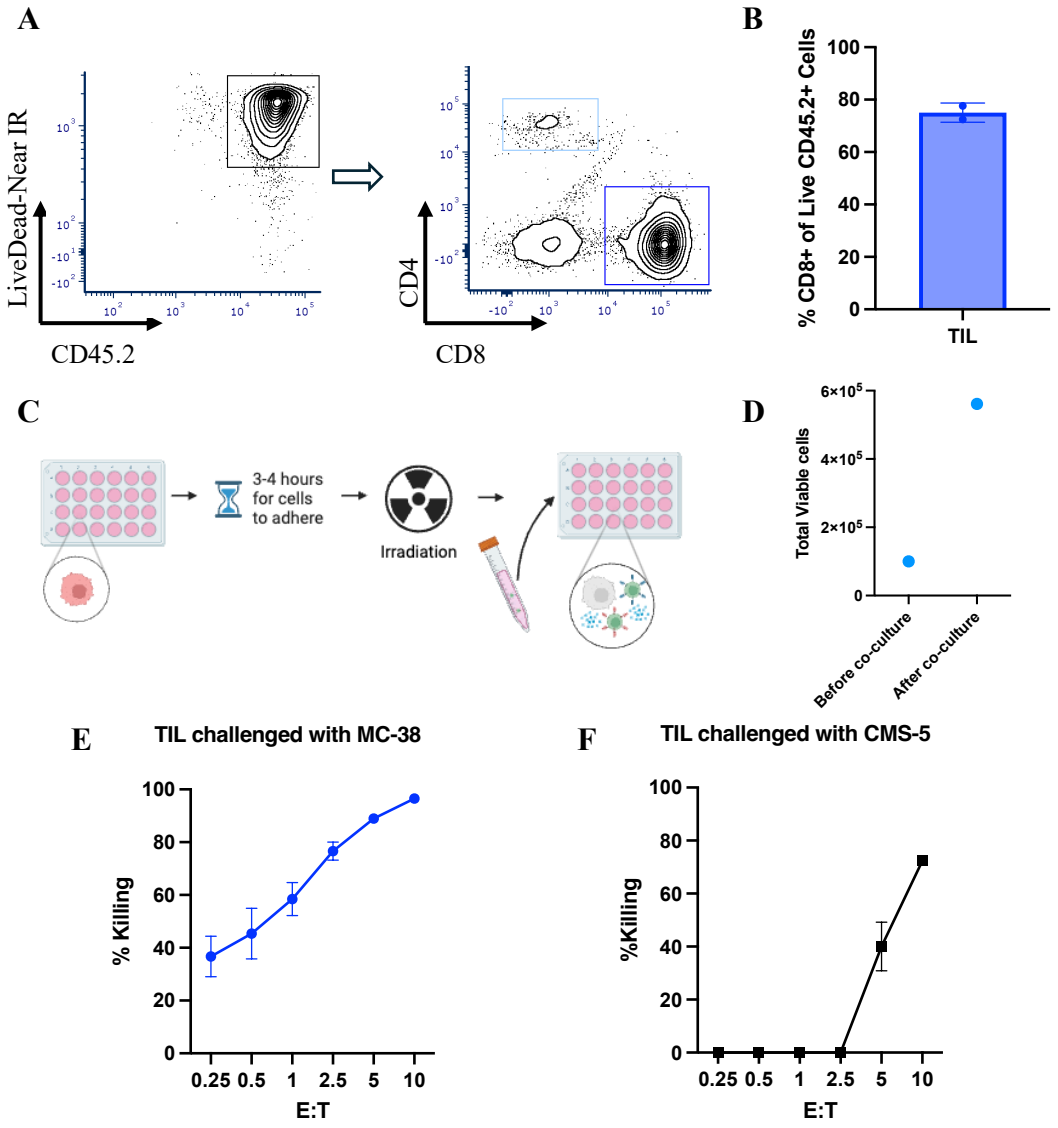

Figure 3.2: CD8+ T cells can be expanded from bulk tumour-isolated cells and can show cytotoxic effects on tumour targets.(A) (B) On day 10 of culture, the cells were stained with a fixable viability dye and a αCD8, αCD4 and αCD45.2 for assessment of cell populations by flow cytometry. (A) Shows two representative flow plots of live (LiveDead-NearIR +) and CD45.2+ cells and downstream gated CD4 and CD8+ cells. (C) A schematic representation of the co-culture where the TIL were placed in culture with irradiated tumour target cells (D) Viability of cultures were assessed before and after the 5-day co-culture using an automated cell counter and AOPI staining. (E) (F) *In vitro* luciferase-based cytotoxicity assays, where cytotoxicity is measured as the % viability of target cells following incubation with effector cells. Enhanced luciferase (effLuc)-expressing target cells were plated with T cells that had been co-cultured in cytokine supplemented media for 5-days with the tumour target. TIL were either challenged with their tumour target cells MC-38 (E) or an arbitrary tumour target cells CMS-5 (F). Cells are plated at effector to target (E:T) ratios from 0.25 - 10. After ~19-hours, firefly luciferin substrate was added to each well and luminescence was quantified. If killing analysis calculated a negative number, 0 was denoted as the % killing.

3.1.3 Engineering and functionally testing T cells isolated from tumour-draining lymph nodes (TDLN)

Tumour-draining lymph nodes (TDLN) are also a potential source of TIL as they are where anti-tumour lymphocytes are primed to tumour-specific antigens and play pivotal roles in immune responses against tumours[117]. We hypothesized that the TDLN could be a source of more viable tumour-specific T cells, which could provide a more facile source of multi-specific tumour-reactive T cells than TIL. Using our standard culture protocol as outlined in Figure 3.3A, T cells isolated from the TDLN were engineered with 28ζ-BCMACAR. The engineered T cell culture was analyzed on day 7 of culture to assess CAR expression, relative proportion of CD4+ and CD8+ T cells and memory phenotype (Figure 3.3). The cells expanded successfully (Figure 3.3 FigureB) and expressed the BCMACAR on a high fraction of cells (Figure 3.3C/D) and showed a memory phenotype skew of predominately central memory T cells (FigureE) which is optimal for our model. This demonstrated the successful isolation, culture and transduction of TDLN-derived T cells.

To determine whether the engineered T cells could respond to the CAR target (BCMA) and tumour antigen, we assessed the proliferative and cytotoxic capacity of the engineered TDLN from mice bearing the CMS-5 tumour. The T cells were co-cultured with either parental CMS-5 cells or relapsed CMS-5 engineered to express BCMA (CMS-5-TR-BCMA). We first assessed the BCMACAR T cells derived from CMS-5-tumour bearing mice TDLN (CMS-CAR-TDLN). Proliferative capacity was evaluated using a CellTrace Violet (CTV)-based proliferation assay and killing was assessed using a luciferase-based assay (Figure 3.4). The CMS-CAR-TDLN T cells proliferated well when stimulated with the CAR target (BCMA) but demonstrated minimal proliferation when stimulated with CMS-5 cells (Figure 3.4A/B). No cytotoxicity was observed (Figure 3.4). This is most likely due to the expansion of all TDLN-derived T cells isolated. The proportion of T cells specific for CMS-5 in the TDLN is possibly low and therefore not capable of forming a successful anti-tumour response in a short time period.

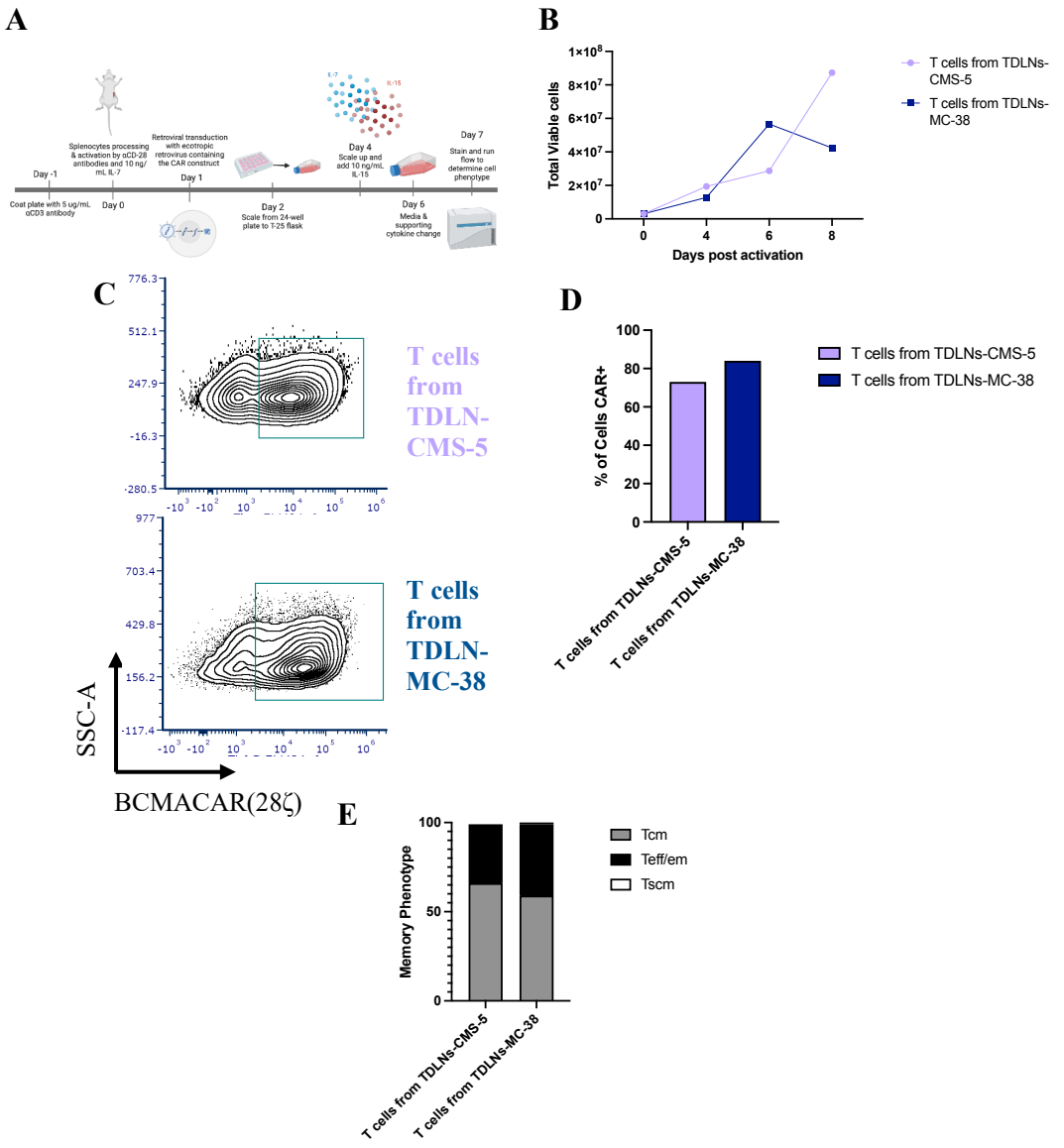

Figure 3.3: TDLN-derived T cells from tumour-bearing mice were engineered to express the 28ζBCMA-CAR.

(A) Schematic indicating experimental protocol followed. T cells were activated from TDLN isolates, transduced with ecotropic retrovirus containing the CAR construct, and cultured for 7 days post-activation. Day 7 T cells were stained with fluorescent antibodies against the CAR construct marker prior to flow cytometric analysis. (B) Cell viability of T cell cultures was assessed every two days for a 7-day culture period post-activation using an automated cell counter and AOPI staining. (C) Shows a representative flow plot and (D) summarizes the phenotypes. (E) Represents the memory phenotype of the cells (Tcm= Central Memory T cells [CD62L+CD44+]; T eff/em= Effector T cells [CD62L-CD44+]; Tscm- Stem Cell Memory T cells [CD62L-CD44-]). Gating strategy: Live Cells>Lymphocytes>CD45.2+>CAR+>CD4+ and CD8+

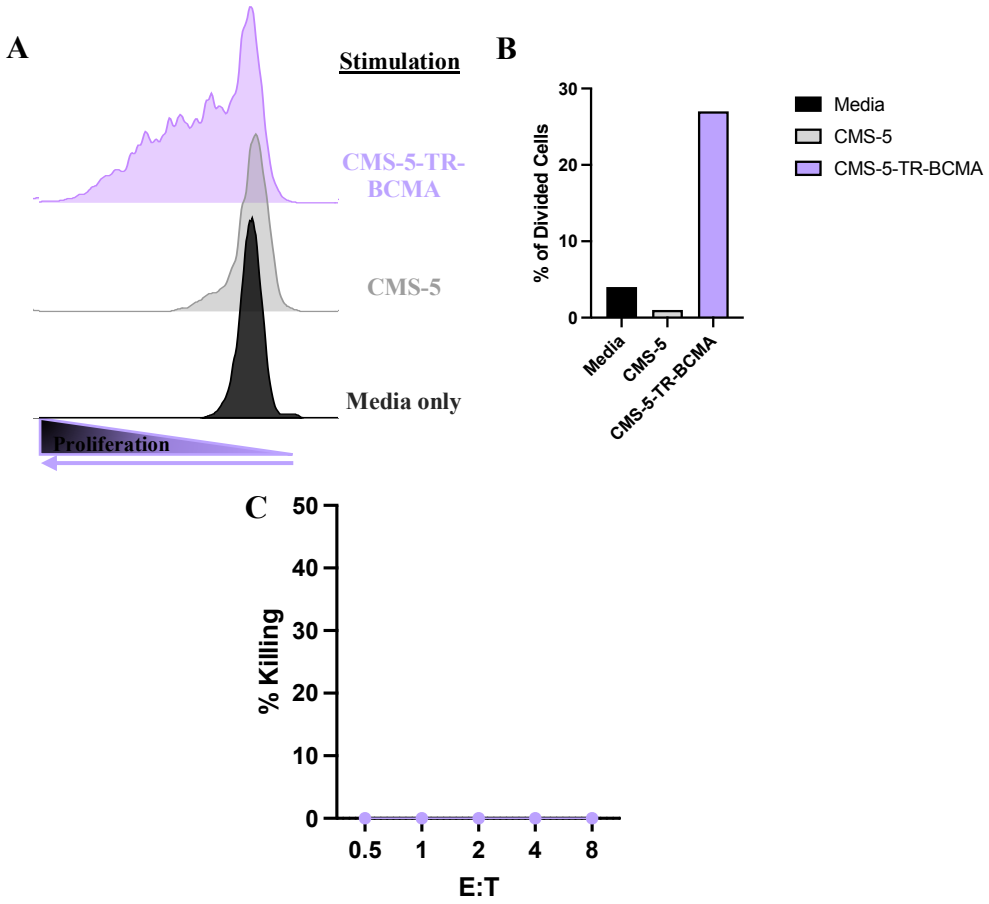

Figure 3.4: T cells isolated from TDLN of CMS-5 tumour-bearing mice proliferated only when stimulated through the CAR and were unable to kill tumour targets. T cells were activated from TDLN isolates, transduced with ecotropic retrovirus containing the CAR construct, and cultured for 7 days post-activation. (A) CellTrace Violet (CTV) dilution assay to assess *in vitro* proliferation of BCMACAR T cells upon stimulation with BCMA (CAR target)- or mERK (CMS-5)-expressing target cells. CTV-labelled T cells were co-cultured with target cells for 4 days followed by flow cytometric analysis. Cells shown in these plots were gated down from live cells > lymphocytes > single cells > CD45.2+ cells > CD8+ cells. (B) Summarizes the percentage of divided cells in each group. (C) *In vitro* luciferase-based cytotoxicity assays, where cytotoxicity is measured as the %viability of target cells following incubation with effector cells. Enhanced luciferase (effLuc)-expressing CMS-5 target cells were plated with BCMACAR- T cells at effector to target (E: T) ratios from 0.5 - 8. After ~19-hours, firefly luciferin substrate was added to each well and luminescence was quantified**.** If killing analysis calculated a negative number, 0 was denoted at the % killing.

3.1.4 Invigorating the cytotoxic capacity of BCMACAR-T cells derived from TDLN

We hypothesized that tumour-specific T cells from TDLN were rare and required a stimulus to expand prior to being challenged with the tumour target. So, we co-cultured engineered-TDLN from an MC-38 tumour-bearing mouse (MC-38-CAR-TDLN) with MC-38 tumour cells. The T cell media was supplemented with IL-2 (500 IU/mL) to facilitate activation of the T cells and 10 ng/mL of IL-7 to promote survival. Following the co-culture period, the stimulated MC-38-CAR-TDLN were evaluated for cytotoxicity

against MC-38 tumour cells in a luciferase-based cytotoxicity assay and some cytotoxicity was observed at high E:T (Figure 3.5A).

The MC-38-CAR-TDLN were then co-cultured with either MC-38 or CMS-5-BCMA to stimulate the cells through the TCRs or the CAR, respectively (Figure 3.5B). For this experiment, cytotoxicity was assessed after four days of co-culture (Figure 3.5C/D/E). T cells from both co-culture conditions displayed cytotoxicity against MC-38 and CMS-5 tumour cells.

As an alternate strategy to assess TCR-mediated and CAR mediated activation of the T cells, we elected to assess cytokine production following stimulation using intracellular cytokine staining (ICS). Cryopreserved MC-38-CAR-TDLN and non-engineered MC-38-TDLN were thawed and rested overnight in complete medium with IL-2 and IL-7. After the overnight rest, the T cells were stimulated with MC-38 cells, CMS-5 cells and CMS-5-BCMA cells. Cells were also stimulated with ionomycin and phorbol myristate acetate (PMA) as a positive control. IFN-γ and TNF-α production was measured as a read-out for activation by the stimulation. The positive control caused almost 100% of the T cells to produce both cytokines, confirming that the T cells were functional. A fraction of the T cells produced cytokine in response to CAR stimulation (Figure 3.6B/C), but the cells did not produce cytokine in response to MC-38 stimulation, which indicates a low frequency of MC-38-specific T cells in the TDLN, if any.

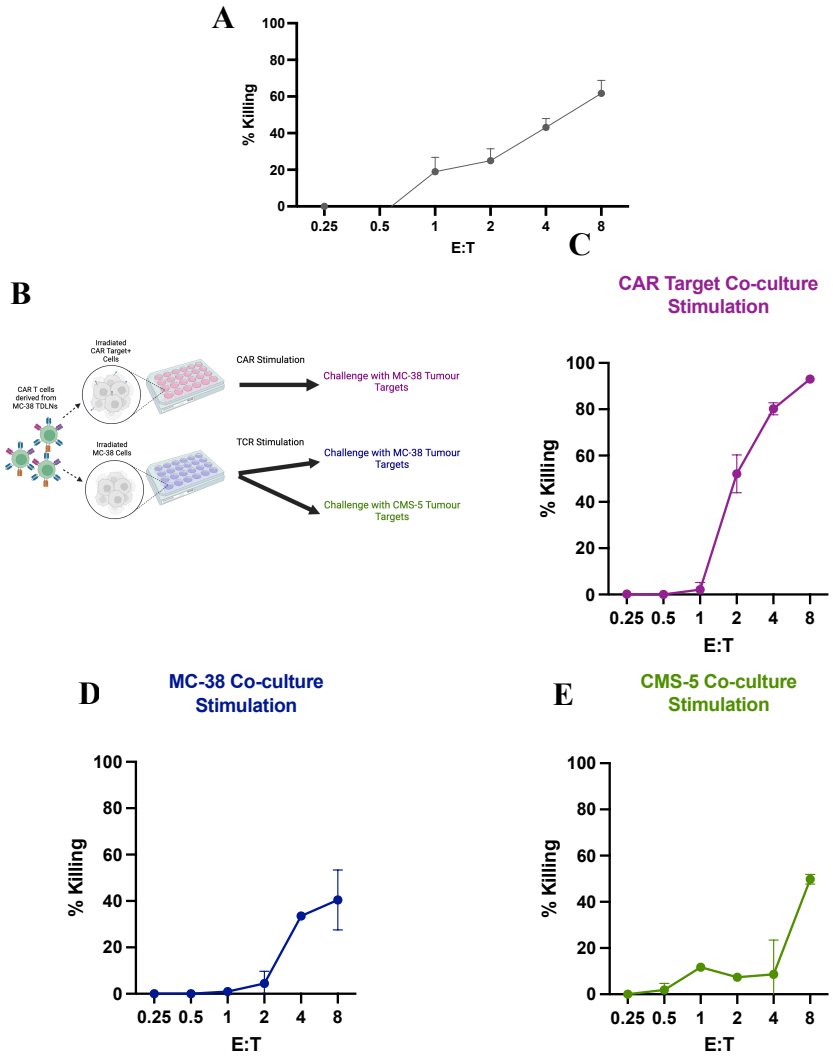

Figure 3.5: T cells isolated from TDLN of MC-38 tumour-bearing mice show cytotoxic effects after co-culture stimulation.(A) TDLN were placed in culture with irradiated tumour target cells and challenged in an *in vitro* killing assay (described below). (B) Schematic overview of experiment. (A, B, C, D) *In vitro* luciferase-based cytotoxicity assays, where cytotoxicity is measured as the % viability of target cells following incubation with effector cells. Enhanced luciferase (effLuc)-expressing target cells were plated with CAR-T cells that had been co-cultured in cytokine supplemented media for 5-days with the CAR target (C) or the tumour target cell (A,C,D). T cells isolated from TDLN of MC-38 tumour-bearing mice were challenged with (A,C,D) MC-38 (E) CMS-5 tumour cells to assess for non-specific killing. Cells are plated at effector to target (E:T) ratios from 0.25 - 8. After ~19-hours, firefly luciferin substrate was added to each well and luminescence was quantified. If killing analysis calculated a negative number, 0 was denoted at the % killing.

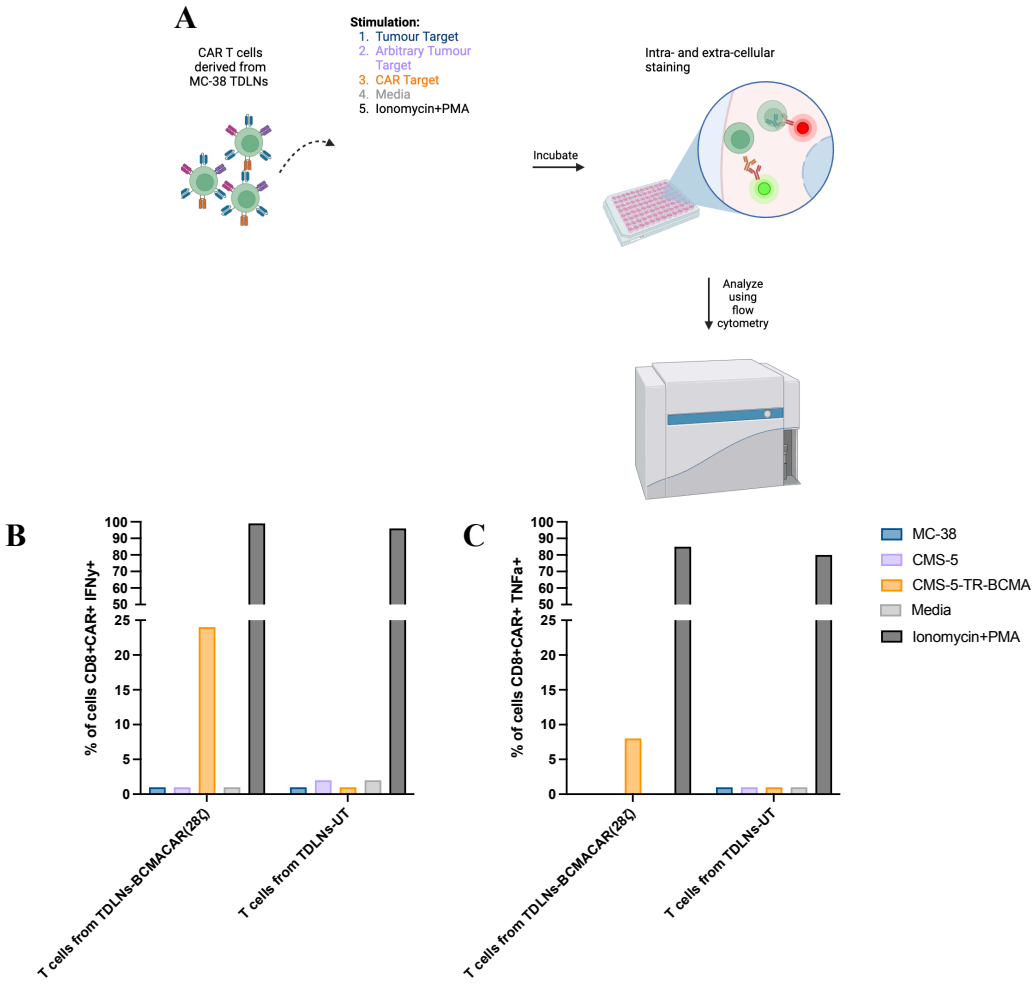

Figure 3.6: T cells isolated from TDLN of MC-38 tumour-bearing mice do not produce inflammatory cytokines in response to stimulation with tumour target.(A) Schematic indicating experimental protocol followed. (B, C) *In vitro* intracellular cytokine staining assay where T cells derived from TDLN were stimulated with various tumour targets and the cytokine response of IFN-γ (B) and TNF-α (C) was assessed at a per cell basis using. Cells were then stained using αCD8, αCD4, αCD45.2, αCAR, αTNF-α and αIFN-γ antibodies and assessed by flow cytometry.

3.2 Evaluating a CAR-mediated OV vaccine boost in the DUC18/CMS-5 model

3.2.1 Depleting CD4+ T cells from splenocytes and mERK-activation of splenocytes to evaluate effects on memory phenotype and function

In preliminary *in vivo* experiments with adoptively transferred CD4+CD8+ DUC18 T cells, 5 days post-VSV-hBCMA vaccination, no boosting or persistence of the infused T cells were present in the peripheral blood (Figure 1.3). We hypothesized that the CD4+ T cells grown alongside CD8+ T cells in DUC18 cultures were having some sort of negative impact on the boosting capacity of the DUC18 T cells. To assess this, we used magnetic separation to isolate the CD4+ cell population from unaltered splenocytes, to

maintain the most similarity between the CD4-negative (CD4- cell population) and CD4+CD8+ (unaltered) DUC18 T cell populations. We then cultured the CD4-negative and CD4+CD8+ cell populations in the P14 culture conditions, as shown in Figure 3.7A, and evaluated differences in growth, BCMACAR expression and phenotype. We chose to conduct a head-to-head comparison of two pre-existing CAR constructs (CD28ζ-signalling and BBζ- signalling) within these experiments to ensure we selected the most effective CAR in the anti-cancer response. Depleting the CD4+ T cells did not alter growth (Figure 3.7B) or BCMACAR (Figure 3.7C) expression, but the T cells engineered from the CD4-depleted splenocytes skewed towards the T_{cm} cell phenotype (Figure 3.7D). This was considered a favorable outcome as previous reports from our group have demonstrated that T cells with T_{cm} phenotype are more therapeutically effective in the combination ACT with rhabdovirus boost strategy[94,95,96]. Neither CAR construct seemed to exhibit superiority in expansion, CAR engineering or memory phenotype. Consistent with the shift towards Tcm, the CAR-T cells engineered from the CD4-depleted DUC18 splenocytes displayed greater proliferation than CAR-T cells engineered from the unsorted splenocytes (Figure 3.7E).

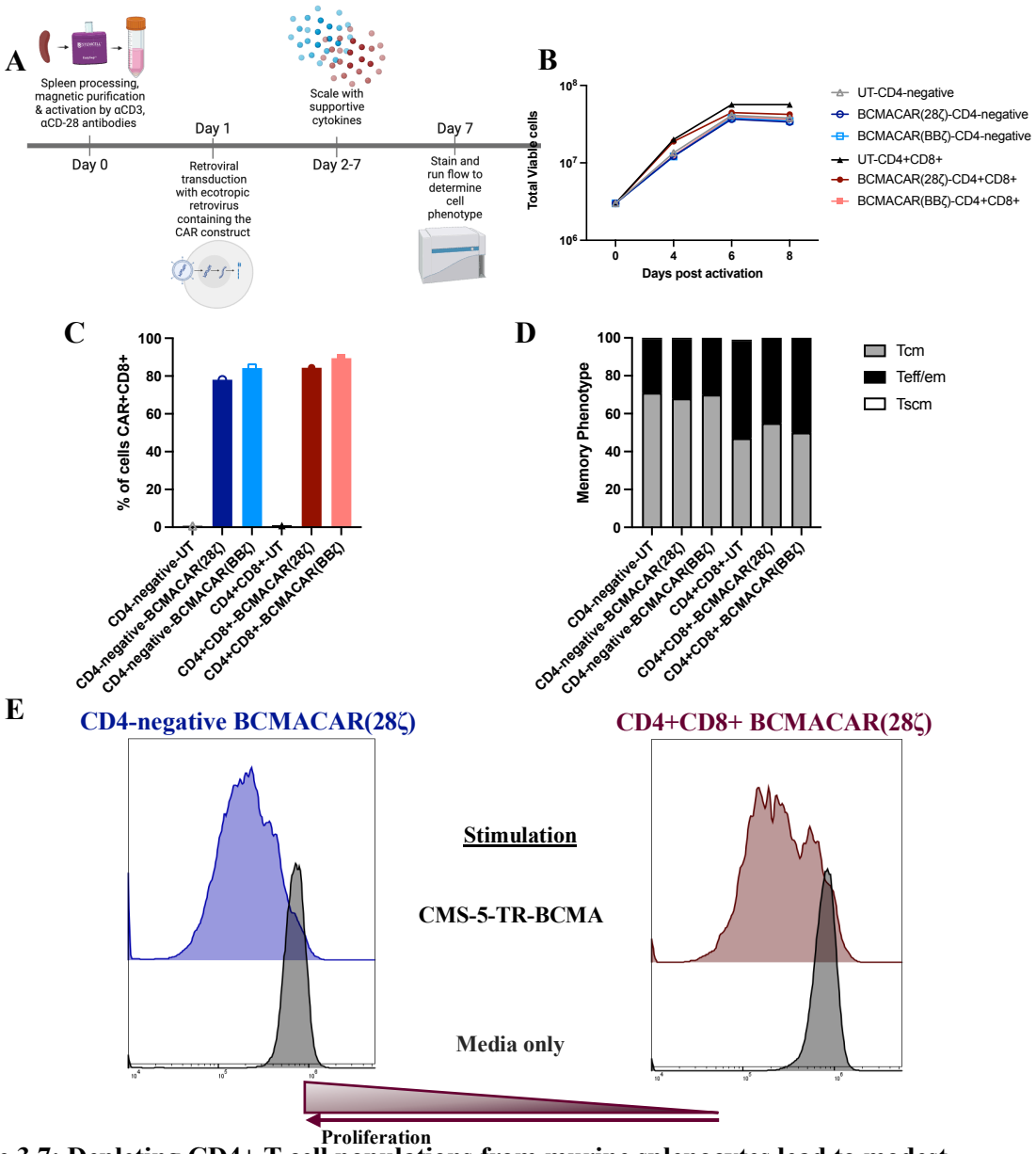

Figure 3.7: Depleting CD4+ T cell populations from murine splenocytes lead to modest differences in memory phenotype bias and proliferative capacity.(A) Schematic indicating cell manufacturing protocol followed. DUC18 splenocytes were depleted or not of CD4+ T cells and activated with plate-bound αCD3e at 5 ug/mL,αCD28 antibodies and transduced with BCMACAR-CD28z or BCMACAR-BBz retrovirus. They then were cultured for 7 days post-activation in media supplemented with 10 ng/mL rhIL-7 and 10 ng/mL rhIL-15 after day 4 of culture prior to phenotype analysis. (B) Cell viability of T cell cultures was assessed every two days for a 7-day culture period post-activation using an automated cell counter and AOPI staining. (C and D) T cells were collected and stained with fluorescently conjugated anti-mouse antibodies against transduction and phenotype (CD62L, CD44) markers prior to FACS analysis. Gating strategy: Lymphocytes> single cells > Thy1.1+ cells > CD4+ and CD8+. (E) CellTrace Violet (CTV) dilution assay to assess *in vitro* proliferation of BCMACAR T cells upon stimulation with BCMA- or mERK-expressing target cells. CTV-labelled T cells were co-cultured with target cells for 4 days followed by flow cytometric analysis. Cells shown in these plots were gated down from live cells > lymphocytes > single cells > Thy1.1+ cells > CD8+ cells.

It is also important to note that the DUC18 transgene displays lower penetrance than the P14 transgene. As such, the mERK-specific TCR is only present on 35%–50% of the T cell repertoire in DUC18 transgenic mice whereas the gp33-specific TCR is present on >99% of the T cell repertoire of P14 mice. To selectively engineer and expand the mERK-specific CD8+ T cells from DUC18 splenocytes, the splenocytes were stimulated with mERK peptide as we had described previously[94,95,96] and engineered with the BCMACAR retrovirus. As a control, the same splenocytes were activated and engineered according to our conventional protocol using antibody activation. The peptide-stimulated splenocytes displayed reduced expansion, which is not unexpected since only a fraction of the T cells will be stimulated by mERK peptide whereas all the T cells will be activated in our conventional protocol (Figure 3.8A). Peptide-based activation resulted in reduced overall transduction and expression of the BCMACAR (Figure 3.8B) but resulted in a striking enhancement of T cells with a memory phenotype (Figure 3.8C) much more skewed toward the T_{cm} cell phenotype. To assess the cytotoxic capacity of these differently activated cells, a Luciferase-based killing assay was performed. We hypothesized that the antigen-activated T cells would exhibit superior killing of the CMS-5 cells upon challenge. When this experiment was performed, no adjustments were made for Vβ8.3+ (mERK specific) DUC18 T cells. A modest difference in killing was observed (Figure 3.8D). It can be assumed that the slightly higher effector phenotype of the antibody-activated cells facilitated more killing of tumour targets in this short period, but regardless neither set of cells completely cleared the tumour targets. This also indicates that mERK-TCR selective culture conditions do not seemingly confer superior cytotoxic ability of DUC18 T cells in this assay.

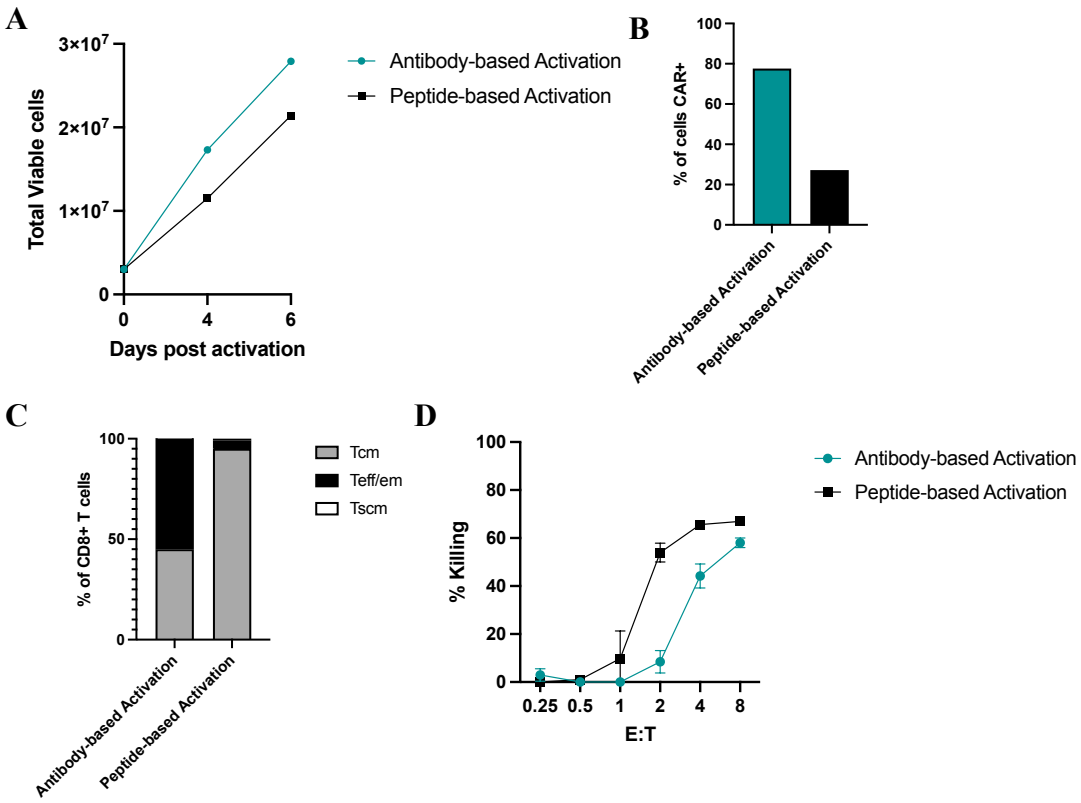

Figure 3.8: Activating murine DUC18 splenocytes with mERK peptide led to some differences in growth and cell phenotype but does not lead to superior killing capacity. DUC18 splenocytes were activated with plate-bound αCD3e at 5 ug/mL,αCD28 antibodies or the mERK peptide at 0.1ug/mL and transduced with BCMACAR-CD28z retrovirus. They then were cultured for 7 days post-activation in media supplemented with 10 ng/mL rhIL-7 and 10 ng/mL rhIL-15 after day 4 of culture prior to phenotype analysis. (A) Cell viability of T cell cultures was assessed every two days for a 7-day culture period post-activation using an automated cell counter and AOPI staining. (B, C) T cells were collected and stained with fluorescently conjugated anti-mouse antibodies against transduction and phenotype (CD62L, CD44) markers prior to FACS analysis. Gating strategy: Lymphocytes> single cells > Thy1.1+ cells > CD4+ and CD8+ (D) Enhanced luciferase (effLuc)-expressing target cells were plated with CAR-T cells at effector to target (E:T) ratios from 0.25 - 8. After ~19-hours, firefly luciferin substrate was added to each well and luminescence was quantified.

3.2.2 Boosting CD4-negative DUC18 BCMACAR T cells and CD4+CD8+ DUC18 BCMACAR T cells with VSV-hBCMA

Upon confirmation that the CD4-negative and CD4+CD8+ cells had proliferative capacity post-thaw (Figure 3.7), the next step was to assess the cells' capacity to be boosted through the CAR upon VSV-hBCMA vaccination. The outline for the experiment is detailed in

FigureA. Both the BBζ and 28ζ variants of our BCMACAR were included in this first experiment to determine whether one BCMACAR demonstrated superior anti-tumour activity and expansion than the other. BCMACAR-DUC18 T cells generated from CD4-depleted DUC18 splenocytes or total DUC18 splenocytes were transferred into CMS-5

bearing BALB/c mice and the following day, mice were vaccinated with VSV-hBCMA. Transferred T cells were measured by the congenic marker Thy1.1 (CD90.1), a surface marker present on DUC18 T cells, in the peripheral blood 5- and 12-days post-vaccination. Only the CD4-negative 28ζBCMACAR T cells displayed marked expansion of the transferred Thy1.1+CD8+ T cells in the peripheral blood following VSV-hBCMA vaccination (Figure 3.9B). We observed some mice with T cell expansion following infusion with BBζBCMACAR T cells generated from CD4-depleted splenocytes, but this did not achieve significance. Most notably, no expansion was observed in mice infused with T cells manufactured from total lymphocytes, regardless of the CAR used for engineering. Thus, the removal of CD4+ T cells from the splenocytes prior to manufacturing yields a T cell product with improved capacity for expansion following boosting with VSV-hBCMA. Regardless of the expansion observed 5 days following vaccination, very few adoptively transferred T cells persisted 12 days after vaccination with VSV-hBCMA, although CD4-negative 28ζBCMACAR still maintained a higher significantly higher percentage than the CD4+CD8+ T cells (Figure 3.9C). Based on these results, the 28ζBCMACAR was employed exclusively in later experiments. Despite the evidence of early T cell expansion in some groups, there was no tumour regression (Figure 3.9D) or long-term extended survival (Figure 3.9E) in any group.

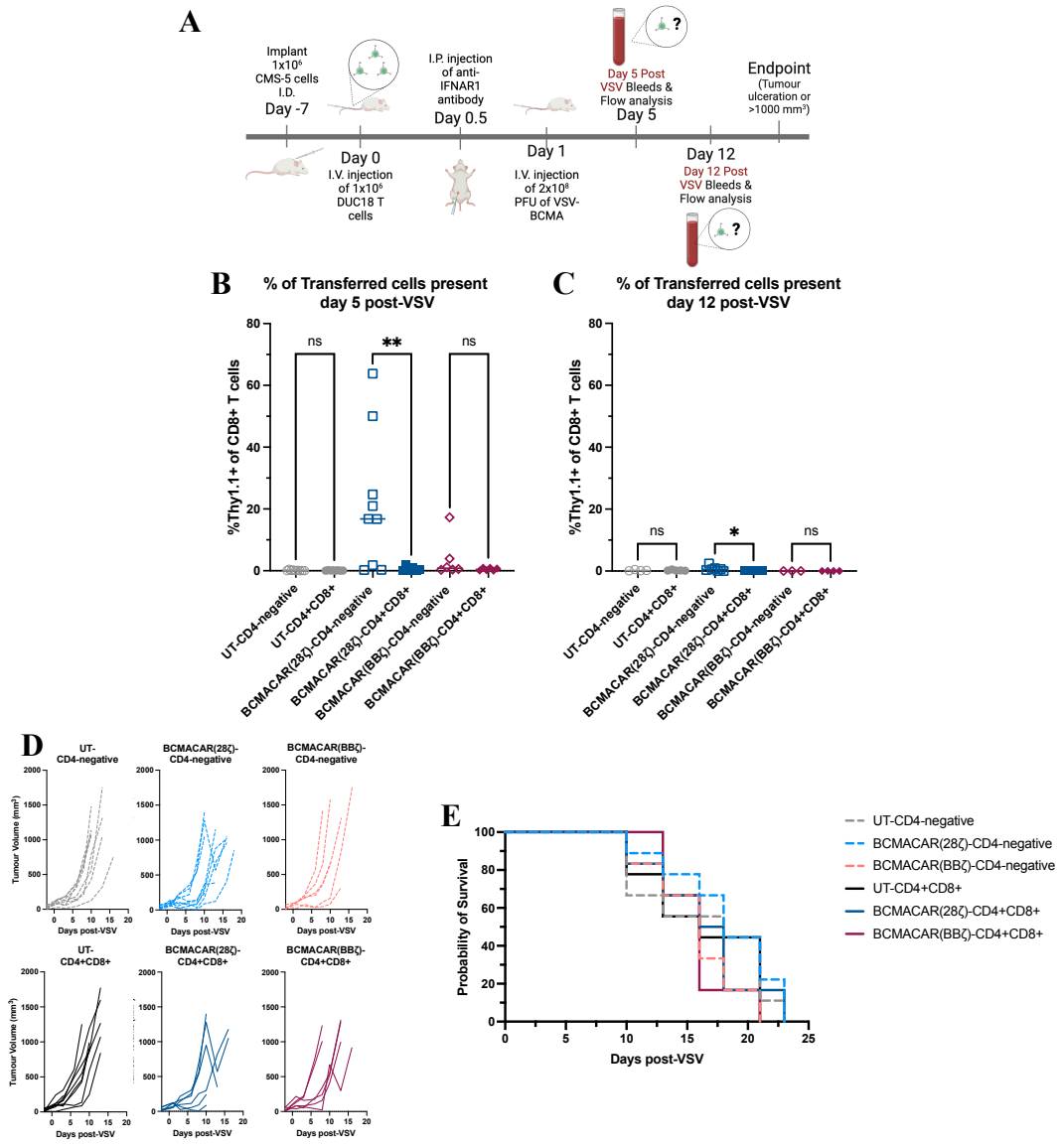

Figure 3.9: ACT and recombinant VSV-hBCMA boosting of CD4-negative and CD4+CD8+ DUC18 CAR-T cells in CMS-5 tumour-bearing mice.(A) Schematic indicating experimental timeline and setup. $1x10^6$ cryopreserved purified or bulk DUC18-Thy1.1+ BCMACAR-T cells or DUC18 UT-T cells were administered intravenously and 0.5 mg of αIFNAR1 blocking antibody was delivered intraperitoneally 7 days after CMS-5 tumours were implanted intradermally (I.D.) in 6–8-week-old BALB/c recipients (n=6-8). Approximately 16 hours prior to vaccination, 0.5 mg of αIFNAR1 antibody was administered interperitoneally (I.P.) to each animal. 24 hours after ACT, $2x10^8$ plaque forming units (PFU) of rVSV-HBCMA was administered through I.V. (B) 5 and (C) 12 days after vaccination, non-terminal bleeds were collected from the facial vein of each mouse. Following ACK lysis to remove erythrocytes, cells were stained with a fixable viability dye and αCD8, αCD4, αThy1.1, and αCAR antibodies for quantification of cell populations by flow cytometry. Plots represent the percentage of total CD8+ T cells in peripheral blood that express the congenic marker, Thy1.1, in each BALB/c recipient post-VSV. 2-way ANOVA statistical analysis was performed. (D) Tumour volume was monitored by manual caliper measurement every 2-3 days for the duration of the experiment. (E) Survival from the time that vaccination was performed (three experiments represented) (n=6-9).

3.2.3 Monitoring DUC18 T cell expansion using non-invasive luminescent imaging

Monitoring T cells in the peripheral blood is a useful method for tracking T cell expansion but it does not accommodate for T cell expansion in specific tissues. Therefore, we elected to engineer T cells with the BCMACAR and luciferase to enable non-invasive imaging of the T cells by bioluminescence. To assess feasibility of this approach, T cells were activated from total DUC18 splenocytes and co-engineered with the BCMACAR and red-shifted firefly luciferase (rsLuc). This luciferase variant emits light at wavelengths greater than 600 nm, avoiding the absorption of blue and green light by hemoglobin and myoglobin, thereby enhancing sensitivity during *in vivo* imaging compared to the wild-type firefly luciferase[118,119]. These co-engineered cells were adoptively transferred into CMS-5 tumour-bearing BALB/C mice and vaccinated with VSV-hBCMA the following day. The mice were imaged the day of and day after VSV vaccination and then imaged every second day until the T cell signal was no longer detectable (Figure 3.10A). Presence of T cells in the periphery was measured using a blood samples 5 days post vaccination, as was previously done. In these data, there appeared to be a peak in the transferred T cells on day four post vaccination, but these cells had completely regressed by day six (Figure 3.10B/D) and were not present in the peripheral blood on day 5 post-vaccination (Figure 3.10C). Based on these results, future experiments will monitor transferred T cells in the peripheral blood on day four post-vaccination instead of day five.

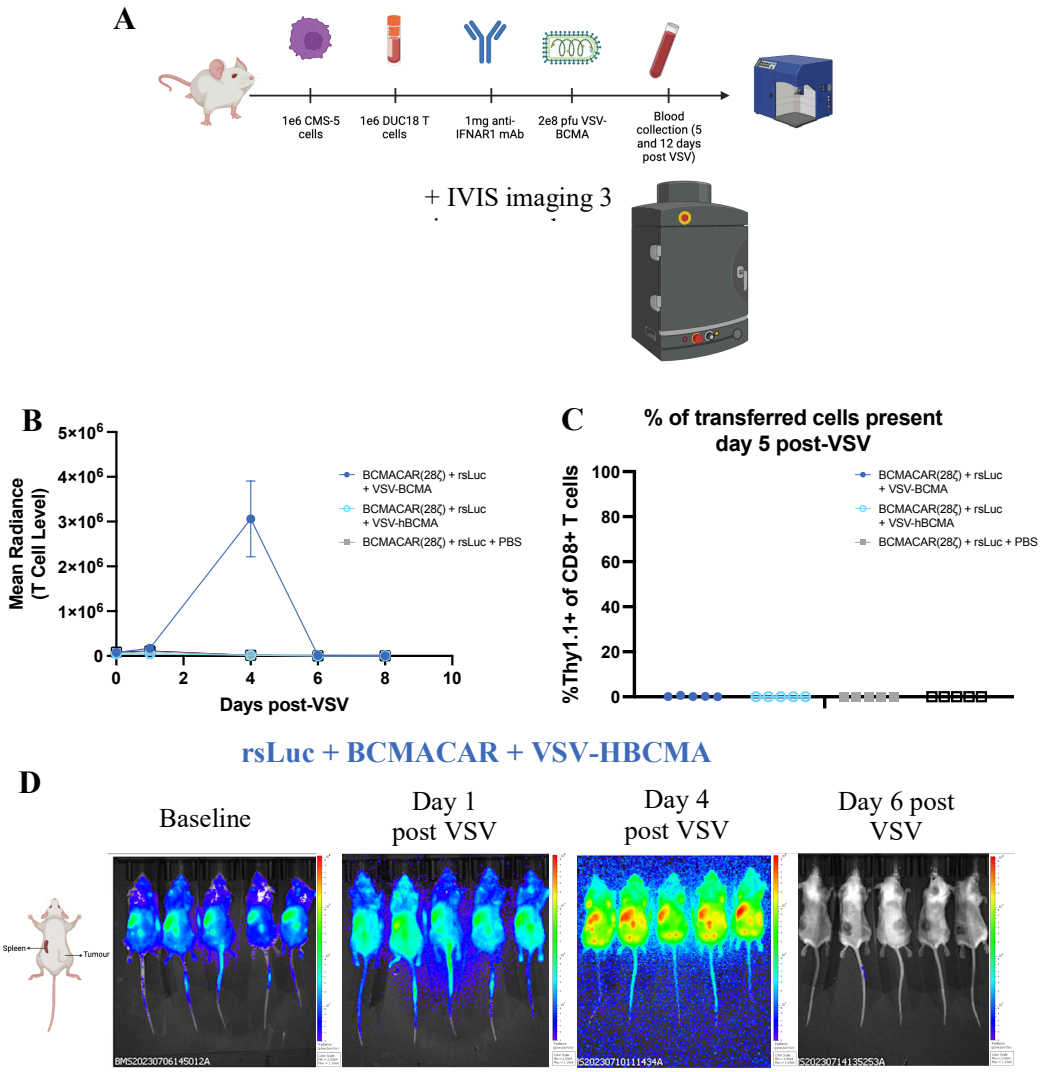

Figure 3.10: Adoptively transferred CD4+CD8+ DUC18 CAR-T cells in CMS-5 tumour-bearing mice peak at 4-days following vaccination with VSV-hBCMA.(A) Schematic indicating experimental timeline and setup. 1x10^6 cryopreserved DUC18 rsLucBCMACAR-T cells or rsLuc T cells were administered intravenously and 0.5 mg of αIFNAR1 blocking antibody was delivered intraperitoneally 5 days after CMS-5 tumours were implanted in 6-8 w.o. BALB/c recipients and baseline images were taken. 24 hours after ACT, 2x10^8 PFU of rVSV-HBCMA was administered intravenously. (B) 4 days after vaccination, non-terminal bleeds were collected from the facial vein of each mouse. Following ACK lysis to remove erythrocytes, cells were stained with a fixable viability dye and αCD8, αCD4, αThy1.1, and αCAR antibodies for quantification of cell populations by flow cytometry. Plots represent the percentage of total CD8+ T cells in peripheral blood that express the congenic marker, Thy1.1, in each BALB/c recipient post-boost. 2-way ANOVA statistical analysis was performed. (C) Mean radiance of images taken of each group (D) Representative images of the data represented in (C) of the DUC18 rsLucBCMACAR-T cells + VSV experimental group. 2-way ANOVA statistical analysis was performed (one experiment represented) (n=3).

To monitor the trafficking of T cells engineered from CD4-negative and CD4+CD8+ splenocytes, we co-engineered T cells manufactured from both starting sources to express the BCMACAR and rsLuc. The cells manufactured from both sources expanded similar (Figure 3.11A) and had expression of both rsLuc and the BCMACAR (Figure 3.11B/C). Upon thawing, the co-transduced cells were assessed for proliferative capacity when stimulated through the CAR and TCR and considered validated for *in vivo* studies as proliferation was observed (Figure 3.11D).

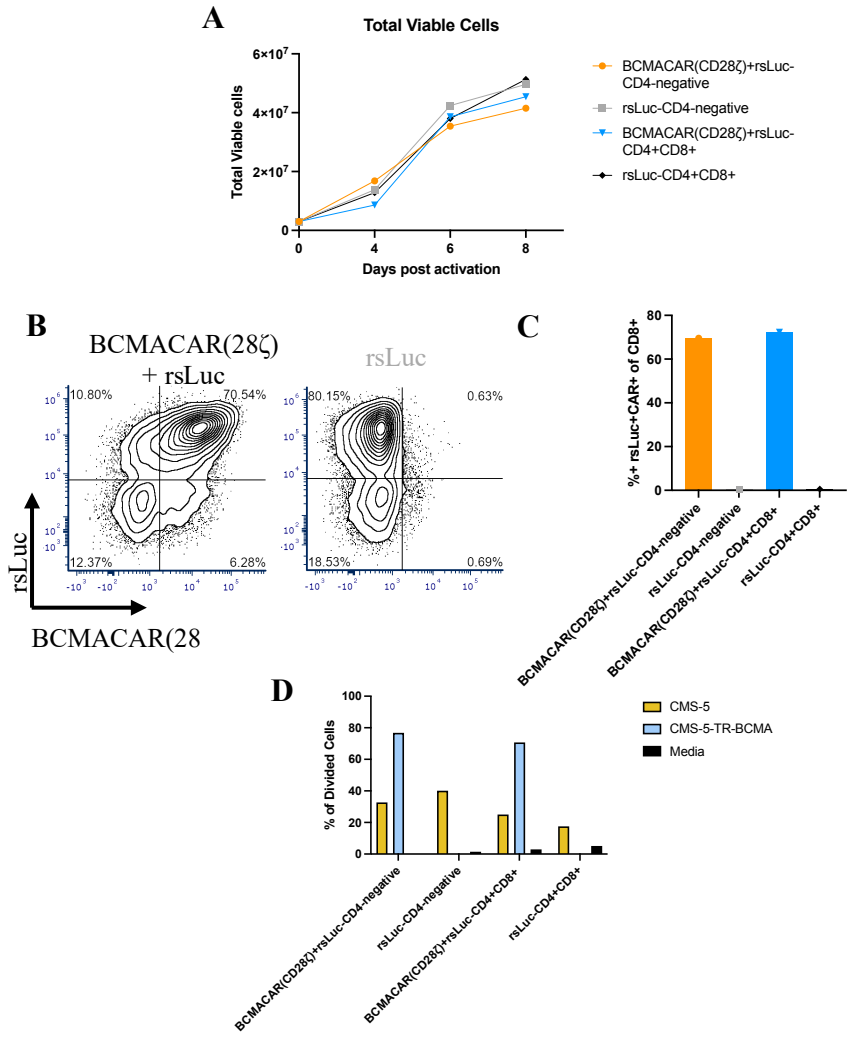

Figure 3.11: CD4-negative and CD4+CD8+ DUC18 T cells were co-engineered with rsLuc and a BCMACAR and proliferative in functional assessments.(A) DUC18 splenocytes were depleted or not of CD4+ T cells and activated with plate-bound αCD3e, αCD28 antibodies and co-transduced with BCMACAR and rsLuc retroviruses. They then were cultured for 7 days post-activation in media supplemented with 10 ng/mL rhIL-7 and 10 ng/mL rhIL-15 after day 4 of culture prior to phenotype analysis. (C) Viability of T cell cultures were assessed every two days for a 7-day culture period post-activation using an automated cell counter and AOPI staining. (D) (E) DUC18 cells were collected and stained with fluorescently conjugated anti-mouse antibodies against transduction and phenotype (CD62L, CD44) markers prior to FACS analysis. Gating strategy: Lymphocytes> single cells > Thy1.1+ cells > CD4+ and CD8+. (D) Shows a representative flow plot and (E) summarizes the data. (F) CellTrace Violet (CTV) dilution assay to assess *in vitro* proliferation of BCMACAR T cells upon stimulation with BCMA- or mERK-expressing target cells. CTV-labelled T cells were co-cultured with target cells for 4 days followed by flow cytometric analysis. Cells shown in these plots were gated down from live cells > lymphocytes > single cells > Thy1.1+ cells > CD8+ cells.

The co-engineered cells from both sources were adoptively transferred into CMS-5 tumour-bearing BALB/C mice and vaccinated with VSV-hBCMA the following day. The mice were imaged the day of and day after VSV vaccination and then imaged every

second day until the T cell signal was no longer detectable. As described, peripheral blood was collected on day 4 post-vaccination instead of day 5 (Figure 3.12A). Each mouse was imaged three times a week until endpoint or luminescence was no longer detectable. In this figure, DUC18 T cells transduced solely with the rsLuc construct serve as the control group, as no T cell boosting is expected in the absence of the BCMACAR construct. In Figure 3.12B, expansion of the transferred Thy1.1+CD8+ T cells in the peripheral blood following VSV-hBCMA vaccination is again predominantly limited to the CD4-depleted group. Similarly to previous results, using a CD4-negative DUC18 T cell product allows for more expansion following vaccination, despite one mouse in the CD4+CD8+ T cell-treated group having similar percentages of transferred cells present. Both CD4-negative and CD4+CD8+ cells become undetectable by 11-days post-vaccination, as was observed in imaging so no peripheral bleeds were collected.
FigureC summarizes the mean radiance data represented in Figure 3.12D and there was no significant difference between the CD4-negative and CD4+CD8+ DUC18 T cells observed. There was no evident difference in cell trafficking between the CD4-negative and CD4+CD8+ DUC18 T cell populations.

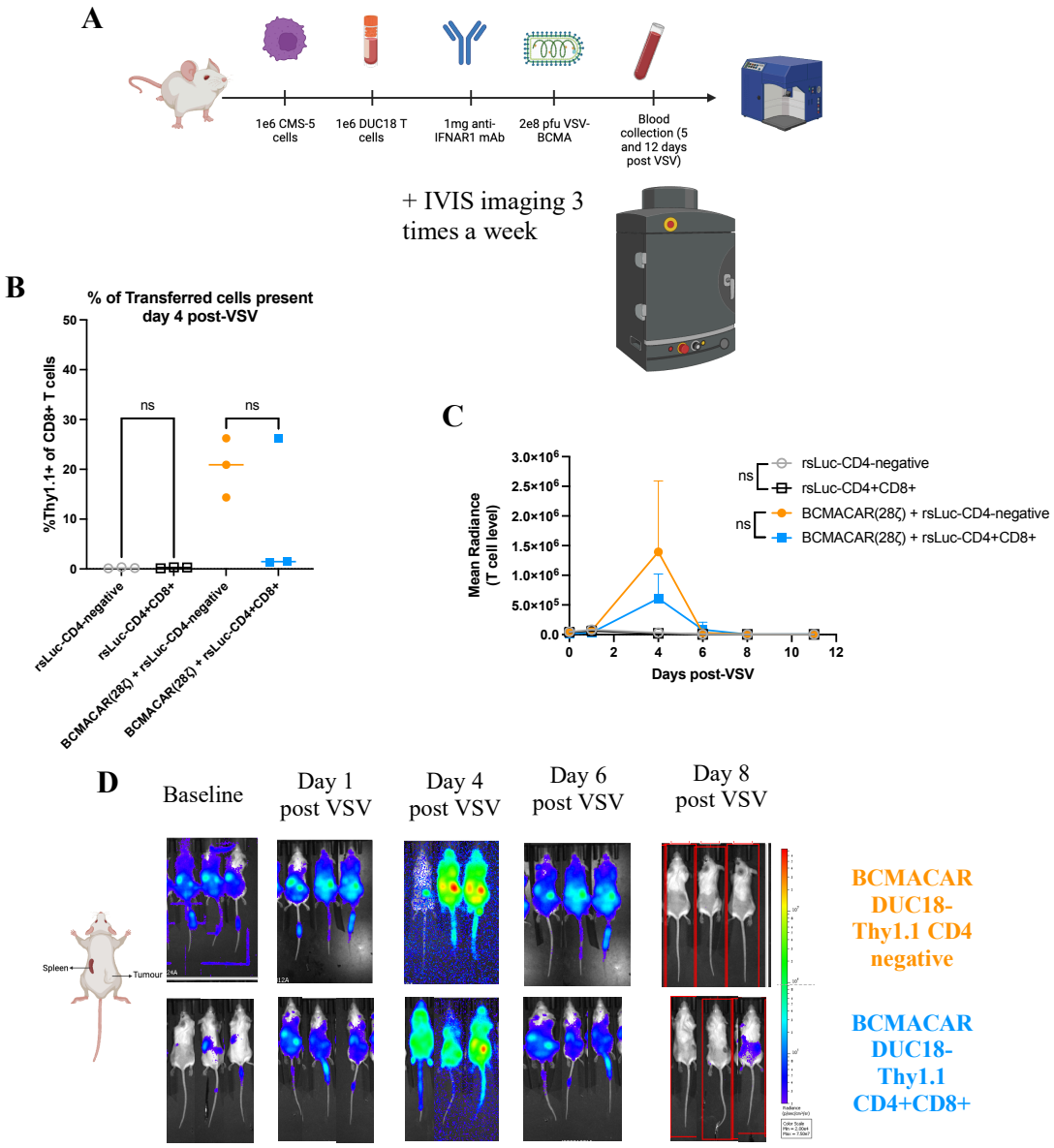

Figure 3.12: Adoptive transfer, recombinant VSV-hBCMA boosting and *in vivo* tracking of CD4-negative and CD4+CD8+ DUC18 CAR-T cells in CMS-5 tumour-bearing mice.(A) Schematic indicating experimental timeline and setup. $1x10^6$ cryopreserved bulk or purified DUC18 rsLucBCMACAR-T cells or rsLucT cells were administered intravenously and 0.5 mg of αIFNAR1 blocking antibody was delivered intraperitoneally 5 days after CMS-5 tumours were implanted in 6-8 w.o. BALB/c recipients and baseline images were taken. 24 hours after ACT, $2x10^8$ PFU of rVSV-HBCMA was administered intravenously. (B) 4 days after vaccination, non-terminal bleeds were collected from the facial vein of each mouse. Following ACK lysis to remove erythrocytes, cells were stained with a fixable viability dye and αCD8, αCD4, αThy1.1, and αCAR antibodies for quantification of cell populations by flow cytometry. Plots represent the percentage of total CD8+ T cells in peripheral blood that express the congenic marker, Thy1.1, in each BALB/c recipient post-boost. 2-way ANOVA statistical analysis was performed. (C) Mean radiance of images taken of each group (D) Representative images of the data represented in (C) of the DUC18 rsLucBCMACAR-T cells + VSV experimental group. 2-way ANOVA statistical analysis was performed (one experiment represented) (n=3).

3.2.4 Comparing the boosting capacity and anti-tumour effects of CD4-negative and CD4+CD8+ DUC18 BCMACAR T cells boosted with VSV-mERK or VSV-hBCMA

Utilizing VSV-mERK alongside VSV-hBCMA allows us to compare TCR-activated boosting and compare it to CAR-activated boosting, using VSV-hBCMA. An experimental schematic is represented in Figure 3.13A. To compare any differences observed when stimulating the CD4-depleted or CD4+CD8+ T cells through the TCR or CAR, engineered T cells were adoptively transferred into CMS-5 tumour-bearing BALB/C mice and vaccinated with VSV-hBCMA or VSV-mERK the following day. As seen in Figure 3.13B, the same trends of reduced CD8+Thy1.1+ T cell expansion when CD4+ T cells are present in the transferred BCMACAR T cell product, regardless of whether the infused T cells were stimulated via their TCR by VSV-mERK or their CAR via VSV-hBCMA. We observed no significant difference in expansion or persistence of the infused T cells whether they were stimulated through their TCR, or their CAR (Figure 3.13C). Tumours relapsed in all mice but two; one in the CD4-negative and one in the CD4+CD8+ DUC18 BCMACAR T cell groups, both boosted with VSV-mERK (Figure 3.13D). Taken together, these data further indicate that there is a benefit to manufacturing engineered T cells from CD4-depleted DUC18 splenocytes, independent of whether boosting through the CAR or TCR.

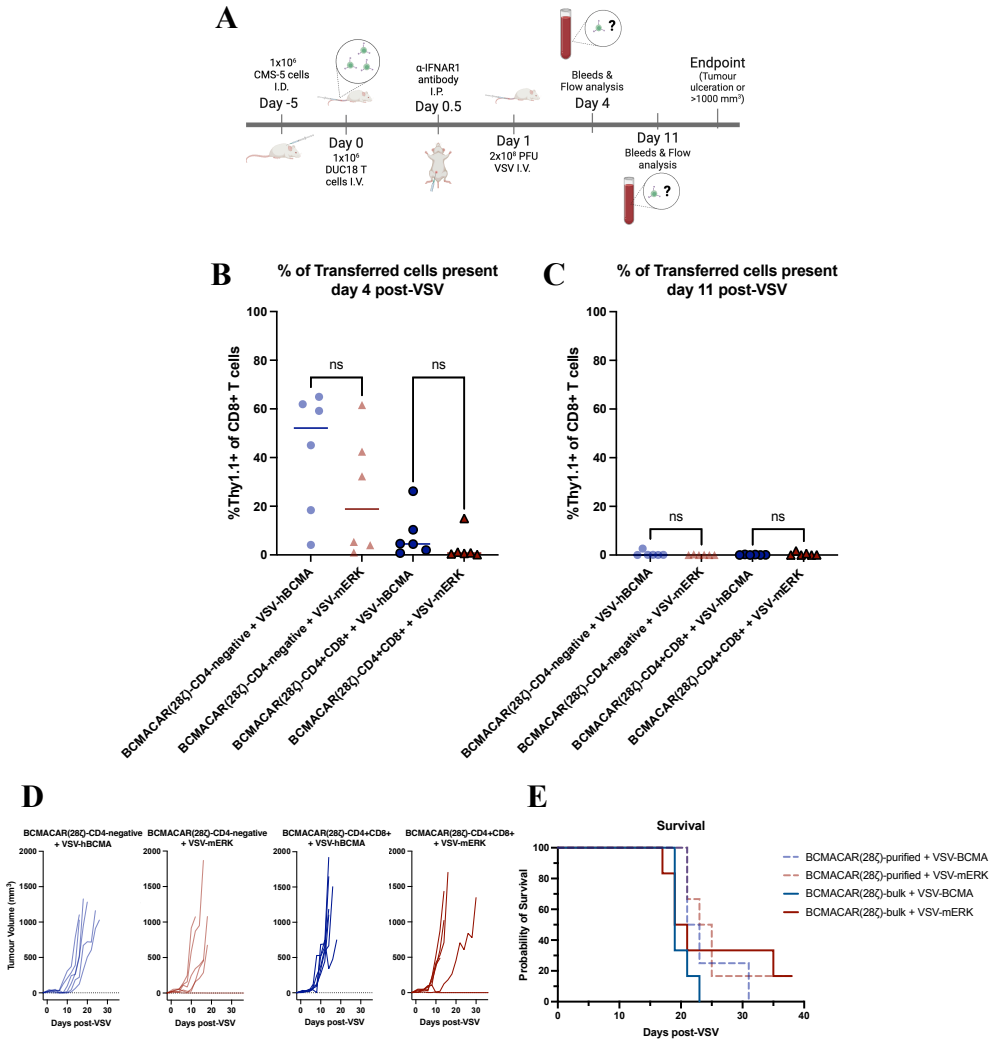

Figure 3.13: Adoptively transferred CD4-negative and CD4+CD8+ DUC18 CAR-T cells in CMS-5 tumour-bearing mice behave similarly in CAR- and TCR-activated boosting following VSV-hBCMA vaccination.(A) Schematic indicating experimental timeline and setup. $1x10^6$ cryopreserved CD4-negative or CD4+CD8+ DUC18 BCMACAR-T cells or DUC18 UT-T cells were administered intravenously and 0.5 mg of αIFNAR1 blocking antibody was delivered intraperitoneally 5 days after CMS-5 tumours were implanted in 6-8 w.o. BALB/c recipients. 24 hours after ACT, $2x10^8$ PFU of rVSV-HBCMA or rVSV-mERK was administered intravenously. (B) 4 and (C) 11 days after vaccination, non-terminal bleeds were collected from the facial vein of each mouse. Following ACK lysis to remove erythrocytes, cells were stained with a fixable viability dye and αCD8, αCD4, αThy1.1, and αCAR antibodies for quantification of cell populations by flow cytometry. Plots represent the percentage of total CD8+ T cells in peripheral blood that express the congenic marker, Thy1.1, in each BALB/c recipient post-boost. 2-way ANOVA statistical analysis was performed. (D) Tumour volume was monitored by manual caliper measurement every 2-3 days for the duration of the experiment. (E) Survival from the time that vaccination was performed (two experiments represented) (n=6).

3.3 Investigating the mechanisms involved in an effective CAR-mediated OV vaccine boost and achieving durable anti-tumour function in the P14/B16.F10-gp33

3.3.1 Investigating the contributions of CD4+ T cells to CD8+ T cell expansion in vivo

The data described above indicated that CD4+ T cells may be detrimental to the manufactured T cell product, but these data cannot discern the impact of the CD4+ T cells on the CD8+ T cells during manufacturing from the impact of the CD4+ T cells on the CD8+ T cells *in vivo*. To address this question, we elected to employ the P14 TCR transgenic system which, as described above, has deep transgene penetrance where the T cell populations are uniformly CD8+ and expressing the gp33-specific TCR. When mice bearing B16F10-gp33 tumours, expressing the target epitope of the P14 TCR, were treated with BCMACAR-engineered P14 cells followed by VSV-hBCMA, we observed robust expansion of the infused T cells and tumour regression; however, the infused T cells failed to persist and the tumour uniformly relapsed (Figure 1.1). We elected to use this model to determine whether adding BCMACAR-engineered CD4+ T cells to the infusion product could improve the durability of the antitumour efficacy. In a preliminary experiment investigating CD4+ T cells within the P14/B16.F10-gp33 model, addition of independently manufactured non-differentiated (ND) wildtype C57BL/6 CD4+ T cells to P14 T cells significantly reduced boosting capacity when compared to P14 CD8+ T cells alone (Figure 3.14B/C). In addition, no benefit in controlling tumour relapse (Figure 3.14D) or survival advantage was observed when including BCMACAR CD4+ T cells (Figure 3.14E).

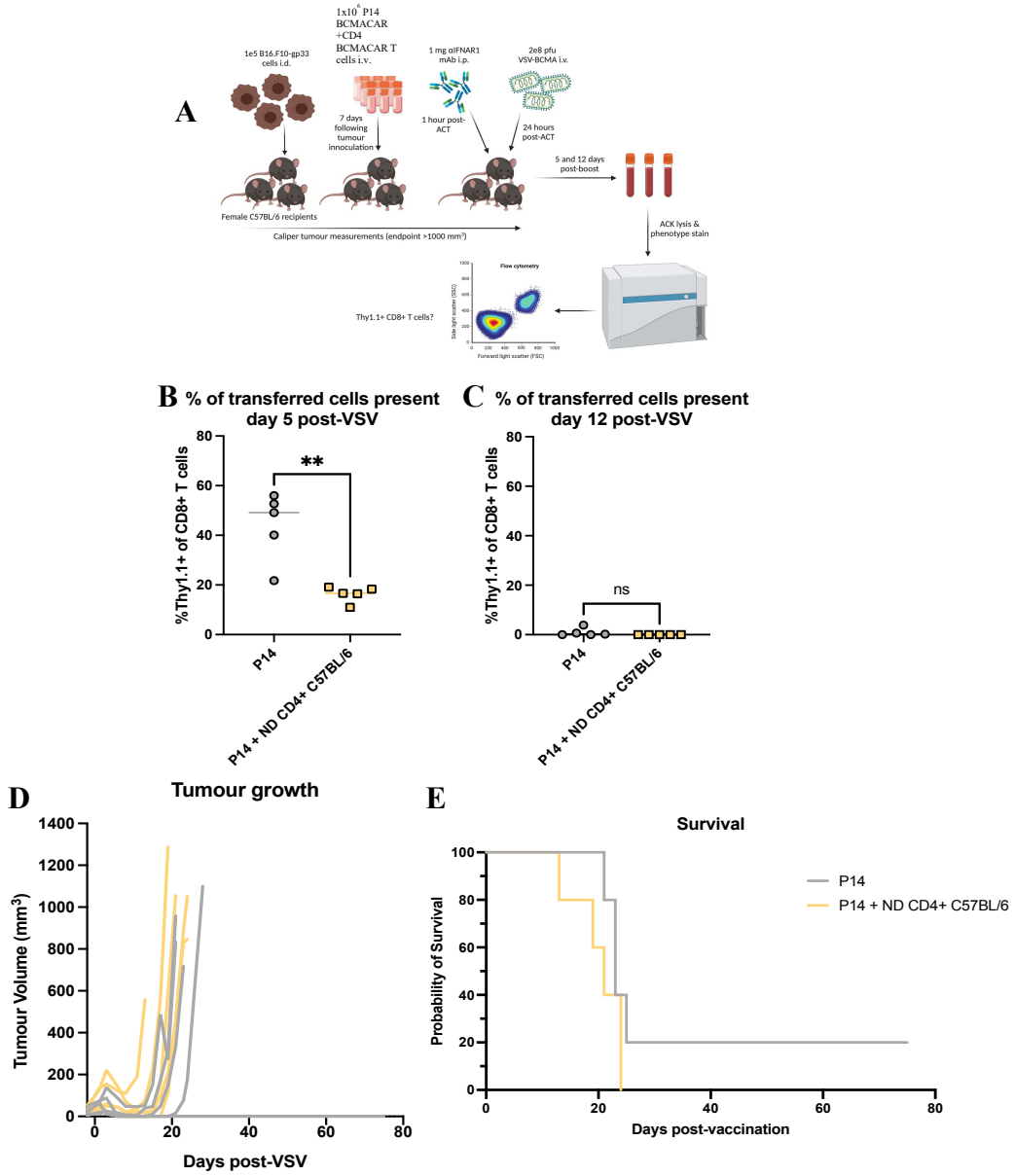

Figure 3.14: Non-differentiated (ND) C57BL/6 CD4+ T cells significantly reduced *in vivo* expansion of P14 T cells when included in the T cell product.(A) Schematic showing experimental procedures. 1x10^6 cryopreserved P14 BCMACAR-T cells or CD4+ C57BL/6 BCMACAR-T cells and P14 BCMACAR-T cells were administered intravenously and 0.5 mg of αIFNAR1 blocking antibody was delivered intraperitoneally 7 days after 1e5 B16-F10-gp33 tumours were implanted in 6-8 w.o. C57BL/6 recipients. 24 hours after ACT, 2x10^8 PFU of rVSV-HBCMA was administered intravenously. (B) 5 and (C) 12 days after vaccination, non-terminal bleeds were collected from the facial vein of each mouse. Following ACK lysis to remove erythrocytes, cells were stained with a fixable viability dye and αCD8, αCD4, αThy1.1, and αCAR antibodies for quantification of cell populations by flow cytometry. Plots represent the percentage of total CD8+ T cells in peripheral blood that express the congenic marker, Thy1.1, in each C57BL/6 recipient post-boost. Student t-test statistical analysis was performed. (D) Tumour volume was monitored by manual caliper measurement every 2-3 days for the duration of the experiment. (E) Survival from the time that vaccination was performed (one experiment represented) (n=5).

To address the question of whether differentiated CD4+ T cells can enhance expansion and/or persistence of the transferred T cells and enhance therapeutic efficacy, we elected to manufacture CAR-engineered CD4+ T cells separately from CAR-engineered CD8+ T cells and pool the T cells after manufacturing, as done by others[66]. We decided to manufacture a differentiated CD4+ T cell population in comparison to our non-differentiated (ND) CD4+ T cell product. The current culture conditions are optimized for CD8+ T cell expansion, as was required in the P14 T cell population. We first aimed to produce a T helper 1 (Th1) CD4+ T cell population. Th1 cells have been well described as critical for an effective anti-tumour response by cytotoxic activity directly, through secretions of IFN-γ or TNF-α, or by stimulating cytotoxic CD8+ T cell activity through production of IL-2[120]. Th1 differentiation requires IL-2 for expansion, IL-12 to promote T-bet expression which is the master regulator of the Th1 genetic program, and αIL-4 to prohibit Th2 differentiation[121-125]. We also included IL-7, as we use in our CD8+ T cell culture for the initial expansion followed by the addition of IL-15[126,127]. The cells were harvested from spleens, CD4+ T cells were magnetically separated and engineered with the BCMACAR through retroviral transduction. Figure 3.15A summarizes this process and describes the media additives included for culturing the ND and Th1 cells. Figure 3.15B shows C57BL/6 CD4+ T cells that were successfully engineered with BCMACAR. To assess whether the manufactured CD4+ T cells were able to produce cytokine when stimulated with CAR target-expressing cells and cytokine production was measured by intracellular cytokine staining. The CD4+CAR+ T cells were assessed for cytokine production as a read-out for activation by the stimulation. The positive control caused almost 100% of the T cells to produce both cytokines, confirming that the T cells were functional. The frequency of CD4+ T cells expressing IFN-γ following the stimulation was assessed as Th1 T cells have been defined as IFN-γ+[122]. The Th1 cells produced IFN-γ in response to the CAR target while the non-differentiated CD4+ T cells, produced no cytokine (Figure 3.15C). While functional it is shown in Figure 3.15D that the viability of the Th1 cells decreases beyond day four of culture.

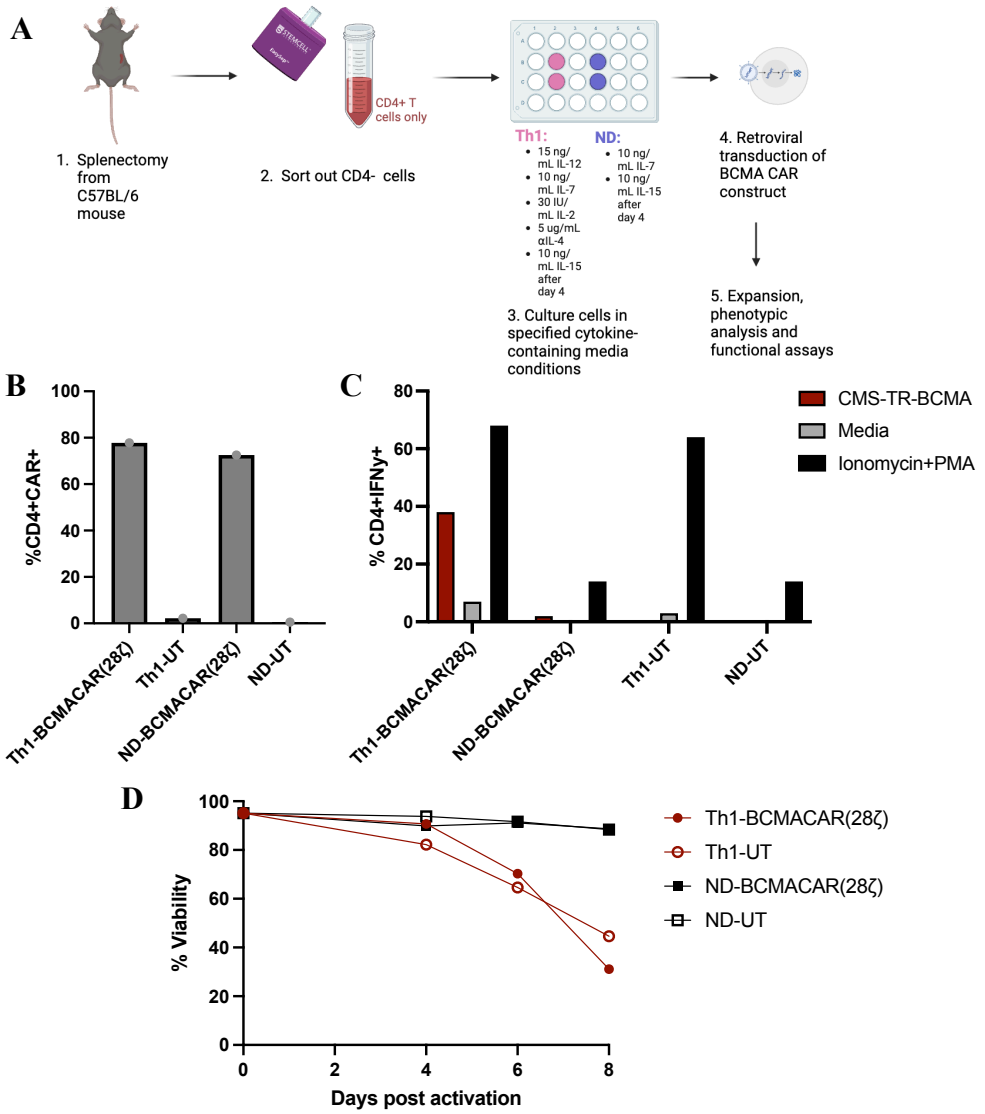

Figure 3.15: T helper 1 (Th1) CD4+ T cells can be engineered with a boosting CAR and produce cytokine in response to CAR stimulation.(A) Schematic indicating experimental protocol followed with the CD4+ T cells. Purified CD4+ T cell populations were isolated from bulk C57BL/6 splenocytes, activated with plate-bound αCD3e, αCD28 antibodies and transduced with BCMACAR retrovirus. They then were cultured for 6 days post-activation in media supplemented with 10 ng/mL rhIL-7, 15 ng/mL rhIL-12, 30 IU/mL IL-2 and 5 ng/mL of αIL-4 and 10 ng/mL rhIL-15 or just IL-7 and IL-15 after day 4 of culture prior to phenotype analysis. Th1 represents T helper 1 CD4+ T cells while ND represents non-differentiated CD4+ T cells (B) C57/BL6 cells were collected and stained with fluorescently conjugated anti-mouse antibodies against transduction and phenotype (CD62L, CD44) markers prior to FACS analysis. Gating strategy: Lymphocytes> single cells > CD45.2+ cells > CD4+ and CD8+ (C) *In vitro* intracellular cytokine staining assay where T cells derived from TDLN were stimulated with various tumour targets and the cytokine response of IFN-γ was assessed at a per cell basis using. Cells were then stained using αCD8, αCD4, αCD45.2, αCAR, αIFN-γ antibodies and assessed by flow cytometry. (B) Viability of T cell cultures were assessed every two days for an 8-day culture period post-activation using an automated cell counter and AOPI staining.

To overcome this loss in viability, engineered CD4+ T cells were collected and cryopreserved five days post-activation where the engineered Th1 T cells displayed no loss of viability (Figure 3.16A) and high expression of the BCMACAR (Figure 3.16B). To then assess whether the engineered-Th1 T cells were capable of proliferating following stimulation of the CAR and to determine whether the engineered-Th1 T cells could provide help to P14 CD8+ T cells, we performed a proliferation assay with each cell population (Th1, P14-CD8) alone or in combination at a 1:1 ratio. The Th1 T cells proliferated modestly, but when combined with CD8+ P14 T cells (Th1 CD4+ and P14 T cells), the P14 T cell population seemed to have a marginally increased proliferation index (Figure 3.16C) and fold expansion (Figure 3.16D) when comparing to the condition where P14 T cells were assessed alone.

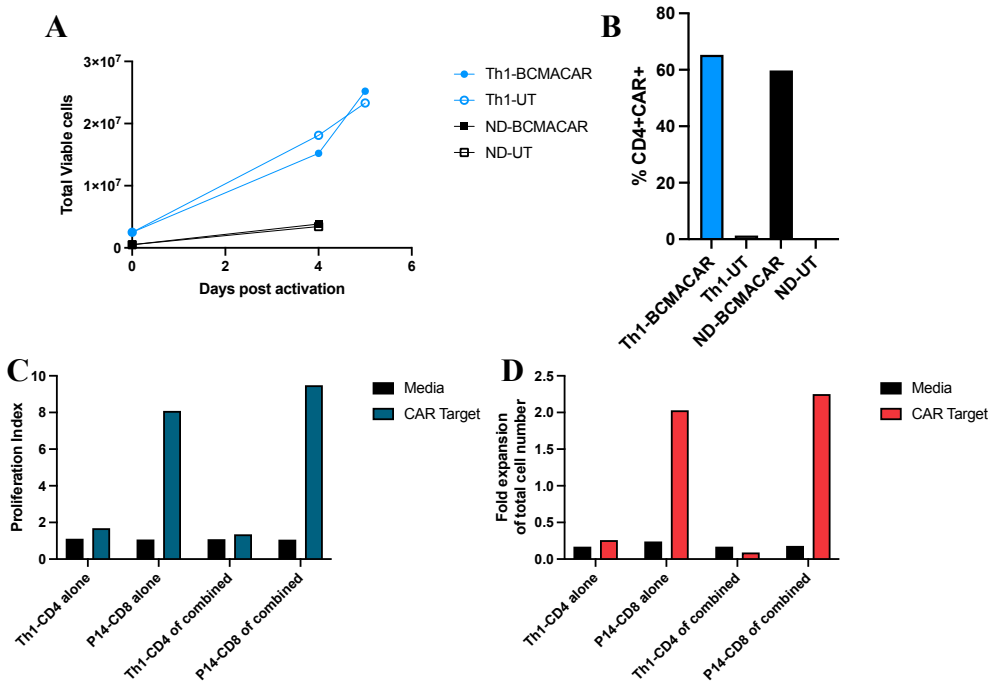

Figure 3.16: Th1 CD4+ T cells can proliferate in response to CAR stimulation and modestly increase proliferative capacity of P14-Thy1.1 T cells *in vitro*. Purified CD4+ T cell populations were isolated from bulk C57BL/6 splenocytes, activated with plate-bound αCD3e, αCD28 antibodies and transduced with BCMACAR retrovirus. They then were cultured for 6 days post-activation in media supplemented with 10 ng/mL rhIL-7, 15 ng/mL rhIL-12, 30 IU/mL IL-2 and 5 ng/mL of αIL-4 and 10 ng/mL rhIL-15 or just IL-7 and IL-15 after day 4 of culture prior to phenotype analysis. Th1 represents T helper 1 CD4+ T cells while ND represents non-differentiated CD4+ T cells. (A) Cell viability of T cell cultures was assessed every two days for a 7-day culture period post-activation using an automated cell counter and AOPI staining. (B) T cells were collected and stained with fluorescently conjugated anti-mouse antibodies against transduction and phenotype (CD62L, CD44) markers prior to FACS analysis. Gating strategy: Lymphocytes> single cells > Thy1.1+ cells > CD4+ and CD8+. (D and E) CellTrace Violet (CTV) dilution assay to assess *in vitro* proliferation of BCMACAR T cells upon stimulation with BCMA- or mERK-expressing target cells. CTV-labelled T cells were co-cultured with target cells for 4 days followed by flow cytometric analysis. (D) Represents proliferation index; (D) represents fold expansion of total cells into the assay versus cells based on events collected vis flow cytometry. Cells shown in these plots were gated down from live cells > lymphocytes > single cells > Thy1.1+ cells > CD8+ cells. One experiment represented.

To assess whether the engineered-Th1 cells could provide help to engineered-P14 T cells *in vivo*, we performed an experiment where the two cell populations were mixed at a 1:1 ratio so that a dosage total of $1x10^6$ T cells total ($5x10^5$ P14 T cells and $5x10^5$ Th1 CD4+ T cells) was given to mice bearing B16F10-gp33 tumours (Figure 3.17A). The engineered Th1 cells were manufactured from C57BL/6 splenocytes and transferred into C57BL/6 recipient mice; as such, we could not distinguish transferred Th1 cells from endogenous CD4+ T cells. We did not include an experimental group treating with P14 T cells alone because an observable difference of persistence beyond 5 days following vaccination would infer that the Th1 cells did ameliorate the P14 T cells persistence. In addition, long-term tumour regression would also indicate successful help. These outcomes would be clearly different from the uniform observation of no presence of P14 T cells by day 12 post-vaccination and tumour relapse. In place of this, representative data of BCMACAR P14 T cell expansion, tumour outgrowth and survival are shown alongside results from this experiment for contrast purposes in Figure 3.17. The analyzed peripheral blood showed an increase in P14 T cell expansion five days after vaccination, reaching about half the level of the representative expansion of P14 T cells alone, which aligns with the half dose of P14 T cells administered (Figure 3.17B). None of these cells persisted to the second peripheral bleed timepoint (Figure 3.17C) and tumours relapsed after a brief regression (Figure 3.17D). All recipient mice eventually succumbed to tumour burden (Figure 3.17E). This suggests that the differentiated CD4+ Th1 T cells are not able to rescue the P14 T cells in terms of persistence and long-term clearance of tumour burdens.

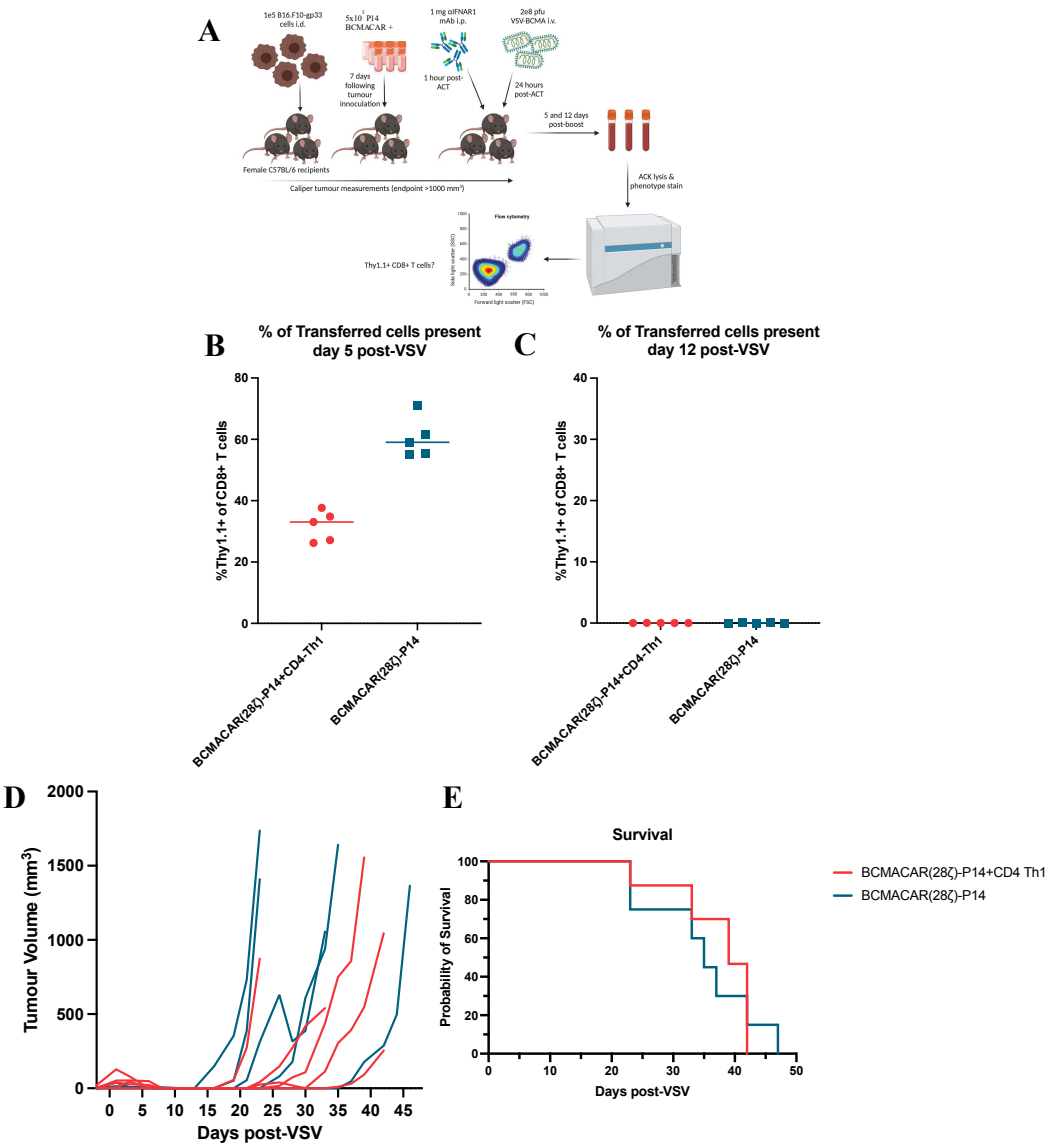

Figure 3.17: Including Th1 CD4+ T cells in ACT and recombinant VSV-hBCMA boosting of P14 T cells does not benefit P14 T cell persistence or prevent tumour relapse in B16-F10-gp33 tumour-bearing mice.(A) Schematic indicating experimental timeline and setup. $5x10^5$ cryopreserved P14 BCMACAR-T cells and $5x10^5$ cryopreserved Th1 C57BL/6 BCMACAR-T cells were mixed at a 1:1 ratio and administered intravenously and 0.5 mg of αIFNAR1 blocking antibody was delivered intraperitoneally 7 days after 1e5 B16-F10-gp33 tumours were implanted in 6-8 w.o. C57BL/6 recipients. 24 hours after ACT, $2x10^8$ PFU of rVSV-HBCMA was administered intravenously. P14 alone data is from a separate experiment and was not preformed alongside the combined experiment. (B) 5 and (C) 12 days after vaccination, non-terminal bleeds were collected from the facial vein of each mouse. Following ACK lysis to remove erythrocytes, cells were stained with a fixable viability dye and αCD8, αCD4, αThy1.1, and αCAR antibodies for quantification of cell populations by flow cytometry. Plots represent the percentage of total CD8+ T cells in peripheral blood that express the congenic marker, Thy1.1, in each C57BL/6 recipient post-boost. The P14 alone data is representative. (D) Tumour volume was monitored by manual caliper measurement every 2-3 days for the duration of the experiment. (E) Survival from the time that vaccination was performed (one experiment represented) (n=5).

3.3.2 Assessing the inclusion of a mIL-15 transgene into the BCMACAR construct to improve T cell persistence and tumour clearance in vivo

Without CD4+ T cell help in priming, CD8+ T cells can display a "helpless" phenotype upon secondary responses and undergo TRAIL-mediated apoptosis or show T cell dysfunction[69,70,71,72]. There is evidence that providing a constitutive IL-15/STAT5 signal to CD8+ T cells can overcome the requirement for CD4 help during T cell priming[128,129]. Co-expression of IL-15 and a CAR had demonstrated increased persistence and anti-tumour effects when compared to control CAR T cells by several groups[130,131,132]. To assess this in our CAR/OVV strategy, a construct was designed to co-express our 28ζ-BCMACAR and secreted murine IL-15 (mIL-15) in a single vector (FigureA). It was hypothesized that this BCMACAR variant could support our "helpless" P14 BCMACAR T cells in place of CD4+ T cells and extend persistence.

In preliminary studies, this construct appeared to increase the number of viable T cells following an *in vitro* functional assay (Figure 3.18B), so we decided to compare it to our BCMACAR construct *in vivo*. C57BL/6 mice bearing B16F10-gp33 tumours were either treated with cells engineered with the 28zBCMACAR construct or with cells engineered with the 28zBCMACAR_mIL-15 construct. The inclusion of the IL-15 transgene did not affect the expansion of engineered T cells measured five days after vaccination (Figure 3.18C); however, neither group persisted until twelve days post-vaccination (Figure 3.18D). Mice in both groups had tumours relapse at very similar timepoints following vaccination, showing that the inclusion of the IL-15 transgene is not advantageous in the anti-tumour response (Figure 3.18E). All experimental mice in both groups succumbed to their tumour burden with no significant difference between the BCMACAR and BCMACAR_mIL-15 treated groups survival probability (Figure 3.18F), indicating no benefit for T cell persistence and tumour-free survival.

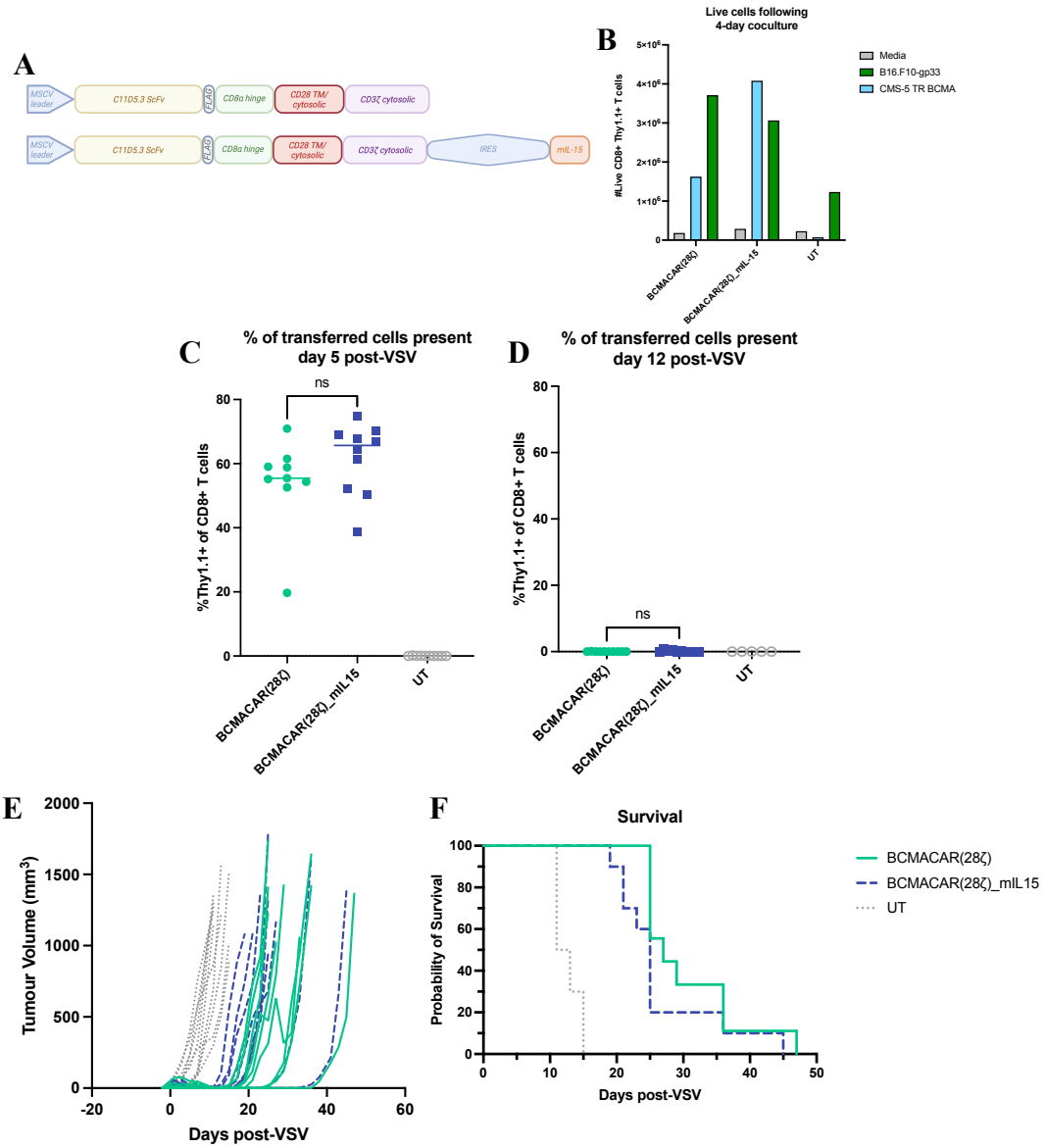

Figure 3.18: Adoptive transfer and recombinant VSV boosting of BCMACAR (28ζ)_mIL-15 P14 T cells does not augment T cell persistence in B16-F10-gp33 tumour-bearing mice.

(A) Schematic indicating experimental timeline and setup. (B) P14 BCMACARmIL-15-T cells increased T cell number following *in vitro* CAR-stimulation. 1x10^6 cryopreserved P14 BCMACAR-T cells, P14 BCMACARmIL-15-T cells or P14 UT-T cells were administered intravenously and 0.5 mg of αIFNAR1 blocking antibody was delivered intraperitoneally 7 days after 1e5 B16-F10-gp33 tumours were implanted in 6-8 w.o. C57BL/6 recipients. 24 hours after ACT, 2x10^8 PFU of rVSV-HBCMA was administered intravenously. (C) 5 and (D) 12 days after vaccination, non-terminal bleeds were collected from the facial vein of each mouse. Following ACK lysis to remove erythrocytes, cells were stained with a fixable viability dye and αCD8, αCD4, αThy1.1, and αCAR antibodies for quantification of cell populations by flow cytometry. Plots represent the percentage of total CD8+ T cells in peripheral blood that express the congenic marker, Thy1.1, in each C57BL/6 recipient post-boost. Student t-test statistical analysis was performed. (D) Tumour volume was monitored by manual caliper measurement every 2-3 days for the duration of the experiment. (F) Survival from the time that vaccination was performed (two experiments represented) (n=10).

3.3.3 Tracking bioluminescent-VSV-hBCMA in vivo to investigate viral kinetics and distribution with transient type I IFN blockade

To gain a better understanding of the *in vivo* kinetics and trafficking of the recombinant VSVΔM51 combined with transferred CAR-T cells, we developed dual-expression constructs containing the surface-expressed hBCMA chimeric antigen (VSV-hBCMA) and a red-shifted firefly luciferase (rsLuc) transgene (VSV-rsLuc-hBCMA) (Figure 3.19). These constructs were cloned and incorporated into the VSVΔM51 backbone, followed by plaque purification, titration, and sequencing to confirm correct transgene integration (data not shown). CMS-5 cells were infected with each virus, and expression of both transgenes was confirmed by flow cytometry and was consistent with VSV-hBCMA (Figure 3.19B/C). The cytotoxicity of the dual-expression virus was comparable to that of the virus expressing only hBCMA, though slightly reduced (Figure 3.19D). Lastly, we confirmed that VSV-expressed rsLuc could be detected *in vivo* following vaccination in C57BL/6 mice. Six hours post-vaccination, the viruses primarily localized to the spleen (Figure 3.19E).

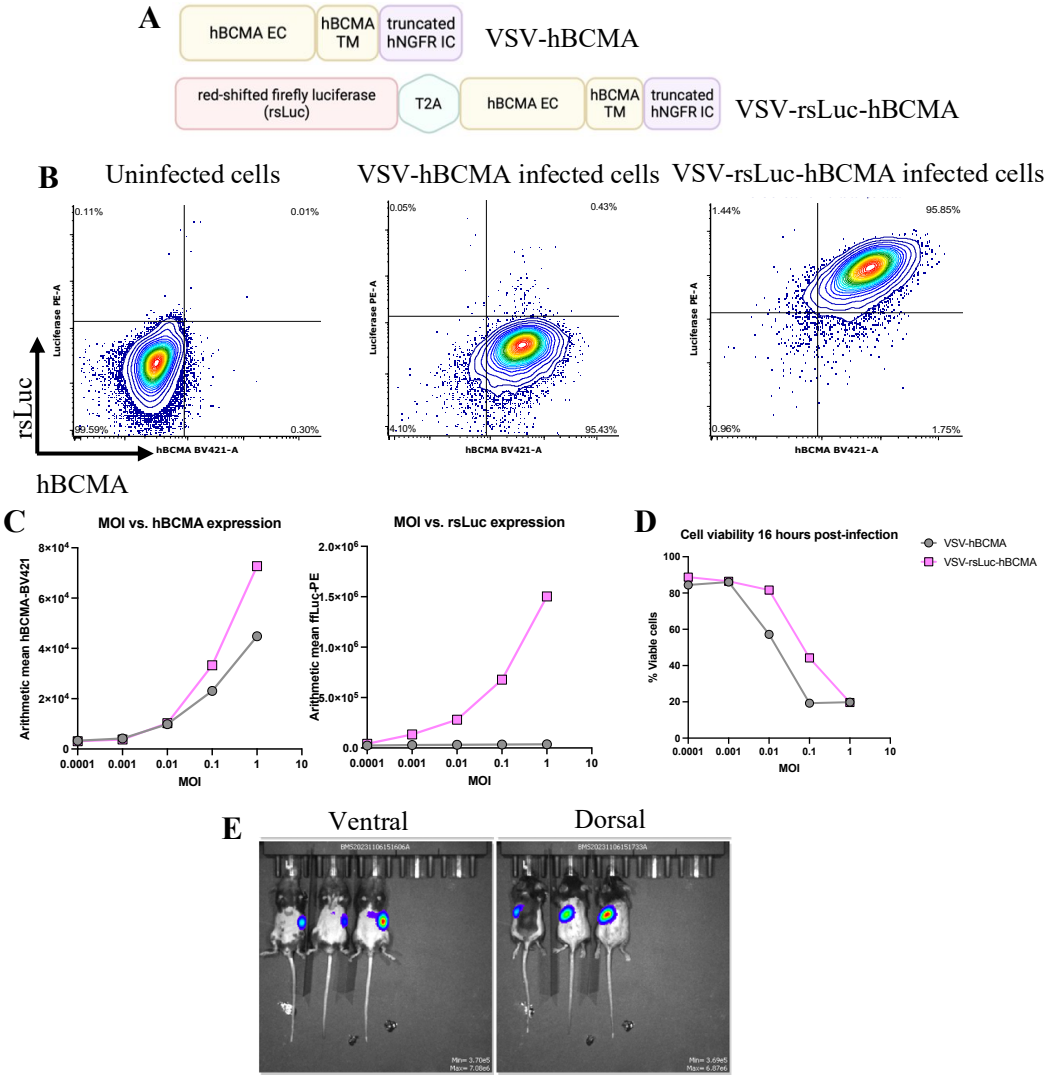

Figure 3.19: Generating and validating VSV-rsLuc-hBCMA.

(A) Schematic representation of single expression and dual-expression antigen constructs. (B) Representative flow plots for co-expression of hBCMAtNGFR and rsLuc transgenes in CMS-5 cells infected with VSV at an MOI of 1.0 for 16 hours. (C) Relative expression of rsLuc, hBCMAtNGFR, and (D) viability of infected CMS-5 cells at different MOIs after 16 hours of infection, determined by flow cytometry. (E) IVIS imaging of naïve C57BL/6 mice 6 hours post-vaccination with VSV-hBCMA/rsLuc viruses. Mice were given αIFNAR1 antibody intraperitoneally 24 hours prior to vaccination (one experiment represented) (n=3).

In the context of the CAR-mediated boosting of adoptively transferred T cells, we infuse recipients with αIFNAR1 antibody prior to vaccine administration. Blocking type I interferon is required to maximize the magnitude of the boost and anti-tumour function of transferred T cells in both the P14 and DUC18 systems. To understand how the interferon

blockade affects VSV distribution, replication and persistence, we used the validated VSV-rsLuc-hBCMA to track our viral replication in the presence and absence of type I IFNs. Albino C57BL/6 mice were used for these experiments to limit absorbance of the bioluminescence. The VSV-rsLuc-hBCMA was administered intravenously and mice were imaged at 6-, 48- and 96-hours following vaccination to assess for virus level and localization in each group (Figure 3.20A). The transferred cells expanded in the periphery as expected, with only the BCMACAR+ αIFNAR1 group having measurable P14 T cells in the peripheral blood five days following vaccination (Figure 3.20B) and a small percentage of these transferred cells in this group persisted to twelve days following vaccination (Figure 3.20C). This increased persistence may be a feature of the albino C57BL/6 mice as we rarely see persistence in wild type C57BL/6 mice. Inclusion of transient IFNAR1 blockade increased viral replication in both BCMACAR and UT groups at all timepoints (Figure 3.20D). At the 48- and 96-hour timepoints, we see a consistently slightly higher level of the virus in the presence of UT P14 T cells, indicating potential on-going antigen clearance by BCMACAR P14 T cells that may have been delayed. This suggests that inclusion of the transient type I IFN blockade increases the longevity and availability of the viral transgene when compared to PBS controls.
We observed an immediate trafficking of the virus to the spleen in all groups at the earliest timepoint (Figure 3.20E). Interestingly, by the next timepoint (48 hours), the virus appears to concentrate in the lower abdominal or pelvic region of mice only in the αIFNAR1-treated groups, while the virus remains in the spleen in the PBS control groups and this is also observed at the last timepoint (96 hours). This could suggest that inclusion of the transient type I IFN blockade allows for more robust infection and trafficking of the virus to other regions of the body as well as increasing overall viral load, leading to the boosting of transferred BCMACAR T cells.

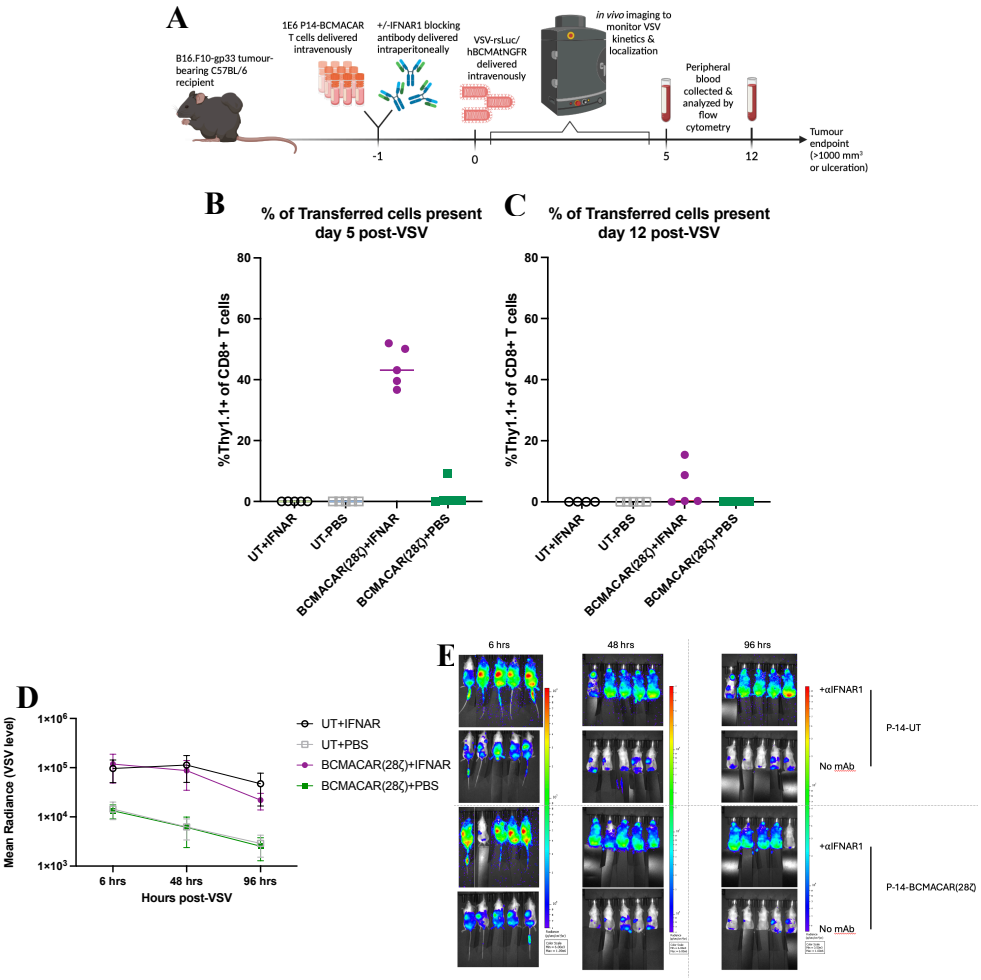

Figure 3.20: Tracking VSV-rsLuc-hBCMA with and without αIFNAR1 blockade shows differences in viral kinetics and infection levels.

(A) Schematic indicating experimental timeline and setup. Mice received 1x10^6 P14-BCMACAR or P14-UT T cells I.V. and 0.5 mg of αIFNAR1 blocking antibody or PBS intraperitoneally. 24 hours after T cell administration, mice received 2x10^8 PFU of VSV-rsLuc-BCMA I.V. At 6 hours, 48 hours, and 96 hours post-vaccination, mice were given luciferin substrate intraperitoneally and imaged using the IVIS live cell imager under gas anesthesia (isoflurane). (B) (C) 5 and 12 days after vaccination, non-terminal bleeds were collected from the facial vein of each mouse. Following ACK lysis to remove erythrocytes, cells were stained with a fixable viability dye and αCD8, αCD4, αThy1.1, and αCAR antibodies for quantification of cell populations by flow cytometry. Plots represent the percentage of total CD8+ T cells in peripheral blood that express the congenic marker, Thy1.1, in each recipient post-boost. (D) Mean radiance of images taken of each group (E) Summarized images of the dorsal view of data represented in (D) (one experiment represented) (n=5).

4 Discussion

Adoptive CAR T cell therapies have demonstrated remarkable efficacy in treating hematological malignancies, but significant biological and practical challenges hinder their clinical success against solid tumours. Such challenges include a lack of robustly expressed tumour-exclusive target antigens, and inefficient homing to an intratumorally heterogeneous antigen landscape. These factors limit treatment safety and efficacy and promote antigen escape. Genetic insertion of synthetic antigen receptors specific to tumour antigens into bulk polyclonal T cell populations can enable large numbers of tumour-reactive T cells to be rapidly produced for adoptive transfer. However, the success of this approach relies on prior knowledge of targetable tumour-associated antigens and expression of the target antigen uniformly across all cancer cells. Some solid tumours do have tumour-related antigens, such as human epidermal growth factor receptor 2 (HER2) in breast, gastric, ductal, pancreatic, non-small cell lung cancer and glioblastoma[133], prostate-specific membrane antigen (PSMA) in prostrate cancer[134] and Claudin 18.2 in gastric cancers[135]. Unfortunately, solid tumours consistently lose expression of these targets and outgrowth of antigen-negative, resistant cells can negate the efficacy of these single-targeted receptors. Additionally, the engraftment of transferred T cells depends on a lymphodepleting pre-treatment step which is necessary in achieving the anti-cancer activity and can create a niche for transferred cells but can also eliminate any anti-tumour activity by endogenous cells. The findings presented in this thesis aimed to develop a novel approach to ACT through proof-of-concept work, wherein reduced numbers of tumour-specific memory T cells are engineered with a CAR and engaged with a paired vaccine that expresses the CAR target to drive *in vivo* expansion and differentiation of the engineered T cells.

Endogenous tumour reactive T cells such as tumour infiltrating lymphocytes (TIL), or T cells derived from tumour-draining lymph nodes (TDLN) are an attractive T cell source to engineer with our CAR as no prior tumour antigen knowledge is required. As these T cells are isolated from either tumour tissue (TIL) or proximal lymph nodes to the solid tumour (TDLN), they can already recognize multiple tumour antigens through their native TCRs. We succeeded in isolating and engineering TDLN-derived T cells with the BCMACAR, but the engineering of TIL requires further investigation. We saw minimal expansion in our isolated populations, and we did not successfully engineer our TIL with a synthetic receptor. It is possible that modifications to expansion protocols, such as the Rapid Expansion Protocol (REP) that has been used to engineer CAR-TIL from companion dog, mice and human tissues[110-112,136], could be beneficial in achieving the expansion we lacked in what was reported and could lead to successful engineering. The use of some components of REP, like using feeder immune cells from irradiated splenocytes, with modifications to lower levels of IL-2 required, could allow for the required expansion of TIL and allow successful transduction.

To investigate another naturally occurring tumour-specific T cell source, we begin culturing and engineering T cells derived from TDLN. We demonstrated in this thesis the successful expansion, engineering and CAR-functionality of these TDLN-derived T cells. Complications emerged within the cytotoxic capacity of these T cells when re-challenged with tumour targets from which they were derived. When TDLN-derived T cells were

assessed for cytokine production in response to a short-term incubation with target tumour cells, we observed no cytokine production. The TDLN-derived T cells did produce cytokine in response to stimulation with the cells expressing hBCMA (the CAR target) and the positive control (Ionomycin and PMA), proving their functionality. As we activated and expanded TDLN-derived cells using anti-CD3 and anti-CD28 antibodies, we did not select for tumour reactivity in the engineered population. It is possible that a small fraction of all TDLN-derived T cells isolated were tumour-specific and our experimental assays did not account for this factor.

Some solid tumours do express targetable antigens, including HER2, PSMA and Claudin18.2, which have all been targeted clinically with CAR T cells[137,138,139]. A possible method of modifying our universal CAR/OVV could utilize these "shared" tumour-related antigens as our boosting antigen instead of an unrelated antigen. For example, in HER2+ tumours, polyclonal T cells could be isolated from tumour tissues and engineered with a HER2-specific CAR. In parallel VSV-ΔM51 could be engineered with a HER2 transgene. These multi-specific HER2CAR T cells could then be infused back into a patient and expanded upon vaccination. As tumour cells and virally infected cells could express HER2, this could allow for a dual-specific attack, as T cells would confer cytotoxicity through the TCR and the HER2CAR. While not entirely universal, this method could be broadly applied to patients with cancers expressing shared antigens. As we have seen success in treating solid tumours when vaccinating using a TAA, utilizing these shared antigens could allow for successful expansion of transferred T cells and potentially engaging endogenous immune cells through antigen spreading and broad immunostimulation from OV vaccination.

Other groups have also proposed similar hypotheses. For example, Zhu et. al have engineered murine colorectal cancer cells lines with human CD19, isolated TIL from tumour-bearing mice and engineered cells with a CD19CAR-TIL[136]. They observed that adoptively transferred CAR-TIL controlled tumour growth in immunocompetent hosts without "on-target off-tumour" toxicities. Following these findings, they hypothesize that, combining engineered OVs with CAR-TIL, could achieve overexpression of engineered tumour antigens in the TME, engage both CAR-TIL and endogenous T cells in an anti-tumour response. Indeed, another group has shown that recombinant oncolytic HSV-1 VC2-OVA expressing a fragment of ovalbumin (OVA) can also act as a vector to deliver antigens to the TME and stimulate strong anti-tumour immunity in syngeneic models[140]. As we have also shown VSV to be a promising vector to deliver transgenes, it is possible that using this broader targeting method in our CAR/OVV system with CAR-TIL or T cells from TDLN could demonstrate superior activity than utilizing an unrelated antigen.

The DUC18-Thy1.1/CMS-5 model has revealed interesting avenues to explore in the context of the universal boost strategy. T cell manufacturing from CD4-depleted DUC18 splenocytes achieved T cell expansion upon VSV-HBCMA vaccination when using the 28ζ-BCMACAR variant. When manufacturing T cells from bulk splenocytes, we did not observe any T cell expansion upon VSV-HBCMA vaccination. CD28 co-stimulus has also been shown to prompt more rapid and intense CAR T cell activity than 4-1BB co-stimulus[141]. This can result in increased T cell exhaustion when using CD28 co-stimulus. In CD4-negative DUC18 T cells, this may also be the case. CAR interactions

with viral antigens may lead to superior CAR T cell expansion in the periphery when driven by CD28 co-stimulation, compared to 4-1BB co-stimulation, due to the initial enhanced activity prompted by CD28. This superior expansion may also lead to subsequent exhaustion and CAR T cell dysfunction that results in a failure to demonstrate anti-tumour activity and persistence we observed.

We next tracked the CD4-negative and CD4+CD8+ DUC18 CAR T cells following VSV-hBCMA vaccination *in vivo* and found no observable difference in T cell trafficking or expansion levels relative to mean radiance. This led us to assess whether CD4-depletion has any effects on *in vivo* expansion when the engineered T cells were boosted with a vaccine that stimulates the DUC18 TCR. We found that the CAR T cell *in vivo* expansion was consistent regardless of the receptor as CD4-negative CAR T cells still expanded marginally more than mixed CAR T cells. We also observed long-term survival of two mice who received vaccines that stimulate the TCR, and this outcome was not affected by the presence or absence of CD4+ T cells in the manufactured product. The adoptively transferred T cells were not measurable in either long term survivor. We suspect the durable tumour clearance was due to endogenous tumour-specific T cells that emerge through antigen spreading described previously by our group[95].

However, this does not explain the consistent lack of expansion and tumour control we observed by transferring the CD4+CD8+ T cells into recipient mice. Additional observations in the P14 model showed detrimental effects on T cell expansion when transferring undifferentiated CD4+ T cells alongside CD8+ P14 T cells. This led us to further investigate the CD4+ T cell population we were transferring. In this regard, we optimized the culture and engineering of Th1 T cells, due to their potential capacity to support our tumour-specific CD8+ T cells. We confirmed that the engineered Th1 cells produced cytokines (IFN-γ and TNF-α) in response to CAR-stimulus. In the context of mixed cultures with Th1 and P14 CD8+ T cells, we observed modest enhancement of P14 CD8+ T cell proliferation. However, the P14 CD8+ T cells are highly proliferative and, thus, may not benefit from additional CD4+ T cell help *in vitro*. When the CAR-Th1 cells were mixed with CAR-P14 CD8+ T cells prior to infusion, we observed no clear benefit in the context of P14 CD8+ T cell persistence or tumour control relative to historic controls, but further work is required to make firm conclusions on this matter.

It is possible that Th1 cells are not optimal for this system. Th9 cells, which produce IL-9, may be a better choice as a CD4+ T cell product than Th1 cells for adoptive transfer as they have been shown to activate and prime CD8+ T cells more effectively than Th1 cells[142]. When co-transferring CD8+ T cells alongside Th1 or Th9 T cells, Lu et al. observed increased percentages and larger numbers of CD8+ T cells in tumour tissues when Th9 cells were co-transferred[142]. Th9 cells were also proven to help CD8+ T cell activation at a higher incidence than Th1 cells by increasing chemokine-dependent recruitment of DCs to the tumour tissues[142]. The authors indicated that this superior recruitment led to additional delivery and presentation of tumour antigens to CD8+ T cells in TDLN. Incorporating Th9 cells into the CAR/OVV boosting strategy may address the limited persistence of the P14 CD8+ T cells. If Th9 CAR T cells can replicate this superior activation of CD8+ T cells and promote antigen presentation, Th9 CAR cell may provide better support than Th1 CAR T cells exhibited in this thesis. We have shown that

TCR-mediated engagement of transferred T cells with viral antigens depends on DC presentation to CD8+ T cells[97]. If DCs play a similar role in in CAR-mediated engagement and expansion and Th9 cells can better facilitate this process, it is possible this may improve T cell persistence and anti-tumour activity.

As was described, without CD4+ T cell help in priming, CD8+ T cells can display a "helpless" phenotype upon secondary responses which can dimmish anti-cancer efficacy. There is evidence that providing a constitutive IL-15 signals to CD8+ T cells can overcome the requirement for CD4 help during T cell priming[128-132], so we explored the possibility of augmenting IL-15 signalling in the engineered T cell product. When comparing T cells engineered to co-express BCMACAR(28ζ) and a full-length murine IL-15 transgene to T cells expressing only BCMACAR(28ζ), we did not observe any difference in the expansion or persistence of the T cells, nor did we observe any advantage on tumour control or survival of treated mice. Therefore, IL-15 alone may not be sufficient to overcome the need for CD4+ T cell help and/or co-stimulation by a licensed DC in our CAR/OVV system. These findings support the notion that perhaps more factors are affecting the transferred T cells in our universal system that *in-situ* IL-15 cannot rescue.

In attempts to better understand our viral distribution and kinetic upon vaccination, we also tracked an rsLuc-engineered version of our VSV-HBCMA *in vivo*. We noted that inclusion of the αIFNAR antibody allowed for higher levels of the transgene presence for longer when comparing to the PBS treated controls. Using VSV-HBCMA, which contains the ΔM51 mutation and leads to an inability to infect healthy cells with intact IFN response as previously described, it is logically sound that a temporal systemic blockade of type I IFN signalling aids in viral replication and spread. At 6 hours post-vaccination, we observed localization of the virus to the spleen in all groups. Interestingly, though, independent of the T cell treatment, in mice with transient IFNAR blockade, the strongest signal emanated from the lower pelvic region of the mice. As we have seen previously that VSV- ΔM51 has preference for secondary lymphoid organs, it is possible that the IFNAR blockade allowed for viral spread to the iliac, mesenteric or sciatic lymph nodes. It is also possible that other tertiary lymphoid organs located in the digestive tract, such as the gut-associated lymphoid tissue (GALT) and Peyer's patches may also become a viral reservoir in the lower pelvic region and contribute to this increased signal.

It is well known that CARs activate T cells in a faster and more robust manner when compared to TCR-mediated T cell activation and that this may lead to activation-induced cell death (AICD)[143,144]. Indeed, Wachsmann et al. (2021) demonstrated this using human-derived T cells engineered with a CD19 targeting CAR and TCR (eTCRs) and found that CAR T cells only outperform eTCRs functionally under low antigen pressure[145]. They claimed that the efficacy of CAR T cells over eTCR T cells is a function of antigen exposure as continued presence of antigen led to significantly impaired CAR T cell expansion and higher incidences of activation-induced cell death (AICD) *in vitro*[145]. AICD is an important process in homeostasis and occurs when activated cells undergo apoptosis when interacting with a death factor and its receptor[146]. In addition, Haffner et al. compared the persistence of human HER2CAR-TIL to unengineered TIL in HER2+

tumour-bearing NSG mice following ACT[134]. They saw a significant reduction of CD3+CD45+ cells present in HER2CAR-TIL-treated mice when comparing to un-engineered TIL-treated mice[134]. While the authors do not comment on these data, this observed contraction may also be an example of CAR-T cells experiencing ACID to a higher incidence than T cells stimulated through their TCR. The administration dose of VSV (2e8 PFU) was derived from T cell transfer experiments wherein T cells were expanded following TCR-mediated expansion[95]. Despite this, the VSV-hBCMA dosage administered to recipient mice to expand transferred CAR T cells was never modified or examined in our studies. When we blocked type I IFN signalling in the CAR/OVV system, we observed increased levels of VSV-hBCMA for longer durations in comparison to when IFN signalling is left intact. This allows T cells to expand more than what is observed without blocked type I IFN signalling, but it is also possible that this increased signal is too much for the BCMACAR T cells for extended periods. This increased antigen pressure due to increased duration and spread of our virus may cause our transferred T cells to undergo AICD and demonstrate the observed lack of persistence following the initial expansion. It is possible that the dosage of VSV and subsequent level of transient antigen present that was sufficient for activation and expansion of TCR-activated vaccination is overpowering for CAR-activated vaccination. Employing a lower dose of VSV in combination with transient IFNAR blockade would be an interesting investigation. This strategy may avoid this ablation of transferred cells and allow for persistence of transferred cells.

We do not perform any lymphodepletion prior to adoptive T cell transfer. In previous work done in our group, a VSV encoding a TAA was used to expand unengineered T cells through TCR-activation. Endogenous CD8+ T cells complemented adoptively transferred cells in the anti-tumour response and formed a long-term memory pool for immune surveillance[95]. This indicated that lymphodepletion prior to ACT/OVV may damper the long-term tumour control observed. A core difference between this TCR/OVV strategy and our CAR/OVV system is the presence of a CAR. CAR T cells can have the potential to induce anti-CAR immune responses to non-self-components of the CAR constructs[52]. Therefore, it is possible that the widespread infection from blocking type I IFN signalling and subsequent CAR T cell expansion elicits a stronger endogenous immune response against the transferred CAR T cells, instead of against tumour antigens. This may also cause the lack of transferred T cell persistence observed in both TCR transgenic models. In the clinic, lymphodepletion has been deemed critical in reaching superior outcomes with CAR-T cell treatments and its inclusion has led to greater transferred T cell expansion, persistence and efficacy[147]. In a clinical trial using CD19 targeted CAR T cell therapy, 50% of patients who did not receive lymphodepletion exhibited anti-CAR responses[147]. While endogenous cells were deemed necessary in the long-term anti-tumour response in the TCR/OVV strategy[95], this may not be the case in the CAR/OVV system. It would be interesting to investigate the effects of lymphodepletion on CAR-T cell persistence in the CAR/OVV system by opening engraftment niches and diminishing the likelihood of anti-CAR immunity.

There is still much to learn about the biology of this universal boosting strategy. Unveiling which cell types engage with CAR T cells upon vaccination is an important

component of this system. We have previously described that intravenous administration of recombinant rhabdovirus lead to infection follicular B cell primarily and cross-presentation of rhabdovirus-derived antigen by splenic dendritic cells which led to expansion of transferred central memory T cells via TCR:MHC interactions[97]. While it is possible that the BCMA from VSV-hBCMA is also presented on dendritic cells for presentation to central memory CAR-T cells, it is equally plausible that other cell population, or B cells, are presenting the BCMA because the CAR-T cells do not rely upon MHC-mediated antigen presentation. However, it is clear that the long-term functional outcomes of TCR-mediated boosting are not yet fully recapitulated with our paired universal boosting CAR/OVV system. Further examination of the VSV-hBCMA vaccine and CAR-T cell biology will be helpful for the learning about how synthetic receptors alter immune responses in this combination therapy and others.

5 References:

1. Couzin-Frankel, J. (2013). Cancer Immunotherapy. Science, 342(6165), 1432–1433. https://doi.org/10.1126/science.342.6165.1432
2. Oiseth, S. J., & Aziz, M. S. (2017). Cancer immunotherapy: A brief review of the history, possibilities, and challenges ahead. *Journal of Cancer Metastasis and Treatment*, *3*(10), 250. https://doi.org/10.20517/2394-4722.2017.41
3. McCarthy, E. F. (2006). The toxins of William B. Coley and the treatment of bone and soft-tissue sarcomas. *The Iowa Orthopaedic Journal*, *26*, 154–158.
4. Razi, S., & Rezaei, N. (2023). Introduction on Cancer Immunotherapy. In N. Rezaei (Ed.), *Handbook of Cancer and Immunology* (pp. 1–27). Springer International Publishing. https://doi.org/10.1007/978-3-030-80962-1_180-1
5. Bearman, S. I., Appelbaum, F. R., Buckner, C. D., Petersen, F. B., Fisher, L. D., Clift, R. A., & Thomas, E. D. (1988). Regimen-related toxicity in patients undergoing bone marrow transplantation. *Journal of Clinical Oncology*, *6*(10), 1562–1568. https://doi.org/10.1200/JCO.1988.6.10.1562
6. Thomas, E. D. (2000). Transplante de medula óssea: Uma revisão histórica. *Medicina (Ribeirão Preto)*, *33*(3), 209–218. https://doi.org/10.11606/issn.2176-7262.v33i3p209-218
7. Zitvogel, L., Tesniere, A., & Kroemer, G. (2006). Cancer despite immunosurveillance: Immunoselection and immunosubversion. *Nature Reviews Immunology*, *6*(10), 715–727. https://doi.org/10.1038/nri1936
8. Smyth, M. J., Dunn, G. P., & Schreiber, R. D. (2006). Cancer Immunosurveillance and Immunoediting: The Roles of Immunity in Suppressing Tumour Development and Shaping Tumour Immunogenicity. In *Advances in Immunology* (Vol. 90, pp. 1–50). Elsevier. https://doi.org/10.1016/S0065-2776(06)90001-7
9. Tuthill, M. & Hatzimichael. (2010). Hematopoietic stem cell transplantation. *Stem Cells and Cloning: Advances and Applications*, 105. https://doi.org/10.2147/SCCAA.S6815
10. Atkins, M. B., Lotze, M. T., Dutcher, J. P., Fisher, R. I., Weiss, G., Margolin, K., Abrams, J., Sznol, M., Parkinson, D., Hawkins, M., Paradise, C., Kunkel, L., & Rosenberg, S. A. (1999). High-Dose Recombinant Interleukin 2 Therapy for Patients With Metastatic Melanoma: Analysis of 270 Patients Treated Between 1985 and 1993.

Journal of Clinical Oncology, *17*(7), 2105–2105. https://doi.org/10.1200/JCO.1999.17.7.2105

11. Fyfe, G., Fisher, R. I., Rosenberg, S. A., Sznol, M., Parkinson, D. R., & Louie, A. C. (1995). Results of treatment of 255 patients with metastatic renal cell carcinoma who received high-dose recombinant interleukin-2 therapy. *Journal of Clinical Oncology*, *13*(3), 688–696. https://doi.org/10.1200/JCO.1995.13.3.688
12. Canadian Cancer Society / Société canadienne du cancer. (n.d.). *Immunotherapy*. Canadian Cancer Society. https://cancer.ca/en/treatments/treatment-types/immunotherapy
13. Golomb, H. M., Jacobs, A., Fefer, A., Ozer, H., Thompson, J., Portlock, C., Ratain, M., Golde, D., Vardiman, J., & Burke, J. S. (1986). Alpha-2 interferon therapy of hairy-cell leukemia: A multicenter study of 64 patients. *Journal of Clinical Oncology*, *4*(6), 900–905. https://doi.org/10.1200/JCO.1986.4.6.900
14. Nguyen, L. T., & Ohashi, P. S. (2015). Clinical blockade of PD1 and LAG3—Potential mechanisms of action. *Nature Reviews Immunology*, *15*(1), 45–56. https://doi.org/10.1038/nri3790
15. Eno, J. (2017). Immunotherapy Through the Years. *Journal of the Advanced Practitioner in Oncology*, *8*(7), 747–753.
16. Tarhini, A., Lo, E., & Minor, D. R. (2010). Releasing the Brake on the Immune System: Ipilimumab in Melanoma and Other Tumours. *Cancer Biotherapy and Radiopharmaceuticals*, *25*(6), 601–613. https://doi.org/10.1089/cbr.2010.0865
17. Piccart-Gebhart, M. J., Procter, M., Leyland-Jones, B., Goldhirsch, A., Untch, M., Smith, I., Gianni, L., Baselga, J., Bell, R., Jackisch, C., Cameron, D., Dowsett, M., Barrios, C. H., Steger, G., Huang, C.-S., Andersson, M., Inbar, M., Lichinitser, M., Láng, I., … Gelber, R. D. (2005). Trastuzumab after Adjuvant Chemotherapy in HER2-Positive Breast Cancer. *New England Journal of Medicine*, *353*(16), 1659–1672. https://doi.org/10.1056/NEJMoa052306
18. Weiner, G. J. (2010). Rituximab: Mechanism of Action. *Seminars in Hematology*, *47*(2), 115–123. https://doi.org/10.1053/j.seminhematol.2010.01.011
19. Goldberg, R., & Kirkpatrick, P. (2005). Cetuximab. *Nature Reviews Drug Discovery*, *4*(5), S10–S11. https://doi.org/10.1038/nrd1728

20. Rosenberg, S. A., & Restifo, N. P. (2015). Adoptive cell transfer as personalized immunotherapy for human cancer. *Science (New York, N.Y.)*, *348*(6230), 62–68. https://doi.org/10.1126/science.aaa4967
21. Delorme, E. (1964). TREATMENT OF PRIMARY FIBROSARCOMA IN THE RAT WITH IMMUNE LYMPHOCYTES. *The Lancet*, *284*(7351), 117–120. https://doi.org/10.1016/S0140-6736(64)90126-6
22. Waldman, A. D., Fritz, J. M., & Lenardo, M. J. (2020). A guide to cancer immunotherapy: From T cell basic science to clinical practice. *Nature Reviews Immunology*, *20*(11), 651–668. https://doi.org/10.1038/s41577-020-0306-5
23. Miller, J. F. A. P., & Mitchell, G. F. (1968). CELL TO CELL INTERACTION IN THE IMMUNE RESPONSE. *The Journal of Experimental Medicine*, *128*(4), 801–820. https://doi.org/10.1084/jem.128.4.801
24. Van Den Broek, T., Borghans, J. A. M., & Van Wijk, F. (2018). The full spectrum of human naive T cells. *Nature Reviews Immunology*, *18*(6), 363–373. https://doi.org/10.1038/s41577-018-0001-y
25. Nikolich-Žugich, J., Slifka, M. K., & Messaoudi, I. (2004). The many important facets of T-cell repertoire diversity. *Nature Reviews Immunology*, *4*(2), 123–132. https://doi.org/10.1038/nri1292
26. Wilson, I. A., & Christopher Garcia, K. (1997). T-cell receptor structure and TCR complexes. *Current Opinion in Structural Biology*, *7*(6), 839–848. https://doi.org/10.1016/S0959-440X(97)80156-X
27. June, C. H., Ledbetter, J. A., Linsley, P. S., & Thompson, C. B. (1990). Role of the CD28 receptor in T-cell activation. *Immunology Today*, *11*, 211–216. https://doi.org/10.1016/0167-5699(90)90085-N
28. Mueller, S. N., Gebhardt, T., Carbone, F. R., & Heath, W. R. (2013). Memory T Cell Subsets, Migration Patterns, and Tissue Residence. *Annual Review of Immunology*, *31*(1), 137–161. https://doi.org/10.1146/annurev-immunol-032712-095954
29. Wherry, E. J. (2011). T cell exhaustion. *Nature Immunology*, *12*(6), 492–499. https://doi.org/10.1038/ni.2035
30. Besser, M. J., Shapira-Frommer, R., Itzhaki, O., Treves, A. J., Zippel, D. B., Levy, D., Kubi, A., Shoshani, N., Zikich, D., Ohayon, Y., Ohayon, D., Shalmon, B., Markel, G., Yerushalmi, R., Apter, S., Ben-Nun, A., Ben-Ami, E., Shimoni, A., Nagler, A., &

Schachter, J. (2013). Adoptive Transfer of Tumour-Infiltrating Lymphocytes in Patients with Metastatic Melanoma: Intent-to-Treat Analysis and Efficacy after Failure to Prior Immunotherapies. *Clinical Cancer Research*, *19*(17), 4792–4800. https://doi.org/10.1158/1078-0432.CCR-13-0380

31. Rosenberg, S. A., Yang, J. C., Sherry, R. M., Kammula, U. S., Hughes, M. S., Phan, G. Q., Citrin, D. E., Restifo, N. P., Robbins, P. F., Wunderlich, J. R., Morton, K. E., Laurencot, C. M., Steinberg, S. M., White, D. E., & Dudley, M. E. (2011). Durable Complete Responses in Heavily Pretreated Patients with Metastatic Melanoma Using T Cell Transfer Immunotherapy. *Clinical Cancer Research : An Official Journal of the American Association for Cancer Research*, *17*(13), 4550–4557. https://doi.org/10.1158/1078-0432.CCR-11-0116
32. Jiang, S.-S., Tang, Y., Zhang, Y.-J., Weng, D.-S., Zhou, Z.-G., Pan, K., Pan, Q.-Z., Wang, Q.-J., Liu, Q., He, J., Zhao, J.-J., Li, J., Chen, M.-S., Chang, A. E., Li, Q., & Xia, J.-C. (2015). A phase I clinical trial utilizing autologous tumour-infiltrating lymphocytes in patients with primary hepatocellular carcinoma. *Oncotarget*, *6*(38), 41339–41349.
33. Robbins, P. F., Dudley, M. E., Wunderlich, J., El-Gamil, M., Li, Y. F., Zhou, J., Huang, J., Powell, D. J., & Rosenberg, S. A. (2004). Cutting Edge: Persistence of Transferred Lymphocyte Clonotypes Correlates with Cancer Regression in Patients Receiving Cell Transfer Therapy. *Journal of Immunology (Baltimore, Md. : 1950)*, *173*(12), 7125–7130.
34. Rosenberg, S. A., Packard, B. S., Aebersold, P. M., Solomon, D., Topalian, S. L., Toy, S. T., Simon, P., Lotze, M. T., Yang, J. C., Seipp, C. A., Simpson, C., Carter, C., Bock, S., Schwartzentruber, D., Wei, J. P., & White, D. E. (1988). Use of Tumour-Infiltrating Lymphocytes and Interleukin-2 in the Immunotherapy of Patients with Metastatic Melanoma. *New England Journal of Medicine*, *319*(25), 1676–1680. https://doi.org/10.1056/NEJM198812223192527
35. Ben-Avi, R., Farhi, R., Ben-Nun, A., Gorodner, M., Greenberg, E., Markel, G., Schachter, J., Itzhaki, O., & Besser, M. J. (2018). Establishment of adoptive cell therapy with tumour infiltrating lymphocytes for non-small cell lung cancer patients. *Cancer Immunology, Immunotherapy*, *67*(8), 1221–1230. https://doi.org/10.1007/s00262-018-2174-4
36. Hall, M., Liu, H., Malafa, M., Centeno, B., Hodul, P. J., Pimiento, J., Pilon-Thomas, S., & Sarnaik, A. A. (2016). Expansion of tumour-infiltrating lymphocytes (TIL) from human

pancreatic tumours. *Journal for ImmunoTherapy of Cancer*, *4*(1), 61. https://doi.org/10.1186/s40425-016-0164-7

37. Liu, Z., Meng, Q., Bartek, J., Poiret, T., Persson, O., Rane, L., Rangelova, E., Illies, C., Peredo, I. H., Luo, X., Rao, M. V., Robertson, R. A., Dodoo, E., & Maeurer, M. (2017). Tumour-infiltrating lymphocytes (TIL) from patients with glioma. *OncoImmunology*, *6*(2), e1252894. https://doi.org/10.1080/2162402X.2016.1252894
38. Mullard, A. (2024). FDA approves first tumour-infiltrating lymphocyte (TIL) therapy, bolstering hopes for cell therapies in solid cancers. *Nature Reviews Drug Discovery*, *23*(4), 238–238. https://doi.org/10.1038/d41573-024-00035-1
39. Muranski, P., Boni, A., Wrzesinski, C., Citrin, D. E., Rosenberg, S. A., Childs, R., & Restifo, N. P. (2006). Increased intensity lymphodepletion and adoptive immunotherapy—How far can we go? *Nature Clinical Practice Oncology*, *3*(12), 668–681. https://doi.org/10.1038/ncponc0666
40. Schwartz, R. N., Stover, L., & Dutcher, J. P. (2002). Managing toxicities of high-dose interleukin-2. *Oncology (Williston Park, N.Y.)*, *16*(11 Suppl 13), 11–20.
41. Kishton, R. J., Vodnala, S. K., Vizcardo, R., & Restifo, N. P. (2022). Next generation immunotherapy: Enhancing stemness of polyclonal T cells to improve anti-tumour activity. *Current Opinion in Immunology*, *74*, 39–45. https://doi.org/10.1016/j.coi.2021.10.001
42. Parkhurst, M. R., Robbins, P. F., Tran, E., Prickett, T. D., Gartner, J. J., Jia, L., Ivey, G., Li, Y. F., El-Gamil, M., Lalani, A., Crystal, J. S., Sachs, A., Groh, E., Ray, S., Ngo, L. T., Kivitz, S., Pasetto, A., Yossef, R., Lowery, F. J., … Rosenberg, S. A. (2019). Unique Neoantigens Arise from Somatic Mutations in Patients with Gastrointestinal Cancers. *Cancer Discovery*, *9*(8), 1022–1035. https://doi.org/10.1158/2159-8290.CD-18-1494
43. Hulen, T. M., Chamberlain, C. A., Svane, I. M., & Met, Ö. (2021). ACT Up TIL Now: The Evolution of Tumour-Infiltrating Lymphocytes in Adoptive Cell Therapy for the Treatment of Solid Tumours. *Immuno*, *1*(3), Article 3. https://doi.org/10.3390/immuno1030012
44. Riddell, S. R., & Greenberg, P. D. (2021, March 21). High efficiency transduction of T lymphocytes using rapid expansion methods ("REM").
45. Flyer, D. C., & Clary, K. W. (2001, November 13). Modified rapid expansion methods ("modified-REM") for in vitro propagation of T lymphocytes.

46. Klebanoff, C. A., Gattinoni, L., Torabi-Parizi, P., Kerstann, K., Cardones, A. R., Finkelstein, S. E., Palmer, D. C., Antony, P. A., Hwang, S. T., Rosenberg, S. A., Waldmann, T. A., & Restifo, N. P. (2005). Central memory self/tumour-reactive CD8+ T cells confer superior antitumour immunity compared with effector memory T cells. *Proceedings of the National Academy of Sciences of the United States of America*, *102*(27), 9571–9576. https://doi.org/10.1073/pnas.0503726102
47. Zhou, J., Shen, X., Huang, J., Hodes, R. J., Rosenberg, S. A., & Robbins, P. F. (2005). Telomere Length of Transferred Lymphocytes Correlates with In Vivo Persistence and Tumour Regression in Melanoma Patients Receiving Cell Transfer Therapy. *The Journal of Immunology*, *175*(10), 7046–7052. https://doi.org/10.4049/jimmunol.175.10.7046
48. Tran, K. Q., Zhou, J., Durflinger, K. H., Langhan, M. M., Shelton, T. E., Wunderlich, J. R., Robbins, P. F., Rosenberg, S. A., & Dudley, M. E. (2008). Minimally Cultured Tumour-infiltrating Lymphocytes Display Optimal Characteristics for Adoptive Cell Therapy. *Journal of Immunotherapy*, *31*(8), 742–751.
49. Kalia, V., Sarkar, S., Subramaniam, S., Haining, W. N., Smith, K. A., & Ahmed, R. (2010). Prolonged Interleukin-2Rα Expression on Virus-Specific CD8+ T Cells Favors Terminal-Effector Differentiation In Vivo. *Immunity*, *32*(1), 91–103. https://doi.org/10.1016/j.immuni.2009.11.010
50. Zhou, Z., Tao, C., Li, J., Tang, J. C., Chan, A. S., & Zhou, Y. (2022). Chimeric antigen receptor T cells applied to solid tumours. *Frontiers in Immunology*, *13*, 984864. https://doi.org/10.3389/fimmu.2022.984864
51. Porter, D. L., Levine, B. L., Kalos, M., Bagg, A., & June, C. H. (2011). Chimeric Antigen Receptor–Modified T Cells in Chronic Lymphoid Leukemia. *New England Journal of Medicine*, *365*(8), 725–733. https://doi.org/10.1056/NEJMoa1103849
52. Wagner, D. L., Fritsche, E., Pulsipher, M. A., Ahmed, N., Hamieh, M., Hegde, M., Ruella, M., Savoldo, B., Shah, N. N., Turtle, C. J., Wayne, A. S., & Abou-el-Enein, M. (2021). Immunogenicity of CAR T cells in cancer therapy. Nature Reviews Clinical Oncology, 18(6), 379–393. https://doi.org/10.1038/s41571-021-00476-2
53. Brudno, J. N., Lam, N., Vanasse, D., Shen, Y., Rose, J. J., Rossi, J., Xue, A., Bot, A., Scholler, N., Mikkilineni, L., Roschewski, M., Dean, R., Cachau, R., Youkharibache, P., Patel, R., Hansen, B., Stroncek, D. F., Rosenberg, S. A., Gress, R. E., & Kochenderfer, J. N. (2020). Safety and feasibility of anti-CD19 CAR T cells with fully human binding

domains in patients with B-cell lymphoma. *Nature Medicine*, *26*(2), 270–280. **https://doi.org/10.1038/s41591-019-0737-3**

54. Feucht, J., Sun, J., Eyquem, J., Ho, Y.-J., Zhao, Z., Leibold, J., Dobrin, A., Cabriolu, A., Hamieh, M., & Sadelain, M. (2019). Calibration of CAR activation potential directs alternative T cell fates and therapeutic potency. *Nature Medicine*, *25*(1), 82–88. https://doi.org/10.1038/s41591-018-0290-5
55. Kershaw, M. H., Westwood, J. A., Parker, L. L., Wang, G., Eshhar, Z., Mavroukakis, S. A., White, D. E., Wunderlich, J. R., Canevari, S., Rogers-Freezer, L., Chen, C. C., Yang, J. C., Rosenberg, S. A., & Hwu, P. (2006). A Phase I Study on Adoptive Immunotherapy Using Gene-Modified T Cells for Ovarian Cancer. *Clinical Cancer Research*, *12*(20), 6106–6115. https://doi.org/10.1158/1078-0432.CCR-06-1183
56. Mullard, A. (2017). FDA approves first CAR T therapy. *Nature Reviews Drug Discovery*, *16*(10), 669–669. https://doi.org/10.1038/nrd.2017.196
57. Martinez, M., & Moon, E. K. (2019). CAR T Cells for Solid Tumours: New Strategies for Finding, Infiltrating, and Surviving in the Tumour Microenvironment. *Frontiers in Immunology*, *10*, 128. https://doi.org/10.3389/fimmu.2019.00128
58. Morgan, R. A., Yang, J. C., Kitano, M., Dudley, M. E., Laurencot, C. M., & Rosenberg, S. A. (2010). Case Report of a Serious Adverse Event Following the Administration of T Cells Transduced With a Chimeric Antigen Receptor Recognizing ERBB2. *Molecular Therapy*, *18*(4), 843–851. https://doi.org/10.1038/mt.2010.24
59. Grout, J. A., Sirven, P., Leader, A. M., Maskey, S., Hector, E., Puisieux, I., Steffan, F., Cheng, E., Tung, N., Maurin, M., Vaineau, R., Karpf, L., Plaud, M., Begue, A.-L., Ganesh, K., Mesple, J., Casanova-Acebes, M., Tabachnikova, A., Keerthivasan, S., … Salmon, H. (2022). Spatial Positioning and Matrix Programs of Cancer-Associated Fibroblasts Promote T-cell Exclusion in Human Lung Tumours. *Cancer Discovery*, *12*(11), 2606–2625. https://doi.org/10.1158/2159-8290.CD-21-1714
60. Ager, A. (2017). High Endothelial Venules and Other Blood Vessels: Critical Regulators of Lymphoid Organ Development and Function. *Frontiers in Immunology*, *8*. https://doi.org/10.3389/fimmu.2017.00045
61. Renner, K., Singer, K., Koehl, G. E., Geissler, E. K., Peter, K., Siska, P. J., & Kreutz, M. (2017). Metabolic Hallmarks of Tumour and Immune Cells in the Tumour

Microenvironment. *Frontiers in Immunology*, *8*. https://doi.org/10.3389/fimmu.2017.00248

62. Poggi, A., Varesano, S., & Zocchi, M. R. (2018). How to Hit Mesenchymal Stromal Cells and Make the Tumour Microenvironment Immunostimulant Rather Than Immunosuppressive. *Frontiers in Immunology*, *9*, 262. https://doi.org/10.3389/fimmu.2018.00262
63. gKohler, M. E., & Fry, T. J. (2023). CD4+ CAR T cells—More than helpers. *Nature Cancer*, *4*(7), 928–929. https://doi.org/10.1038/s43018-023-00567-2
64. Bove, C., Arcangeli, S., Falcone, L., Camisa, B., El Khoury, R., Greco, B., De Lucia, A., Bergamini, A., Bondanza, A., Ciceri, F., Bonini, C., & Casucci, M. (2023). CD4 CAR-T cells targeting CD19 play a key role in exacerbating cytokine release syndrome, while maintaining long-term responses. *Journal for ImmunoTherapy of Cancer*, *11*(1), e005878. https://doi.org/10.1136/jitc-2022-005878
65. Boulch, M., Cazaux, M., Cuffel, A., Ruggiu, M., Allain, V., Corre, B., Loe-Mie, Y., Hosten, B., Cisternino, S., Auvity, S., Thieblemont, C., Caillat-Zucman, S., & Bousso, P. (2023). A major role for CD4+ T cells in driving cytokine release syndrome during CAR T cell therapy. *Cell Reports Medicine*, *4*(9), 101161. https://doi.org/10.1016/j.xcrm.2023.101161
66. Sommermeyer, D., Hudecek, M., Kosasih, P. L., Gogishvili, T., Maloney, D. G., Turtle, C. J., & Riddell, S. R. (2016). Chimeric antigen receptor-modified T cells derived from defined CD8+ and CD4+ subsets confer superior antitumour reactivity in vivo. *Leukemia*, *30*(2), 492–500. https://doi.org/10.1038/leu.2015.247
67. Moeller, M., Haynes, N. M., Kershaw, M. H., Jackson, J. T., Teng, M. W. L., Street, S. E., Cerutti, L., Jane, S. M., Trapani, J. A., Smyth, M. J., & Darcy, P. K. (2005). Adoptive transfer of gene-engineered CD4+ helper T cells induces potent primary and secondary tumour rejection. *Blood*, *106*(9), 2995–3003. https://doi.org/10.1182/blood-2004-12-4906
68. Melenhorst, J. J., Chen, G. M., Wang, M., Porter, D. L., Chen, C., Collins, M. A., Gao, P., Bandyopadhyay, S., Sun, H., Zhao, Z., Lundh, S., Pruteanu-Malinici, I., Nobles, C. L., Maji, S., Frey, N. V., Gill, S. I., Loren, A. W., Tian, L., Kulikovskaya, I., … June, C. H. (2022). Decade-long leukaemia remissions with persistence of CD4+ CAR T cells. *Nature*, *602*(7897), 503–509. https://doi.org/10.1038/s41586-021-04390-6

69. Yang, T. C., Millar, J., Groves, T., Zhou, W., Grinshtein, N., Parsons, R., Evelegh, C., Xing, Z., Wan, Y., & Bramson, J. (2007). On the Role of CD4+ T Cells in the CD8+ T-Cell Response Elicited by Recombinant Adenovirus Vaccines. *Molecular Therapy*, *15*(5), 997–1006. https://doi.org/10.1038/sj.mt.6300130
70. Busselaar, J., Tian, S., Van Eenennaam, H., & Borst, J. (2020). Helpless Priming Sends CD8+ T Cells on the Road to Exhaustion. *Frontiers in Immunology*, *11*, 592569. https://doi.org/10.3389/fimmu.2020.592569
71. Janssen, E. M., Droin, N. M., Lemmens, E. E., Pinkoski, M. J., Bensinger, S. J., Ehst, B. D., Griffith, T. S., Green, D. R., & Schoenberger, S. P. (2005). CD4+ T-cell help controls CD8+ T-cell memory via TRAIL-mediated activation-induced cell death. *Nature*, *434*(7029), 88–93. https://doi.org/10.1038/nature03337
72. Janssen, E. M., Lemmens, E. E., Wolfe, T., Christen, U., Von Herrath, M. G., & Schoenberger, S. P. (2003). CD4+ T cells are required for secondary expansion and memory in CD8+ T lymphocytes. *Nature*, *421*(6925), 852–856. https://doi.org/10.1038/nature01441
73. Yu, H., Tawab-Amiri, A., Dzutsev, A., Sabatino, M., Aleman, K., Yarchoan, R., Terabe, M., Sui, Y., & Berzofsky, J. A. (2011). IL-15 ex vivo overcomes CD4+ T cell deficiency for the induction of human antigen-specific CD8+ T cell responses. *Journal of Leukocyte Biology*, *90*(1), 205–214. https://doi.org/10.1189/jlb.1010579
74. Andtbacka, R. H. I., Kaufman, H. L., Collichio, F., Amatruda, T., Senzer, N., Chesney, J., Delman, K. A., Spitler, L. E., Puzanov, I., Agarwala, S. S., Milhem, M., Cranmer, L., Curti, B., Lewis, K., Ross, M., Guthrie, T., Linette, G. P., Daniels, G. A., Harrington, K., … Coffin, R. S. (2015). Talimogene Laherparepvec Improves Durable Response Rate in Patients With Advanced Melanoma. *Journal of Clinical Oncology*, *33*(25), 2780–2788. https://doi.org/10.1200/JCO.2014.58.3377
75. Bommareddy, P. K., Shettigar, M., & Kaufman, H. L. (2018). Integrating oncolytic viruses in combination cancer immunotherapy. *Nature Reviews Immunology*, *18*(8), 498–513. https://doi.org/10.1038/s41577-018-0014-6
76. Hanson, R. P., & Karstad, L. (1958). Further studies on enzootic vesicular stomatitis.
77. Bridle, B. W., Chen, L., Lemay, C. G., Diallo, J.-S., Pol, J., Nguyen, A., Capretta, A., He, R., Bramson, J. L., Bell, J. C., Lichty, B. D., & Wan, Y. (2013). HDAC Inhibition Suppresses Primary Immune Responses, Enhances Secondary Immune Responses, and

Abrogates Autoimmunity During Tumour Immunotherapy. *Molecular Therapy*, *21*(4), 887–894. https://doi.org/10.1038/mt.2012.265

78. Petersen, J. M., Her, L.-S., Varvel, V., Lund, E., & Dahlberg, J. E. (2000). The Matrix Protein of Vesicular Stomatitis Virus Inhibits Nucleocytoplasmic Transport When It Is in the Nucleus and Associated with Nuclear Pore Complexes. *Molecular and Cellular Biology*, *20*(22), 8590–8601. https://doi.org/10.1128/MCB.20.22.8590-8601.2000
79. Shinozaki, K., Ebert, O., Suriawinata, A., Thung, S. N., & Woo, S. L. C. (2005). Prophylactic Alpha Interferon Treatment Increases the Therapeutic Index of Oncolytic Vesicular Stomatitis Virus Virotherapy for Advanced Hepatocellular Carcinoma in Immune-Competent Rats. *Journal of Virology*, *79*(21), 13705–13713. https://doi.org/10.1128/JVI.79.21.13705-13713.2005
80. Johnson, J. E., Nasar, F., Coleman, J. W., Price, R. E., Javadian, A., Draper, K., Lee, M., Reilly, P. A., Clarke, D. K., Hendry, R. M., & Udem, S. A. (2007). Neurovirulence properties of recombinant vesicular stomatitis virus vectors in non-human primates. *Virology*, *360*(1), 36–49. https://doi.org/10.1016/j.virol.2006.10.026
81. Stojdl, D. F., Lichty, B. D., tenOever, B. R., Paterson, J. M., Power, A. T., Knowles, S., Marius, R., Reynard, J., Poliquin, L., Atkins, H., Brown, E. G., Durbin, R. K., Durbin, J. E., Hiscott, J., & Bell, J. C. (2003). VSV strains with defects in their ability to shutdown innate immunity are potent systemic anti-cancer agents. *Cancer Cell*, *4*(4), 263–275. https://doi.org/10.1016/S1535-6108(03)00241-1
82. Simon, I. D., Van Rooijen, N., & Rose, J. K. (2010). Vesicular Stomatitis Virus Genomic RNA Persists *In Vivo* in the Absence of Viral Replication. *Journal of Virology*, *84*(7), 3280–3286. https://doi.org/10.1128/JVI.02052-09
83. Patel, M. R., Jacobson, B. A., Ji, Y., Drees, J., Tang, S., Xiong, K., Wang, H., Prigge, J. E., Dash, A. S., Kratzke, A. K., Mesev, E., Etchison, R., Federspiel, M. J., Russell, S. J., & Kratzke, R. A. (2015). Vesicular stomatitis virus expressing interferon-β is oncolytic and promotes antitumour immune responses in a syngeneic murine model of non-small cell lung cancer. *Oncotarget*, *6*(32), 33165–33177. https://doi.org/10.18632/oncotarget.5320
84. Jenks, N., Myers, R., Greiner, S. M., Thompson, J., Mader, E. K., Greenslade, A., Griesmann, G. E., Federspiel, M. J., Rakela, J., Borad, M. J., Vile, R. G., Barber, G. N., Meier, T. R., Blanco, M. C., Carlson, S. K., Russell, S. J., & Peng, K.-W. (2010). Safety Studies on Intrahepatic or Intratumoural Injection of Oncolytic Vesicular Stomatitis Virus

Expressing Interferon-β in Rodents and Nonhuman Primates. *Human Gene Therapy*, *21*(4), 451–462. https://doi.org/10.1089/hum.2009.111

85. Merchan, J. R., Patel, M., Cripe, T. P., Old, M. O., Strauss, J. F., Thomassen, A., Diaz, R. M., Peng, K. W., Russell, S. J., Russell, L., Reckner, M., Wiegert, E., Bexon, A. S., & Powell, S. F. (2020). Relationship of infusion duration to safety, efficacy, and pharmacodynamics (PD): Second part of a phase I-II study using VSV-IFNβ-NIS (VV1) oncolytic virus in patients with refractory solid tumours. *Journal of Clinical Oncology*, *38*(15_suppl), 3090–3090. https://doi.org/10.1200/JCO.2020.38.15_suppl.3090
86. *VSV-hIFNbeta-NIS With or Without Ruxolitinib Phosphate in Treating Stage IV or Recurrent Endometrial Cancer*. Clinicaltrials.gov. (2017, April 19). https://clinicaltrials.gov/ct2/show/NCT03120624
87. *VSV-hIFNbeta-NIS in Treating Patients With Relapsed or Refractory Multiple Myeloma, Acute Myeloid Leukemia or Lymphoma*. Clinicaltrials.gov. (2017a, January 11). https://clinicaltrials.gov/study/NCT03017820
88. Cook, J., Peng, K. W. W., Witzig, T. E., Broski, S. M., Villasboas, J. C., Paludo, J., Patnaik, M. M., Rajkumar, V. V., Dispenzieri, A., Leung, N., Buadi, F., Bennani, N. N., Ansell, S. M., Zhang, L., Packiriswamy, N., Balakrishnan, B., Brunton, B., Giers, M., Ginos, B., … Lacy, M. Q. (2022). Clinical Activity of Single Dose Systemic Oncolytic VSV Virotherapy in Patients with Relapsed Refractory T-Cell Lymphoma. *Blood Advances*, bloodadvances.2021006631. https://doi.org/10.1182/bloodadvances.2021006631
89. Obuchi, M., Fernandez, M., & Barber, G. N. (2003). Development of Recombinant Vesicular Stomatitis Viruses That Exploit Defects in Host Defense To Augment Specific Oncolytic Activity. *Journal of Virology*, *77*(16), 8843–8856. https://doi.org/10.1128/JVI.77.16.8843-8856.2003
90. Boudreau, J. E., Bridle, B. W., Stephenson, K. B., Jenkins, K. M., Brunellière, J., Bramson, J. L., Lichty, B. D., & Wan, Y. (2009). Recombinant Vesicular Stomatitis Virus Transduction of Dendritic Cells Enhances Their Ability to Prime Innate and Adaptive Antitumour Immunity. Molecular Therapy, 17(8), 1465–1472. https://doi.org/10.1038/mt.2009.95
91. Bridle, B. W., Boudreau, J. E., Lichty, B. D., Brunellière, J., Stephenson, K., Koshy, S., Bramson, J. L., & Wan, Y. (2009). Vesicular stomatitis virus as a novel cancer vaccine

vector to prime antitumour immunity amenable to rapid boosting with adenovirus. *Molecular Therapy: The Journal of the American Society of Gene Therapy*, *17*(10), 1814–1821. https://doi.org/10.1038/mt.2009.154

92. Bridle, B. W., Stephenson, K. B., Boudreau, J. E., Koshy, S., Kazdhan, N., Pullenayegum, E., Brunellière, J., Bramson, J. L., Lichty, B. D., & Wan, Y. (2010). Potentiating Cancer Immunotherapy Using an Oncolytic Virus. *Molecular Therapy*, *18*(8), 1430–1439. https://doi.org/10.1038/mt.2010.98
93. Bridle, B. W., Clouthier, D., Zhang, L., Pol, J., Chen, L., Lichty, B. D., Bramson, J. L., & Wan, Y. (2013). Oncolytic vesicular stomatitis virus quantitatively and qualitatively improves primary CD8+ T-cell responses to anticancer vaccines. *Oncoimmunology*, *2*(8), e26013. https://doi.org/10.4161/onci.26013
94. Nguyen, A., Ho, L., Workenhe, S. T., Chen, L., Samson, J., Walsh, S. R., Pol, J., Bramson, J. L., & Wan, Y. (2018). HDACi Delivery Reprograms Tumour-Infiltrating Myeloid Cells to Eliminate Antigen-Loss Variants. *Cell Reports*, *24*(3), 642–654. https://doi.org/10.1016/j.celrep.2018.06.040
95. Walsh, S. R., Simovic, B., Chen, L., Bastin, D., Nguyen, A., Stephenson, K., Mandur, T. S., Bramson, J. L., Lichty, B. D., & Wan, Y. (n.d.). Endogenous T cells prevent tumour immune escape following adoptive T cell therapy. *The Journal of Clinical Investigation*, *129*(12), 5400–5410. https://doi.org/10.1172/JCI126199
96. Klebanoff, C. A., Gattinoni, L., Torabi-Parizi, P., Kerstann, K., Cardones, A. R., Finkelstein, S. E., Palmer, D. C., Antony, P. A., Hwang, S. T., Rosenberg, S. A., Waldmann, T. A., & Restifo, N. P. (2005). Central memory self/tumour-reactive $CD8^+$ T cells confer superior antitumour immunity compared with effector memory T cells. *Proceedings of the National Academy of Sciences*, *102*(27), 9571–9576. https://doi.org/10.1073/pnas.0503726102
97. Bridle, B. W., Nguyen, A., Salem, O., Zhang, L., Koshy, S., Clouthier, D., Chen, L., Pol, J., Swift, S. L., Bowdish, D. M. E., Lichty, B. D., Bramson, J. L., & Wan, Y. (2016). Privileged Antigen Presentation in Splenic B Cell Follicles Maximizes T Cell Responses in Prime-Boost Vaccination. *The Journal of Immunology*, *196*(11), 4587–4595. https://doi.org/10.4049/jimmunol.1600106

98. Burchett, R., Walsh, S., Wan, Y., & Bramson, J. L. (2020). A rational relationship: Oncolytic virus vaccines as functional partners for adoptive T cell therapy. *Cytokine & Growth Factor Reviews*, *56*, 149–159. https://doi.org/10.1016/j.cytogfr.2020.07.003

99. Reinhard, K., Rengstl, B., Oehm, P., Michel, K., Billmeier, A., Hayduk, N., Klein, O., Kuna, K., Ouchan, Y., Wöll, S., Christ, E., Weber, D., Suchan, M., Bukur, T., Birtel, M., Jahndel, V., Mroz, K., Hobohm, K., Kranz, L., … Sahin, U. (2020). An RNA vaccine drives expansion and efficacy of claudin-CAR-T cells against solid tumours. *Science (New York, N.Y.)*, *367*(6476), 446–453. https://doi.org/10.1126/science.aay5967

100. Zhang, A. Q., Hostetler, A., Chen, L. E., Mukkamala, V., Abraham, W., Padilla, L. T., Wolff, A. N., Maiorino, L., Backlund, C. M., Aung, A., Melo, M., Li, N., Wu, S., & Irvine, D. J. (2023). Universal redirection of CAR T cells against solid tumours via membrane-inserted ligands for the CAR. *Nature Biomedical Engineering*, *7*(9), 1113–1128. https://doi.org/10.1038/s41551-023-01048-8

101. Ma, L., Dichwalkar, T., Chang, J. Y. H., Cossette, B., Garafola, D., Zhang, A. Q., Fichter, M., Wang, C., Liang, S., Silva, M., Kumari, S., Mehta, N. K., Abraham, W., Thai, N., Li, N., Wittrup, K. D., & Irvine, D. J. (2019). Enhanced CAR–T cell activity against solid tumours by vaccine boosting through the chimeric receptor. *Science*, *365*(6449), 162–168. https://doi.org/10.1126/science.aav8692

102. Pule, M. A., Savoldo, B., Myers, G. D., Rossig, C., Russell, H. V., Dotti, G., Huls, M. H., Liu, E., Gee, A. P., Mei, Z., Yvon, E., Weiss, H. L., Liu, H., Rooney, C. M., Heslop, H. E., & Brenner, M. K. (2008). Virus-specific T cells engineered to coexpress tumour-specific receptors: Persistence and antitumour activity in individuals with neuroblastoma. *Nature Medicine*, *14*(11), 1264–1270. https://doi.org/10.1038/nm.1882

103. Tanaka, M., Tashiro, H., Omer, B., Lapteva, N., Ando, J., Ngo, M., Mehta, B., Dotti, G., Kinchington, P. R., Leen, A. M., Rossig, C., & Rooney, C. M. (2017). Vaccination targeting native receptors to enhance the function and proliferation of chimeric antigen receptor (CAR)-modified T cells. *Clinical Cancer Research : An Official Journal of the American Association for Cancer Research*, *23*(14), 3499–3509. https://doi.org/10.1158/1078-0432.CCR-16-2138

104. Pircher, H., Bürki, K., Lang, R., Hengartner, H., & Zinkernagel, R. M. (1989). Tolerance induction in double specific T-cell receptor transgenic mice varies with antigen. *Nature*, *342*(6249), 559–561. https://doi.org/10.1038/342559a0

105. VanSeggelen, H., Tantalo, D. G., Afsahi, A., Hammill, J. A., & Bramson, J. L. (2015). Chimeric antigen receptor-engineered T cells as oncolytic virus carriers. *Molecular Therapy Oncolytics*, *2*, 15014. https://doi.org/10.1038/mto.2015.14

106. Hammill, J. A., VanSeggelen, H., Helsen, C. W., Denisova, G. F., Evelegh, C., Tantalo, D. G. M., Bassett, J. D., & Bramson, J. L. (2015). Designed ankyrin repeat proteins are effective targeting elements for chimeric antigen receptors. *Journal for Immunotherapy of Cancer*, *3*, 55. https://doi.org/10.1186/s40425-015-0099-4

107. Evgin, L., Huff, A. L., Wongthida, P., Thompson, J., Kottke, T., Tonne, J., Schuelke, M., Ayasoufi, K., Driscoll, C. B., Shim, K. G., Reynolds, P., Monie, D. D., Johnson, A. J., Coffey, M., Young, S. L., Archer, G., Sampson, J., Pulido, J., Perez, L. S., & Vile, R. (2020). Oncolytic virus-derived type I interferon restricts CAR T cell therapy. *Nature Communications*, *11*(1), 3187. https://doi.org/10.1038/s41467-020-17011-z

108. Lukhele, S., Rabbo, D. A., Guo, M., Shen, J., Elsaesser, H. J., Quevedo, R., Carew, M., Gadalla, R., Snell, L. M., Mahesh, L., Ciudad, M. T., Snow, B. E., You-Ten, A., Haight, J., Wakeham, A., Ohashi, P. S., Mak, T. W., Cui, W., McGaha, T. L., & Brooks, D. G. (2022). The transcription factor IRF2 drives interferon-mediated CD8+ T cell exhaustion to restrict anti-tumour immunity. *Immunity*, *55*(12), 2369-2385.e10. https://doi.org/10.1016/j.immuni.2022.10.020

109. Walsh, S. R., Bastin, D., Chen, L., Nguyen, A., Storbeck, C. J., Lefebvre, C., Stojdl, D., Bramson, J. L., Bell, J. C., & Wan, Y. (2018). Type I IFN blockade uncouples immunotherapy-induced antitumour immunity and autoimmune toxicity. *Journal of Clinical Investigation*, *129*(2), 518–530. https://doi.org/10.1172/JCI121004

110. Forsberg, E. M. V., Riise, R., Saellström, S., Karlsson, J., Alsén, S., Bucher, V., Hemminki, A. E., Olofsson Bagge, R., Ny, L., Nilsson, L. M., Rönnberg, H., & Nilsson, J. A. (2023). Treatment with Anti-HER2 Chimeric Antigen Receptor Tumour-Infiltrating Lymphocytes (CAR-TIL) Is Safe and Associated with Antitumour Efficacy in Mice and Companion Dogs. *Cancers*, *15*(3), Article 3. https://doi.org/10.3390/cancers15030648

111. Mills, J. K., Henderson, M. A., Giuffrida, L., Petrone, P., Westwood, J. A., Darcy, P. K., Neeson, P. J., Kershaw, M. H., & Gyorki, D. E. (2021). Generating CAR T cells from tumour-infiltrating lymphocytes. *Therapeutic Advances in Vaccines and Immunotherapy*, *9*, 251513552110171. https://doi.org/10.1177/25151355211017119

112. Ollé Hurtado, M., Wolbert, J., Fisher, J., Flutter, B., Stafford, S., Barton, J., Jain, N., Barone, G., Majani, Y., & Anderson, J. (2019). Tumour infiltrating lymphocytes expanded from pediatric neuroblastoma display heterogeneity of phenotype and function. *PLOS ONE*, *14*(8), e0216373. https://doi.org/10.1371/journal.pone.0216373

113. Hanson, H. L., Donermeyer, D. L., Ikeda, H., White, J. M., Shankaran, V., Old, L. J., Shiku, H., Schreiber, R. D., & Allen, P. M. (2000). Eradication of Established Tumours by CD8+ T Cell Adoptive Immunotherapy. *Immunity*, *13*(2), 265–276. https://doi.org/10.1016/S1074-7613(00)00026-1

114. Zhang, Y., & Nagalo, B. M. (2022). Immunovirotherapy Based on Recombinant Vesicular Stomatitis Virus: Where Are We? *Frontiers in Immunology*, *13*, 898631. https://doi.org/10.3389/fimmu.2022.898631

115. Kobayashi, T., Kumagai, S., Doi, R., Afonina, E., Koyama, S., & Nishikawa, H. (2022). Isolation of tumour-infiltrating lymphocytes from preserved human tumour tissue specimens for downstream characterization. *STAR Protocols*, *3*(3), 101557. https://doi.org/10.1016/j.xpro.2022.101557

116. Lafreniere, R., Borkenhagen, K., & Bryant, L. D. (1990). MC-38 adenocarcinoma tumour infiltrating lymphocytes: Correlation of cytotoxicity with time of tumour harvest after tumour inoculation. *Journal of Surgical Oncology*, *43*(1), 8–12. https://doi.org/10.1002/jso.2930430104

117. Okamura, K., Nagayama, S., Tate, T., Chan, H. T., Kiyotani, K., & Nakamura, Y. (2022). Lymphocytes in tumour-draining lymph nodes co-cultured with autologous tumour cells for adoptive cell therapy. *Journal of Translational Medicine*, *20*, 241. https://doi.org/10.1186/s12967-022-03444-1

118. Liang, Y., Walczak, P., & Bulte, J. W. M. (2012). Comparison of red-shifted firefly luciferase Ppy RE9 and conventional Luc2 as bioluminescence imaging reporter genes for in vivo imaging of stem cells. *Journal of Biomedical Optics*, *17*(1), 016004. https://doi.org/10.1117/1.JBO.17.1.016004

119. Branchini, B. R., Ablamsky, D. M., Davis, A. L., Southworth, T. L., Butler, B., Fan, F., Jathoul, A. P., & Pule, M. A. (2010). Red-emitting luciferases for bioluminescence reporter and imaging applications. *Analytical Biochemistry*, *396*(2), 290–297. https://doi.org/10.1016/j.ab.2009.09.009

120. Basu, A., Ramamoorthi, G., Albert, G., Gallen, C., Beyer, A., Snyder, C., Koski, G., Disis, M. L., Czerniecki, B. J., & Kodumudi, K. (2021). Differentiation and Regulation of TH Cells: A Balancing Act for Cancer Immunotherapy. *Frontiers in Immunology*, *12*, 669474. https://doi.org/10.3389/fimmu.2021.669474

121. Szabo, S. J., Kim, S. T., Costa, G. L., Zhang, X., Fathman, C. G., & Glimcher, L. H. (2000). A Novel Transcription Factor, T-bet, Directs Th1 Lineage Commitment. *Cell*, *100*(6), 655–669. https://doi.org/10.1016/S0092-8674(00)80702-3

122. Flaherty, S., & Reynolds, J. M. (2015). Mouse Naïve CD4+ T Cell Isolation and In vitro Differentiation into T Cell Subsets. *Journal of Visualized Experiments : JoVE*, *98*, 52739. https://doi.org/10.3791/52739

123. Siracusa, F., Muscate, F., & Perez, L. G. (2021). Murine T-Helper Cell Differentiation and Plasticity. In F. Annunziato, L. Maggi, & A. Mazzoni (Eds.), *T-Helper Cells: Methods and Protocols* (pp. 65–75). Springer US. https://doi.org/10.1007/978-1-0716-1311-5_5

124. Read, K. A., Powell, M. D., Sreekumar, B. K., & Oestreich, K. J. (2019). In Vitro Differentiation of Effector CD4+ T Helper Cell Subsets. In I. C. Allen (Ed.), *Mouse Models of Innate Immunity: Methods and Protocols* (pp. 75–84). Springer. https://doi.org/10.1007/978-1-4939-9167-9_6

125. Nishimura, T., Iwakabe, K., Sekimoto, M., Ohmi, Y., Yahata, T., Nakui, M., Sato, T., Habu, S., Tashiro, H., Sato, M., & Ohta, A. (1999). Distinct Role of Antigen-Specific T Helper Type 1 (Th1) and Th2 Cells in Tumour Eradication in Vivo. *The Journal of Experimental Medicine*, *190*(5), 617–628.

126. Bradley, L. M., Haynes, L., & Swain, S. L. (2005). IL-7: Maintaining T-cell memory and achieving homeostasis. *Trends in Immunology*, *26*(3), 172–176. https://doi.org/10.1016/j.it.2005.01.004

127. Coppola, C., Hopkins, B., Huhn, S., Du, Z., Huang, Z., & Kelly, W. J. (2020). Investigation of the Impact from IL-2, IL-7, and IL-15 on the Growth and Signaling of Activated CD4+ T Cells. *International Journal of Molecular Sciences*, *21*(21), 7814. https://doi.org/10.3390/ijms21217814

128. Oh, S., Perera, L. P., Terabe, M., Ni, L., Waldmann, T. A., & Berzofsky, J. A. (2008). IL-15 as a mediator of CD4+ help for CD8+ T cell longevity and avoidance of

TRAIL-mediated apoptosis. *Proceedings of the National Academy of Sciences*, *105*(13), 5201–5206. https://doi.org/10.1073/pnas.0801003105

129. Yu, H., Tawab-Amiri, A., Dzutsev, A., Sabatino, M., Aleman, K., Yarchoan, R., Terabe, M., Sui, Y., & Berzofsky, J. A. (2011). IL-15 ex vivo overcomes CD4+ T cell deficiency for the induction of human antigen-specific CD8+ T cell responses. *Journal of Leukocyte Biology*, *90*(1), 205–214. https://doi.org/10.1189/jlb.1010579

130. Lanitis, E., Rota, G., Kosti, P., Ronet, C., Spill, A., Seijo, B., Romero, P., Dangaj, D., Coukos, G., & Irving, M. (2021). Optimized gene engineering of murine CAR-T cells reveals the beneficial effects of IL-15 coexpression. *The Journal of Experimental Medicine*, *218*(2), e20192203. https://doi.org/10.1084/jem.20192203

131. Gargett, T., Ebert, L. M., Truong, N. T. H., Kollis, P. M., Sedivakova, K., Yu, W., Yeo, E. C. F., Wittwer, N. L., Gliddon, B. L., Tea, M. N., Ormsby, R., Poonnoose, S., Nowicki, J., Vittorio, O., Ziegler, D. S., Pitson, S. M., & Brown, M. P. (2022). GD2-targeting CAR-T cells enhanced by transgenic IL-15 expression are an effective and clinically feasible therapy for glioblastoma. *Journal for Immunotherapy of Cancer*, *10*(9), e005187. https://doi.org/10.1136/jitc-2022-005187

132. Shi, H., Li, A., Dai, Z., Xue, J., Zhao, Q., Tian, J., Song, D., Wang, H., Chen, J., Zhang, X., Zhou, K., Wei, H., & Qin, S. (2023). IL-15 armoring enhances the antitumour efficacy of claudin 18.2-targeting CAR-T cells in syngeneic mouse tumour models. *Frontiers in Immunology*, *14*, 1165404. https://doi.org/10.3389/fimmu.2023.1165404

133. Vranic, S., & Gatalica, Z. (2020). Targeting HER2 expression in cancer: New drugs and new indications. *Bosnian Journal of Basic Medical Sciences*. https://doi.org/10.17305/bjbms.2020.4908

134. Haffner, M. C., Kronberger, I. E., Ross, J. S., Sheehan, C. E., Zitt, M., Mühlmann, G., Öfner, D., Zelger, B., Ensinger, C., Yang, X. J., Geley, S., Margreiter, R., & Bander, N. H. (2009). Prostate-specific membrane antigen expression in the neovasculature of gastric and colorectal cancers. *Human Pathology*, *40*(12), 1754–1761. https://doi.org/10.1016/j.humpath.2009.06.003

135. Sahin, U., Koslowski, M., Dhaene, K., Usener, D., Brandenburg, G., Seitz, G., Huber, C., & Türeci, Ö. (2008). Claudin-18 Splice Variant 2 Is a Pan-Cancer Target Suitable for Therapeutic Antibody Development. *Clinical Cancer Research*, *14*(23), 7624–7634. https://doi.org/10.1158/1078-0432.CCR-08-1547

136. Zhu, C., Zhao, Y., He, J., Zhao, H., Ni, L., Cheng, X., Chen, Y., Mu, L., Zhou, X., Shi, Q., & Sun, J. (2023). TIL-Derived CAR T Cells Improve Immune Cell Infiltration and Survival in the Treatment of CD19-Humanized Mouse Colorectal Cancer. *Cancers*, *15*(23), 5567. https://doi.org/10.3390/cancers15235567

137. Hegde, M., Navai, S., DeRenzo, C., Joseph, S. K., Sanber, K., Wu, M., Gad, A. Z., Janeway, K. A., Campbell, M., Mullikin, D., Nawas, Z., Robertson, C., Mathew, P. R., Zhang, H., Mehta, B., Bhat, R. R., Major, A., Shree, A., Gerken, C., … Ahmed, N. (2024). Autologous HER2-specific CAR T cells after lymphodepletion for advanced sarcoma: A phase 1 trial. *Nature Cancer*, *5*(6), 880–894. https://doi.org/10.1038/s43018-024-00749-6

138. Junghans, R. P., Ma, Q., Rathore, R., Gomes, E. M., Bais, A. J., Lo, A. S. Y., Abedi, M., Davies, R. A., Cabral, H. J., Al-Homsi, A. S., & Cohen, S. I. (2016). Phase I Trial of Anti-PSMA Designer CAR-T Cells in Prostate Cancer: Possible Role for Interacting Interleukin 2-T Cell Pharmacodynamics as a Determinant of Clinical Response. *The Prostate*, *76*(14), 1257–1270. https://doi.org/10.1002/pros.23214

139. Qi, C., Gong, J., Li, J., Liu, D., Qin, Y., Ge, S., Zhang, M., Peng, Z., Zhou, J., Cao, Y., Zhang, X., Lu, Z., Lu, M., Yuan, J., Wang, Z., Wang, Y., Peng, X., Gao, H., Liu, Z., … Shen, L. (2022). Claudin18.2-specific CAR T cells in gastrointestinal cancers: Phase 1 trial interim results. *Nature Medicine*, *28*(6), 1189–1198. https://doi.org/10.1038/s41591-022-01800-8

140. Uche, I. K., Stanfield, B. A., Rudd, J. S., Kousoulas, K. G., & Rider, P. J. F. (2022). Utility of a Recombinant HSV-1 Vaccine Vector for Personalized Cancer Vaccines. *Frontiers in Molecular Biosciences*, *9*, 832393. https://doi.org/10.3389/fmolb.2022.832393

141. Salter, A. I., Ivey, R. G., Kennedy, J. J., Voillet, V., Rajan, A., Alderman, E. J., Voytovich, U. J., Lin, C., Sommermeyer, D., Liu, L., Whiteaker, J. R., Gottardo, R., Paulovich, A. G., & Riddell, S. R. (2018). Phosphoproteomic analysis of chimeric antigen receptor signaling reveals kinetic and quantitative differences that affect cell function. *Science Signaling*, *11*(544), eaat6753. https://doi.org/10.1126/scisignal.aat6753

142. Lu, Y., Hong, S., Li, H., Park, J., Hong, B., Wang, L., Zheng, Y., Liu, Z., Xu, J., He, J., Yang, J., Qian, J., & Yi, Q. (2012). Th9 cells promote antitumour immune responses in vivo. *Journal of Clinical Investigation*, *122*(11), 4160–4171. https://doi.org/10.1172/JCI65459

143. Yun, K., Siegler, E. L., & Kenderian, S. S. (2023). Who wins the combat, CAR or TCR? *Leukemia*, *37*(10), 1953–1962. https://doi.org/10.1038/s41375-023-01976-z

144. Davenport, A. J., Cross, R. S., Watson, K. A., Liao, Y., Shi, W., Prince, H. M., Beavis, P. A., Trapani, J. A., Kershaw, M. H., Ritchie, D. S., Darcy, P. K., Neeson, P. J., & Jenkins, M. R. (2018). Chimeric antigen receptor T cells form nonclassical and potent immune synapses driving rapid cytotoxicity. *Proceedings of the National Academy of Sciences*, *115*(9). https://doi.org/10.1073/pnas.1716266115

145. Wachsmann, T. L. A., Wouters, A. K., Remst, D. F. G., Hagedoorn, R. S., Meeuwsen, M. H., van Diest, E., Leusen, J., Kuball, J., Falkenburg, J. H. F., & Heemskerk, M. H. M. (n.d.). Comparing CAR and TCR engineered T cell performance as a function of tumour cell exposure. *Oncoimmunology*, *11*(1), 2033528. https://doi.org/10.1080/2162402X.2022.2033528

146. Green, D. R., Droin, N., & Pinkoski, M. (2003). Activation-induced cell death in T cells. *Immunological Reviews*, *193*(1), 70–81. https://doi.org/10.1034/j.1600-065X.2003.00051.x

147. Turtle, C. J., Berger, C., Sommermeyer, D., Hanafi, L.-A., Pender, B., Robinson, E. M., Melville, K., Budiarto, T. M., Steevens, N. N., Chaney, C., Cherian, S., Wood, B. L., Soma, L., Chen, X., Heimfeld, S., Jensen, M. C., Riddell, S. R., & Maloney, D. G. (2015). Anti-CD19 Chimeric Antigen Receptor-Modified T Cell Therapy for B Cell Non-Hodgkin Lymphoma and Chronic Lymphocytic Leukemia: Fludarabine and Cyclophosphamide Lymphodepletion Improves In Vivo Expansion and Persistence of CAR-T Cells and Clinical Outcomes. *Blood*, *126*(23), 184–184. https://doi.org/10.1182/blood.V126.23.184.184